MIT Libraries | DSpace@MIT

MIT Open Access Articles

Thermodynamics, Exergy, and Energy Efficiency in Desalination Systems

The MIT Faculty has made this article openly available. ***Please share*** how this access benefits you. Your story matters.

Citation: J.H. Lienhard V, K.H. Mistry, M.H. Sharqawy, and G.P. Thiel, "Thermodynamics, Exergy, and Energy Efficiency in Desalination Systems," in Desalination Sustainability: A Technical, Socioeconomic, and Environmental Approach, Chpt. 4, H.A. Arafat, editor. Elsevier Publishing Co., 2017.

Publisher: Elsevier

Persistent URL: http://hdl.handle.net/1721.1/109737

Version: Author's final manuscript: final author's manuscript post peer review, without publisher's formatting or copy editing

Terms of use: Creative Commons Attribution-Noncommercial-Share Alike

Massachusetts Institute of Technology

Chapter 4

Thermodynamics, Exergy, and Energy Efficiency in Desalination Systems

John H. Lienhard V
Department of Mechanical Engineering
Massachusetts Institute of Technology, Cambridge MA 02139, USA

Karan H. Mistry
Department of Mechanical Engineering
Massachusetts Institute of Technology, Cambridge MA 02139, USA

Mostafa H. Sharqawy
School of Engineering
University of Guelph, Ontario N1G 2W1, Canada

Gregory P. Thiel
Department of Mechanical Engineering
Massachusetts Institute of Technology, Cambridge MA 02139, USA

J.H. Lienhard V, K.H. Mistry, M.H. Sharqawy, and G.P. Thiel, "Thermodynamics, Exergy, and Energy Efficiency in Desalination Systems," in *Desalination Sustainability: A Technical, Socioeconomic, and Environmental Approach*, Chpt. 4, H.A. Arafat, editor. Elsevier Publishing Co., 2017. ISBN: 978-0-12-809791-5.

Abstract

Desalination is the thermodynamic process of separating fresh water from water that contains dissolved salts. This chapter introduces the concepts and methods required for thermodynamic analysis of desalination systems. Thermodynamic laws are summarized along with the chemical thermodynamics of electrolytes. Exergy analysis is introduced. The work and heat of separation are defined, and the roles of entropy generation and exergy destruction are identified. Important sources of entropy generation are discussed. Examples are given for the application of these methods to several representative desalination systems.

KEYWORDS: Thermodynamics, exergy, entropy generation, efficiency, physical properties, desalination systems

Contents

4.1 Introduction . . . 3
4.2 Thermodynamic Essentials . . . 4
4.2.1 Thermodynamic Analysis of Open Systems . . . 5
4.2.2 Thermodynamic Properties of Mixtures . . . 6
4.2.3 Activity Coefficient Models for Electrolytes . . . 11
4.2.4 Colligative Properties: Boiling Point Elevation, Freezing Point Depression, Vapor Pressure Lowering and Osmotic Pressure . . . 15
4.3 Exergy Analysis . . . 19
4.3.1 Exergy Variation . . . 22
4.3.2 Seawater Exergy . . . 26
4.4 Thermodynamic Analysis of Desalination . . . 28
4.4.1 Derivation of Performance Parameters for Desalination . 28
4.4.2 Analysis of Entropy Generation Mechanisms in Desalination 38
4.5 Entropy Generation in Desalination Systems . . . 45
4.5.1 Multiple Effect Distillation . . . 45
4.5.2 Direct Contact Membrane Distillation . . . 49
4.5.3 Mechanical Vapor Compression . . . 51
4.5.4 Reverse Osmosis . . . 53
4.6 Second Law Efficiency for Cogeneration . . . 57
4.7 Summary . . . 63
Appendices . . . 66
4.A Seawater Properties Correlations . . . 66
4.A.1 Specific Volume . . . 66
4.A.2 Specific Enthalpy . . . 67

4.A.3 Specific Entropy 68
4.A.4 Chemical Potential 69
4.A.5 Osmotic Coefficient 70
4.A.6 Specific Heat Capacity at Constant Pressure 71
4.A.7 Tabulated Data 72
4.B Pitzer Parameters **73**
4.C Nomenclature **75**
References **79**

4.1 Introduction

Desalination is an energy intensive process, and reduction of energy consumption is central to the development and design of all desalination processes. At the heart of the process is the chemical energy of separating water and dissolved salts. This minimum amount of energy will always be required, no matter how desalination is to be accomplished. The entire desalination system, however, brings additional energy consumption to the process of desalinating water, as a result of a variety of inefficiencies that are present in any real system. The total energy consumed is normally several times greater than the minimum chemical energy of separation. Identifying and reducing this additional energy consumption requires thermodynamic analysis of the desalination system.

The minimum separation energy can be characterized as work, in the thermodynamic sense of the word. Examples of thermodynamic work include the work done by high pressure pumps in moving water, the work done by the rotating shaft of an electric motor, and the work done by current flowing in an electric field. So, we commonly speak of the minimum or least work of separation as defining the thermodynamic limit of performance for a desalination process. The least work is usually higher when the salinity of the source water is higher.

A real desalination system will require greater amounts of work, owing to factors such as losses in pumps, hydraulic pressure behind membranes that greatly exceeds osmotic pressure, or incomplete energy recovery from high pressure brines. From a thermodynamic viewpoint, the losses or irreversibilities of components in a desalination system can be measured in terms of the entropy they generate. Entropy production directly increases the energy requirements of a system that produces a given amount of desalinated water. Entropy is produced whenever friction occurs and when heat is transferred through a difference in temperature.

Work is a form of energy transfer, but it is distinct from energy in the form of heat. Most often, work is generated by heat transferred from a high temperature source (perhaps a burning fuel in a combustor), through some process (expansion of steam through a turbine perhaps), to a low temperature sink (the cooling water in a plant condenser). The number of joules of work generated (by the steam turbine) is substantially less than the number of joules of heat transferred from the high temperature source, with the difference between them ending up as heat transfer to the low temperature sink. This difference is greater when the high temperature

source is cooler. Any inefficiencies in the system, perhaps from friction or from large temperature differences in heat exchangers, will reduce the amount of work that can be produced.

The difference between heat and work is essential to characterizing and evaluating thermal desalination processes, and more so because many desalination systems that are driven by heat also consume significant electrical energy, which is a form of work. Heat and work cannot be added or compared directly. Heat gains its potential to do work from the presence of a significant temperature difference between the high temperature source and the low temperature sink. Consequently, thermodynamic methods, in the form of exergy analysis, are essential in assessing the efficiency of a thermal desalination process, especially when comparing such a process to a work-driven desalination process. Heat transfer between two temperatures represents a source of exergy, as does any work transfer, but a given amount of heat transfer provides less exergy when taken from a lower temperature source. Thus, exergetic methods are all the more important when thermal processes are to be driven by low temperature heat sources, such as common solar collectors. Exergy is destroyed by friction or when heat is transferred to a lower temperature. In fact, any process that generates entropy destroys exergy in the process.

In this chapter, we introduce the concepts and methods required for assessing the thermodynamic efficiency of desalination systems. In Section 4.2, thermodynamic laws for open systems (those through which fluids flow) are given, and key results on the chemical thermodynamics of electrolyte mixtures (salts dissolved in water) are summarized, including the Pitzer model. Osmotic pressure and boiling point elevation are discussed. Section 4.3 introduces exergy analysis of desalination. With these tools in hand, Section 4.4 proceeds to the thermodynamic analysis of desalination processes. The work and heat of separation are derived, and the role of entropy generation and exergy destruction are identified. Important sources of entropy production are described and equations for their evaluation are given. Finally, Section 4.5 applies these methods to give brief assessments of the causes of inefficiency in several representative desalination systems. The appendices to this chapter give some useful correlations for the thermodynamic properties of seawater and and further details of one of the electrolyte models.

4.2 Thermodynamic Essentials

This chapter deals with the energy consumption of desalination systems: how it is evaluated, what its limits are, and how to push real systems closer to those limits. The key to answering these questions is a ground-up understanding of efficiency, η – strictly, the *Second Law Efficiency*. Conceptually, η is the fraction of energy consumed that *must* be consumed according to the laws of physics, or

$$\eta = \frac{\text{Minimum Energy Input}}{\text{Actual Energy Input}} \tag{4.1}$$

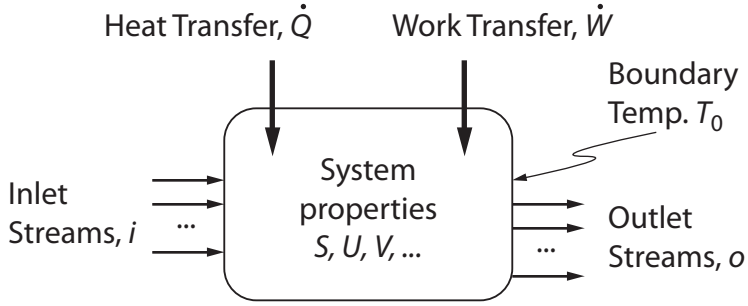

Figure 4.1: In an open system, streams i enter the system at some state, undergo a change of state and exit as outlet streams o. A work transfer $\dot{W}$ and/or a heat transfer $\dot{Q}$ may accompany the change in state. The system has instantaneous properties, such as internal energy U, entropy S, and volume V.

Conceptually, the actual energy input is

$$\begin{aligned}\text{Actual Energy Input} = \text{Minimum Energy Input} \\ + \text{Energy to Overcome Losses}\end{aligned} \tag{4.2}$$

A more rigorous definition of η and the interplay between the three terms above are described in the sections that follow; but first, in order to understand the details of each of these terms, we require some thermodynamic basics. In this section, using the Gibbs free energy as the fundamental thermodynamic function, we will provide a brief overview of the essential thermodynamic concepts and terms used throughout the remainder of the chapter.

4.2.1 Thermodynamic Analysis of Open Systems

An open system, or control volume (CV), is shown in Fig. 4.1: streams flow into the system at some inlet state(s) i, undergo a change of state within the control volume, and exit at state(s) o. A work or heat transfer may occur across the boundary of the system to effect the streams' change of state or as a consequence of their change of state. We fix the system boundary temperature at T_0.

The First Law of Thermodynamics for this system reads

$$\frac{dU}{dt} = \dot{Q} + \dot{W} + \sum_i \dot{H}_i - \sum_o \dot{H}_o \tag{4.3}$$

where U is the internal energy of the system, $\dot{Q}$ is the net heat transfer rate into the system, $\dot{W}$ is the net rate at which work is done on the system, and $\dot{H}_i$ and $\dot{H}_o$ are the enthalpy inflows and outflows, respectively. The Second Law of Thermodynamics for

this system is

$$\frac{dS}{dt} = \frac{\dot{Q}}{T_0} + \sum_i \dot{S}_i - \sum_o \dot{S}_o + \dot{S}_{\text{gen}} \tag{4.4}$$

where S is the entropy of the system, $\dot{Q}/T_0$ is the rate of entropy transfer into the system; $\dot{S}_i$ and $\dot{S}_o$ are the entropy inflows and outflows, respectively; and $\dot{S}_{\text{gen}}$ is the entropy generation rate within the CV.

Multiplying Eq. (4.4) by the boundary temperature T_0 and subtracting it from Eq. (4.3), we find that the heat transfer terms cancel; and at steady state we are left with

$$0 = \dot{W} + \sum_i (\dot{H}_i - T_0\dot{S}_i) - \sum_o (\dot{H}_o - T_0\dot{S}_o) - T_0\dot{S}_{\text{gen}} \tag{4.5}$$

If we define the CV such that the streams enter and exit at T_0, then H and S are also evaluated at T_0, and the preceding reduces to

$$\dot{W} = \sum_o \dot{G}_o - \sum_i \dot{G}_i + T_0\dot{S}_{\text{gen}} \tag{4.6}$$

where the grouping $H - TS$ is the Gibbs free energy, G.

Equation (4.6) illustrates the fundamental variables involved in desalination system energetic analysis. When $\dot{S}_{\text{gen}} = 0$, the system is *reversible*, and $\dot{W}$ becomes $\dot{W}_{\text{rev}}$, the reversible work associated with the streams changing from their inlet to their outlet states:

$$\dot{W}_{\text{rev}} = \sum_o \dot{G}_o - \sum_i \dot{G}_i \tag{4.7}$$

Thus, we see that differences in Gibbs free energy determine a system's reversible limits; consequently $T_0\dot{S}_{\text{gen}}$ is identically equal to the energy required to overcome the losses that produce $\dot{S}_{\text{gen}}$.

In cases where the outlet streams have different temperatures than the inlet stream, a control volume analysis will not isolate Gibbs energy in the same way, and the reversible work would differ because would it be possible to extract additional work from the differences in temperature relative to T_0. In those situations, exergy is discarded with the leaving streams (see discussion in Sec. 4.4.1). Some cases of this type are analyzed in Sec. 4.5. A formulation using flow exergy (Sec. 4.3) would also account for these differences in outlet state.

The two groupings in Eq. 4.6, ΔG and $T_0\dot{S}_{\text{gen}}$, are the building blocks for thermodynamic analysis of desalination systems: G determines the limits, and precise identification of $\dot{S}_{\text{gen}}$ guides avenues for improvement. In addition, as we will see shortly, when G is known for a substance as a function of temperature and pressure, it contains all of the necessary information to compute efficiency, including $T_0\dot{S}_{\text{gen}}$.

4.2.2 Thermodynamic Properties of Mixtures

As discussed in Sec. 4.2.1, G serves two useful purposes in our analyses. First, the property itself defines the reversible work associated with any change in state. Second, because its conjugate variables are temperature and pressure, which are measurable

Table 4.1: Relationships between $G = f(T, p, N_i)$ and several thermodynamic variables

Property	Expression
Entropy	$S = -\left(\frac{\partial G}{\partial T}\right)_{p,N_i}$
Molar Volume	$\overline{v} = \frac{1}{N}\left(\frac{\partial G}{\partial p}\right)_{T,N_i}$
Enthalpy	$H = G - T\left(\frac{\partial G}{\partial T}\right)_{p,N_i} = -T^2\left(\frac{\partial (G/T)}{\partial T}\right)_{p,N_i}$
Heat Capacity	$C_p = -T\left(\frac{\partial^2 G}{\partial T^2}\right)_{p,N_i}$
Chemical Potential	$\mu_i = \left(\frac{\partial G}{\partial N_i}\right)_{T,p}$

and controllable thermodynamic variables, it provides a convenient basis with which to correlate substance behavior. A model describing G for aqueous solutions (*e.g.*, seawater) is thus essential.

Gibbs Energy as a Fundamental Thermodynamic Function

Once a thermodynamic state is fixed, any thermodynamic property *at that state* can be computed as a function of any other complete set of independent properties *at that state*. However, there are specific independent variables, called conjugate variables, that when used to formulate a property, yield all thermodynamic properties of the substance at *any state*.

The conjugate variables for G are temperature, T, pressure, p, and number of moles of species i, N_i (equivalently mole fraction, molality, or other measures of concentration). This can be shown as follows. With the definition of $G = H - TS = U + pV - TS$,

$$dG = dU + p\,dV + V\,dp - T\,dS - S\,dT \tag{4.8}$$

By the fundamental relationship of thermodynamics, $dU = T\,dS - p\,dV + \sum_i \mu_i\,dN_i$, and so

$$dG = -S\,dT + V\,dp + \sum_i \mu_i\,dN_i \tag{4.9}$$

Thus, knowledge of $G = f(T, p, N_i)$ allows one to compute all thermodynamic properties of the substance, as shown for several properties by the relationships in Table 4.1. With these properties, the actual energy consumption, the losses, and the energy required to overcome the losses, $T_0\dot{S}_{\text{gen}}$, can be computed [see Eqs. (4.3) and (4.4)].

Standard Formulations for Gibbs Energy and the Chemical Potential

By definition, any extensive mixture property X can be written as the weighted sum of partial molar properties over each species i:

$$X = \sum_i \left(\frac{\partial X}{\partial N_i}\right)_{T,p,N_{j\neq i}} N_i \tag{4.10}$$

where the partial molar property, $\partial X/\partial N_i$, physically represents the change in mixture X with an incremental addition of species i. Thus, the Gibbs free energy of the solution can be written as

$$G = \sum_i \left(\frac{\partial G}{\partial N_i}\right)_{T,p,N_{j\neq i}} N_i \tag{4.11}$$

But since T and p are the conjugate variables of G [see Eq. (4.9)], the chemical potential μ_i *is* the partial molar Gibbs free energy, $\left(\frac{\partial G}{\partial N_i}\right)_{T,p,N_{j\neq i}}$.

The chemical potential may be written as

$$\mu_i \equiv \left(\frac{\partial G}{\partial N_i}\right)_{T,p,N_{j\neq i}} = \mu_i^\circ + \bar{R}T \ln a_i \tag{4.12}$$

where the superscript $\circ$ denotes the standard (or reference) state, $\bar{R}$ is the molar (universal) gas constant, T is the absolute temperature in kelvin, and a_i is the activity of species i in the solution. For solutes, the reference state is usually a hypothetical solution of infinite dilution and unit concentration (*i.e.*, 1 mol/L or 1 mol/kg, etc.) at the same temperature. For solvents (water), the reference state is typically the pure liquid at the same temperature. Depending on the convention, the reference pressure may or may not be fixed at 1 atm [1, 2].

Chemical activity is often termed a "thermodynamic concentration", and is related to the change in energy of a component as it is added to a mixture, *i.e.*, as its concentration changes. For solutes, it is modeled as the product of the activity coefficient, γ, and a measure of concentration, giving several possible formulations:

$$a_{x,i} = \gamma_{x,i} x_i, \qquad a_{b,i} = \gamma_{b,i} b_i / b^\circ, \qquad a_{c,i} = \gamma_{c,i} c_i / c^\circ \tag{4.13}$$

where x_i is mole fraction, b_i is molality, and c_i is molar concentration (moles per unit volume) of species i. The reference quantities c° and b° usually have a magnitude of unity and thus often not written explicitly.

In the ideal solution model, the first building block in mixture thermodynamics, the rational activity coefficient $\gamma_x = 1$. Physically, in an ideal solution, the introduction of a solute causes little change in the average interaction potential between all species. This can approximate real solution behavior when, *e.g.*, the solution is very dilute[1] and solvent–solvent interactions are negligibly small. The model can also be suitable for mixtures of two chemically similar components. For a mixture of toluene and

[1] In dilute systems, the difference between γ_x, γ_b, and γ_c is generally quite small, so in the ideal solution model, all activity coefficients are commonly taken as unity. Formulas for converting from one activity coefficient scale to another are straightforward to use and can be found in [3].

benzene, *e.g.*, benzene–benzene interactions are like those of benzene–toluene and toluene–toluene [4]. The activity coefficient γ thus represents departures from ideal solution behavior, and is the lynchpin in computing G for electrolyte solutions.

For water, the solvent, deviations from ideality are often expressed as an osmotic coefficient, the form of which is also dependent on the concentration scale:

$$\phi_x = -\frac{\mu_w^\circ - \mu_w}{\bar{R}T \ln x_w} \tag{4.14a}$$

$$\phi_b = \frac{\mu_w^\circ - \mu_w}{\bar{R}TM_w \sum_i b_i} \tag{4.14b}$$

The water activity is related to the osmotic coefficient by the relation $\mu_w - \mu_w^\circ = \bar{R}T \ln a_w$. For an ideal solution, $\phi_x = \phi_b = 1$.

The water activity, a_w, is not independent of the solute activities, and it is usually calculated from solute activity using the Gibbs-Duhem relationship. The latter is found by equating Eq. (4.9) and the differential form of Eq. (4.11), $dG = \sum_i d(\mu_i N_i)$:

$$\sum_i N_i \, d\mu_i = -S \, dT + V \, dP \tag{4.15}$$

All models for activity must satisfy this relationship. At constant temperature and pressure, Eq. (4.15) can be restated on a mole fraction basis by dividing through by N:

$$\sum_i x_i d\mu_i = 0 \tag{4.16}$$

This equation can be manipulated to find the solvent activity, a_w as

$$d \ln a_w = -\frac{1}{x_w} \sum_{i \neq w} \frac{d(\gamma_i x_i)}{\gamma_i} \tag{4.17}$$

Analogous expressions can be found for the other concentration scales.

Ideal Solutions and Deviations from Ideality as Functions of Activity

A common modeling approach for the activity coefficient is to model the energetic contributions that lead to deviations from ideality—the excess Gibbs free energy—and then differentiate to compute an activity coefficient. Because of the relationships between $G = f(T, p, N_i)$ and the suite of thermodynamic properties, such models are also related to deviations from ideality for all other thermodynamic properties: the excess enthalpy, excess entropy, excess volume, etc. These relationships are discussed briefly later.

The Gibbs free energy can be written as the sum of ideal and excess components

$$G = G^{\text{id}} + G^{\text{ex}} \tag{4.18}$$

Based on the definition of chemical potential (Eq. (4.12)) and the osmotic coefficient (Eq. (4.14b)), and the condition for ideality, G^{id} can be written on a mole fraction or

molal concentration scale, respectively as:

$$\frac{G^{\mathrm{id}}}{N} = \sum_i \left(\mu^\circ_{x,i} + \bar{R}T \ln x_i\right) x_i \tag{4.19a}$$

$$\frac{G^{\mathrm{id}}}{m_w} = \left(\mu^\circ_w - \bar{R}TM_w \sum_{j\in\text{solutes}} b_j\right) b_w + \sum_{j\in\text{solutes}} \left(\mu^\circ_{b,j} + \bar{R}T \ln b_j\right) b_j \tag{4.19b}$$

The excess component is similarly written on any of the concentration scales, and yields the following expressions for the activity coefficient:

$$\ln \gamma_{x,i} = \frac{\partial(G^{\mathrm{ex}}/\bar{R}T)}{\partial N_i}, \qquad \ln \gamma_{b,i} = \frac{\partial(G^{\mathrm{ex}}/m_w\bar{R}T)}{\partial b_i} \tag{4.20}$$

Combining this ideal–excess breakdown with the relationships shown in Table 4.1, we can find the properties of ideal solutions and formulate deviations as a function of the activities and their pressure and temperature derivatives. We will show the procedure explicitly for entropy and enthalpy; several other properties are shown in Table 4.2.

For an ideal solution, the entropy and enthalpy are:

$$S^{\mathrm{id}} = -\left(\frac{\partial G^{\mathrm{id}}}{\partial T}\right)_{P,x_i} = -\sum_i N_i \left(\left.\frac{\partial \mu^\circ_i}{\partial T}\right|_P + \bar{R}\ln x_i\right) \tag{4.21}$$

$$H^{\mathrm{id}} = \sum_i N_i \left(\mu^\circ_i - T \left.\frac{\partial \mu^\circ_i}{\partial T}\right|_P\right) \tag{4.22}$$

When a solution undergoes an isothermal, isobaric change of state by the addition (or removal) of some species, the corresponding change in entropy and enthalpy are known as the *entropy of mixing* and the *enthalpy of mixing*, respectively. For an ideal solution, we are left with

$$\Delta S^{\mathrm{id}}_{\mathrm{mix}} = -\bar{R}\Delta\left(\sum_i N_i \ln x_i\right) \tag{4.23}$$

$$\Delta H^{\mathrm{id}}_{\mathrm{mix}} = 0 \tag{4.24}$$

Because ideal solutions have zero enthalpy of mixing, the isothermal, isobaric change in Gibbs free energy—the reversible work associated with salt dissolution or desalination (cf. Eq. (4.7))—is identically equal to $T\Delta S^{\mathrm{id}}_{\mathrm{mix}}$:

$$\Delta G^{\mathrm{id}}_{\mathrm{mix}} = \bar{R}T\Delta\left(\sum_i N_i \ln x_i\right) \tag{4.25}$$

All desalination processes must overcome the entropy of mixing.

Table 4.2: Relationships between partial molar excess thermodynamic properties and the activity coefficient

Property	Expression
Partial Molar Excess Entropy	$-\bar{R}\left(T\left.\frac{\partial \ln \gamma_i}{\partial T}\right\|_P + \ln \gamma_i\right)$
Partial Molar Excess Volume	$\bar{R}T\left.\frac{\partial \ln \gamma_i}{\partial P}\right\|_T$
Partial Molar Excess Enthalpy	$-\bar{R}T^2\left.\frac{\partial \ln \gamma_i}{\partial T}\right\|_P$
Partial Molar Excess Heat Capacity	$-\bar{R}T^2\left(\left.\frac{\partial^2 \ln \gamma_i}{\partial T^2}\right\|_P + \frac{2}{T}\left.\frac{\partial \ln \gamma_i}{\partial T}\right\|_P\right)$

Deviations from these ideal approximations are entirely contained within the temperature and pressure dependence of the activity coefficient. The excess entropy is

$$S^{\text{ex}} = -\left(\frac{\partial G^{\text{ex}}}{\partial T}\right)_{P,N_i} = -\sum_i N_i \underbrace{\bar{R}\left(T\left.\frac{\partial \ln \gamma_i}{\partial T}\right|_{P,x_i} + \ln \gamma_i\right)}_{\text{partial molar excess entropy}} \tag{4.26}$$

and the excess enthalpy is

$$H^{\text{ex}} = G^{\text{ex}} - T\left(\frac{\partial G^{\text{ex}}}{\partial T}\right)_{P,N_i} = -\sum_i N_i \underbrace{\left(\bar{R}T^2\left.\frac{\partial \ln \gamma_i}{\partial T}\right|_{P,x_i}\right)}_{\text{partial molar excess enthalpy}} \tag{4.27}$$

Relationships for the other properties are shown in Table 4.2, and mimic those shown in Table 4.1, with G^{ex} replaced by $\mu^{\text{ex}} = \bar{R}T \ln \gamma_i$.

4.2.3 Activity Coefficient Models for Electrolytes

Thus far, we have seen that knowledge of G allows us to predict the limits of desalination system performance; that knowledge of $G = f(T, P, N_i)$ allows us to predict all properties of a solution; and that γ and ϕ reflect departures from ideal solution behavior. In this section, we will review some common models for activity coefficients in aqueous electrolyte solutions: the Debye-Hückel Limiting Law, the Davies Equation, and the Pitzer Model. For a salt MX that dissociates like

$$\mathrm{M}_{\nu_\mathrm{M}}\mathrm{X}_{\nu_\mathrm{X}} \longleftrightarrow \nu_\mathrm{M}\,\mathrm{M}^{z_\mathrm{M}} + \nu_\mathrm{X}\,\mathrm{X}^{z_\mathrm{X}} \tag{4.28}$$

it is typical to report values of a mean activity coefficient, $\gamma_\pm$, which is defined as

$$\gamma_\pm^\nu = \gamma_M^{\nu_M}\gamma_X^{\nu_X} \tag{4.29}$$

where $\nu = \nu_M + \nu_X$. Values of the mean molal activity coefficient $\gamma_{b,\pm}$ for NaCl are shown in Fig. 4.2: as model complexity increases from the Debye-Hückel Limiting Law, the models are more accurate over larger concentration domains.

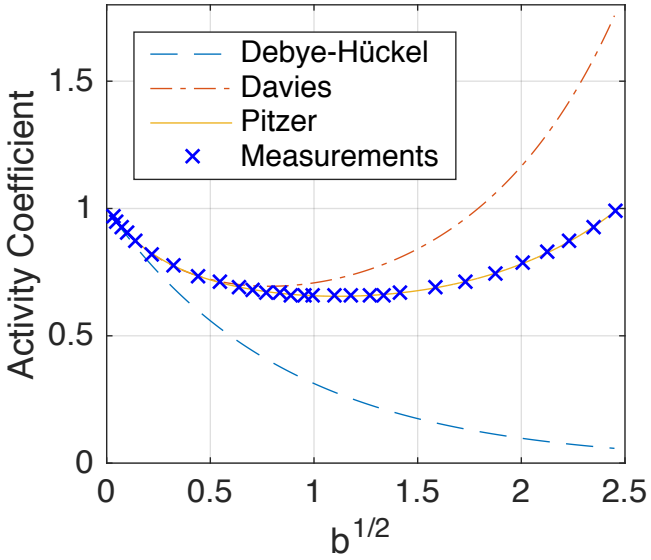

Figure 4.2: A comparison of three models for the activity coefficient of NaCl shows that the simpler Debye-Hückel and Davies models are limited to concentrations below about 0.01 and 0.5 mol/kg, respectively. Measured data is an average over several values in literature provided in [5].

Debye-Hückel Theory For very dilute ionic solutions, the most important addition to mixture energy is that which derives from ionizing the salt as it dissolves, which is reflected in electrostatic interactions between ions. Through a combination of electrostatics and statistical mechanics, Debye-Hückel theory [6] provides an expression for the activity coefficient that is accurate for solutions of ionic strength up to about 0.01 molal. Full derivations can be found in a variety of texts, *e.g.*, [3] and the resulting expression for activity coefficient is

$$\ln \gamma_{x,\pm} = -A\,|z_M z_X|\,\sqrt{I} = -\,|z_M z_X| \left[\frac{e^3\,(2N_A\rho_w)^{1/2}}{8\pi\,(\varepsilon_r\varepsilon_0 k_b T)^{3/2}}\right]\sqrt{I} \tag{4.30}$$

where z_M and z_X are the cation and anion charge numbers, e is the elementary charge, N_A is Avogadro's number, ε_r is the dielectric constant (relative permittivity) of the solvent, ε_0 is the vacuum permittivity, k_B is Boltzmann's constant, ρ_w is the density of pure water, and I is the molal ionic strength. The molal ionic strength is defined as

$$I = \frac{1}{2}\sum_i b_i z_i^2 \tag{4.31}$$

Equation (4.30) is known as the Debye-Hückel Limiting Law, which has a square-root dependence on ionic strength. To first order, most expressions for activity coefficient are characterized by a square-root dependence on ionic strength, reflecting the long-range electrostatic contributions to the excess Gibbs free energy that are the first to appear as solute concentration increases from zero. The temperature dependence of the Debye-Hückel activity coefficient is not quite $T^{-3/2}$ because the dielectric constant is also a function of temperature.

Davies Equation Several other equations exist that extend the Debye-Hückel Limiting Law using mostly empirical or semi-empirical methods, and these can be found in, *e.g.*, [3, 7]. The general approach is to add concentration and/or ionic strength dependent terms to the Debye-Hückel expression to capture the curvature of γ vs. concentration (Fig. 4.2) that arises from the increasing importance of short-range interactions as solute concentration increases further. One particularly useful equation that requires no adjustable parameters for a particular electrolyte is given by Davies [8]:

$$-\log \gamma_{x,\pm} = 0.50|z_M z_X|\left(\frac{\sqrt{I}}{1+\sqrt{I}} - 0.20I\right) \tag{4.32}$$

which is approximate for ionic strengths up to about 0.1 and a temperature of 25° C.

Pitzer Model The Pitzer model [9–12] is based on a virial expansion of the excess Gibbs free energy, and extends the Debye-Hückel model to account for short range interactions between solute pairs and triplets. Detailed derivations are given in references [9, 10, 13]. For calculations beyond the dilute limit, the Pitzer model among those most widely used for single and mixed electrolytes. The model has been validated and used for calculations in several mixed electrolytes, *e.g.*, [7, 14]. Of the three models

discussed in this section, the Pitzer model is the most accurate for seawater and its concentrates.

Expressions are available for the mean molal activity coefficient, but for added flexibility, we will give the single ion expressions here[2]. We also provide an expression for uncharged solutes, which may also exist in mixed-electrolytes or arise as a result of ion-pairing in concentrated mixtures.

The activity coefficient of an individual cation, M, is given by

$$\begin{aligned}\ln \gamma_M = {} & z_M^2 F + \sum_a b_a (2B_{Ma} + ZC_{Ma}) \\ & + \sum_c b_c \left(2\Phi_{Mc} + \sum_a b_a \Psi_{Mca}\right) \\ & + \sum_{a<a'} \sum b_a b_{a'} \Psi_{aa'M} \\ & + |z_M| \sum_c \sum_a b_c b_a C_{ca} + \sum_n b_n (2\lambda_{nM})\end{aligned} \tag{4.33}$$

For an individual anion, X, the expression is analogous:

$$\begin{aligned}\ln \gamma_X = {} & z_X^2 F + \sum_c b_c (2B_{cX} + ZC_{cX}) \\ & + \sum_a b_a \left(2\Phi_{Xa} + \sum_c b_c \Psi_{Xac}\right) \\ & + \sum_{c<c'} \sum b_c b_{c'} \Psi_{cc'X} \\ & + |z_X| \sum_c \sum_a b_c b_a C_{ca} + \sum_n b_n (2\lambda_{nX})\end{aligned} \tag{4.34}$$

The activity coefficient of uncharged species N (*e.g.*, aqueous CO_2) is

$$\ln \gamma_N = \sum_c b_c (2\lambda_{Nc}) + \sum_a b_a (2\lambda_{Na}) \tag{4.35}$$

[2]Of course, as the activity of an individual ion cannot be measured explicitly, the physical meaning of such expressions is unclear. However, as noted by [11], the combination of Eqs. (4.33) and (4.34) in the form of a measurable mean activity coefficient produces the same equation as Pitzer [10], and is far more convenient for calculations in mixed electrolytes.

The molal osmotic coefficient ϕ_b is calculated from the expression

$$\begin{aligned}(\phi-1)\sum_i m_i = 2\Bigg[&\frac{-A^\phi I^{3/2}}{1+1.2\sqrt{I}}\\ &+\sum_c\sum_a b_c b_a (B^\phi_{ca}+ZC_{ca})\\ &+\sum_{c<c'}\sum b_c b_{c'}\left(\Phi^\phi_{cc'}+\sum_a b_a\Psi_{cc'a}\right)\\ &+\sum_{a<a'}\sum b_a b_{a'}\left(\Phi^\phi_{aa'}+\sum_c b_c\Psi_{aa'c}\right)\\ &+\sum_n\sum_a b_n b_a\lambda_{na}+\sum_n\sum_c b_n b_c\lambda_{nc}\Bigg]\end{aligned} \tag{4.36}$$

in which $Z=\sum_i |z_i| m_i$, M_w is the molar mass of water, and the remainder are functions quantifying particular solute interactions, as defined below. Subscript c denotes cations other than M, a denotes anions other than X, and n denotes uncharged (neutral) solutes. Summation over all i indicates a sum over all solutes; likewise summation over all c, a, and n denotes a sum over all cations, anions, and neutral solutes, respectively. The summation notations $c<c'$ and $a<a'$ indicate that the sum should be performed over all distinguishable cation pairs and anion pairs, respectively. Equations for A^ϕ, B_{ij}, B^ϕ_{ij}, F, Φ_{ij}, and Φ^ϕ_{ij} are given in Appendix 4.B.

4.2.4 Colligative Properties: Boiling Point Elevation, Freezing Point Depression, Vapor Pressure Lowering and Osmotic Pressure

Mixture properties that depend on the total mole numbers of dissolved substances, but not the specific chemical species dissolved in a solvent, are called colligative properties. Colligative properties are truly independent of the chemical species dissolved only when the solution is very dilute, so that the solution behaves as an ideal mixture. They must be corrected to some degree at higher concentrations, typically through the osmotic coefficient.

Four colligative properties of great importance in desalination system analysis relate to chemical equilibrium between two phases or two different mixture concentrations: the boiling point elevation, δ_b; the freezing point depression, δ_f; the osmotic pressure, π; and the vapor pressure lowering, Δp_{sat}. In osmotically driven processes, such as reverse osmosis (RO) and forward osmosis (FO), the flux of pure water across the membrane is a function of π. Likewise, in thermal systems, such as multistage flash (MSF), multi-effect distillation (MED), and mechanical vapor compression (MVC), the evaporative flux is a function of δ_b; and in freeze desalination, the ice formation rate is a function of δ_f. In membrane distillation (MD), the flux of water vapor across the membrane is a function of Δp_{sat}. Accurate values of δ_b, δ_f, π, and Δp_{sat} are thus needed for a wide range of salinities and temperatures.

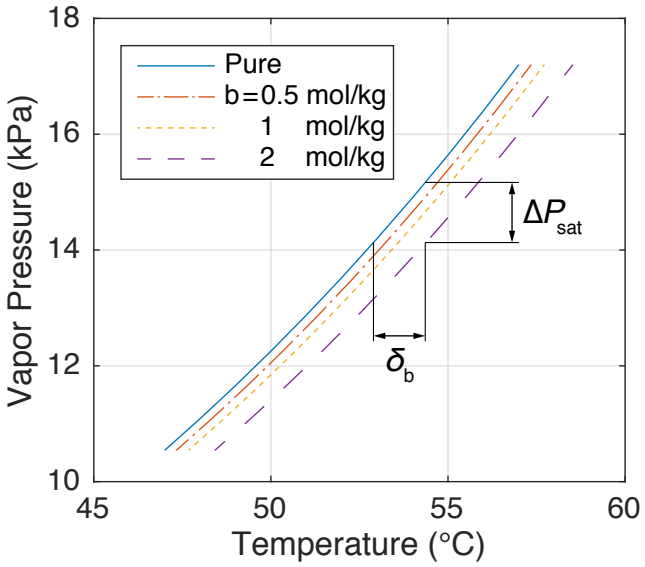

Figure 4.3: The vapor pressure curve for sodium chloride solutions: the boiling point elevation (δ_b) and the vapor pressure lowering (Δp_{sat}) increase with increasing salt concentration (b). The curves are computed from Eq. (4.43) using the equations of Pitzer [2] and Saul and Wagner [15].

Boiling point elevation

Adding salt to water increases its boiling temperature at a given pressure. The boiling point elevation, δ_b, is the difference between the saturation temperatures of a solution, T_{sat}, and of its pure solvent, T°_{sat} at a fixed pressure (Fig. 4.3). It tends to be an increasing function of salt concentration and vapor pressure (equivalently, solvent saturation temperature). As with all of the colligative properties, it is related to the activity of the solvent (water), and can thus be written as a function of ϕ_b:

$$\delta_b = T_{\text{sat}} - T^\circ_{\text{sat}} = \frac{\bar{R} T^{\circ 2}_{\text{sat}}}{h^\circ_{fg}} \phi_b \sum_i b_i \tag{4.37}$$

where $\bar{R}$ is the molar gas constant, and h°_{fg} is enthalpy of vaporization of pure water[3]. For low salinities, ϕ_b is close to one (see Fig. 4.4), and so δ_b has a nearly linear dependence on salinity. A good approximation for the boiling point elevation is therefore given by the linear equation

$$\delta_b = K_b b \tag{4.38}$$

where b is the total molality of the solute ions in moles/kg-solvent, the ebullioscopic constant K_b is defined as

$$K_b = \frac{\bar{R} T^{\circ 2}_{\text{sat}}}{h^\circ_{fg}} \tag{4.39}$$

and T°_{sat} is in kelvin. For water at 1 atm, $K_b = 0.513$ K-kg/mol.

Freezing point depression

The boiling point elevation's analog at the solid–liquid phase boundary is the freezing point depression, δ_f. The freezing point depression is the difference between the freezing temperatures of a solution, T_f, and of its pure solvent, T°_f. A mirror of δ_b, δ_f increases with increasing salt concentration, and can be written similarly[3]:

$$\delta_f = T^\circ_f - T_f = \frac{\bar{R} T^{\circ 2}_f}{h^\circ_{sf}} \phi_b \sum_i b_i \tag{4.40}$$

where h°_{sf} is enthalpy of fusion of pure water. Like the boiling point elevation, we can define a linear relationship for the freezing depression at low salinities, where ϕ_b is near unity:

$$\delta_f = K_f b \tag{4.41}$$

The prefactor K_f is known as the cryoscopic constant:

$$K_f = \frac{\bar{R} T^{\circ 2}_f}{h^\circ_{sf}} \tag{4.42}$$

[3] Eq. (4.37) is valid when $\delta_b \ll T^\circ_{\text{sat}}$ and h°_{fg} does not change significantly between T_{sat} and T°_{sat}, which is true for seawater at typical thermal desalination operating conditions. Likewise, Eq. (4.40) is valid when $\delta_f \ll T^\circ_f$ and h°_{sf} does not change significantly between T_f and T°_f.

Like the ebullioscopic constant, T_f° is an absolute temperature (i.e., in K). For water at 1 atm, $K_f = 1.86$ K-kg/mol.

Vapor pressure lowering

The boiling point elevation is considered at a fixed pressure. The equivalent effect at a fixed temperature is the vapor pressure lowering, Δp_{sat} (Fig. 4.3). A solution maintained at fixed temperature will require a greater vacuum for solvent to evaporate. The vapor pressure of water in solution is related to the activity of water[4] by

$$\ln\left(\frac{p_{\text{sat}}}{p_{\text{sat}}^\circ}\right) = \ln a_w \tag{4.43}$$

The vapor pressure lowering is the difference between the vapor pressures of the solution, p_{sat}, and of the pure solvent, p_{sat}°, at fixed temperature. In terms of the osmotic coefficient, the vapor pressure lowering is thus

$$\ln\left(\frac{\Delta p_{\text{sat}}}{p_{\text{sat}}^\circ} + 1\right) = -\phi_b M_w \sum_i b_i \tag{4.44}$$

where M_w is the molar mass of the solvent. For sufficiently dilute solutions, where ϕ_b is near one, Eq. (4.44) reduces to Raoult's Law for the vapor pressure of the solvent:

$$p_{\text{sat}} = p_{\text{sat}}^\circ x_w = \frac{p_{\text{sat}}^\circ}{1 + M_w \sum_i b_i} \tag{4.45}$$

Osmotic pressure

The osmotic pressure represents the pressure that must be applied to a solution to maintain equilibrium with the pure solvent at a fixed temperature. Osmotic pressure rises as the solute concentration increases, and it is proportional to the absolute temperature. For a non-ideal electrolyte solution such as seawater, the osmotic coefficient characterizes the deviation from ideal solution behavior. The osmotic pressure for a solution composed of multiple solutes may be expressed in terms of the molality of solutes as [3]:

$$\pi = -\frac{\rho_w}{M_w}\bar{R}T \ln a_w = \phi_b \bar{R} T \rho_w b \tag{4.46}$$

where π is the osmotic pressure; ϕ_b is the molal osmotic coefficient [Eq. (4.14b)]; $\bar{R}$ is the molar gas constant; T is the absolute temperature in kelvin; ρ_w is the density of the solvent, in this case pure water; M_w is the molar mass of the solvent; and b is the

[4] Equation (4.43) is valid when the fugacity coefficients and the Poynting correction factor are near unity; that is, when the vapor behaves ideally and the pressure is not too high. For a 2 mol/kg NaCl solution at 80 °C, Eq. (4.43) overpredicts the vapor pressure by less than 0.001% relative to the general expression for vapor-liquid equilibrium that includes fugacity coefficients and the Poynting correction factor; see [1] for details.

total molality of the solute ions in moles/kg-solvent[5]. The total molality of the ions in seawater can be written as a function of the salinity as:

$$b = 31.843 \frac{w_s}{1 - w_s} \tag{4.47}$$

where w_s is the salt mass fraction of the solution in kg-salt/kg-solution, and 31.843 is a constant which takes into account the weighted average of the molecular weight of each dissolved solute of the seawater constituents which have the same relative composition at any salt concentration.

The osmotic coefficient is a function of salinity and temperature (see Section 4.A.5). Using a piecewise fit for the osmotic coefficient function [i.e., Eq. (4.A.11) and (4.A.13)], the osmotic pressure of seawater can be calculated from Eq. (4.46) for a range of salinity of 0–120 g/kg and a range of temperature of 0–200 °C.

In the literature, a linearized expression for the osmotic pressure modeled on the van 't Hoff equation is widely used for quick calculation of the seawater osmotic pressure. The van 't Hoff equation itself applies to very dilute (or ideal) solutions ($\phi_b = 1$):

$$\pi = i\bar{R}Tc \tag{4.48}$$

where i is the van 't Hoff factor (accounting for dissociation of the solute), and c is the molarity of the solution (mol/L). We can define a modified van 't Hoff coefficient to make a linear approximation to the osmotic pressure function, Eqs. (4.46) and (4.47), as follows:

$$\pi = Cw_s \tag{4.49}$$

The modified van 't Hoff coefficient, C, is determined to be 73.45 kPa-kg/g for seawater at 25 °C. The linear model represented by Eq. (4.49) can be used for a salinity range of 0 to 70 g/kg, which is a typical range for many desalination applications. For this range, the maximum deviation from the nonlinear osmotic pressure function, Eq. (4.46), is 6.8%. The osmotic pressure, Eq. (4.46), the osmotic coefficient, Eqs. (4.A.11) and (4.A.12), and the linear osmotic pressure, Eq. (4.49), are shown as a function of salinity in Fig. 4.4.

4.3 Exergy Analysis

Exergy is the maximum amount of work obtainable when a thermodynamic system is brought into equilibrium from its initial state to the environmental (dead) state. In this regard, the state of the environment must be specified. The system is considered to be at zero exergy when it reaches the environment state, which is called the dead state. The equilibrium can be divided into thermal, mechanical and chemical equilibrium. These equilibria are achieved when the temperature (T), pressure (p) and concentration

[5]Eq. (4.46) is valid when water can be modeled as an incompressible fluid and when μ_w° is pressure dependent (see Sec. 4.2.2). Strictly, therefore, a_w should be evaluated at the reference pressure plus π, but evaluating it at 1 bar only leads to small errors up to moderately high pressures (*e.g.*, for a 4 mol/kg NaCl solution at 25 °C, ln a_w at 200 bar is 0.8% higher than at 1 bar). Glasstone [1] provides an alternative formulation of osmotic pressure for a pressure-independent reference state.

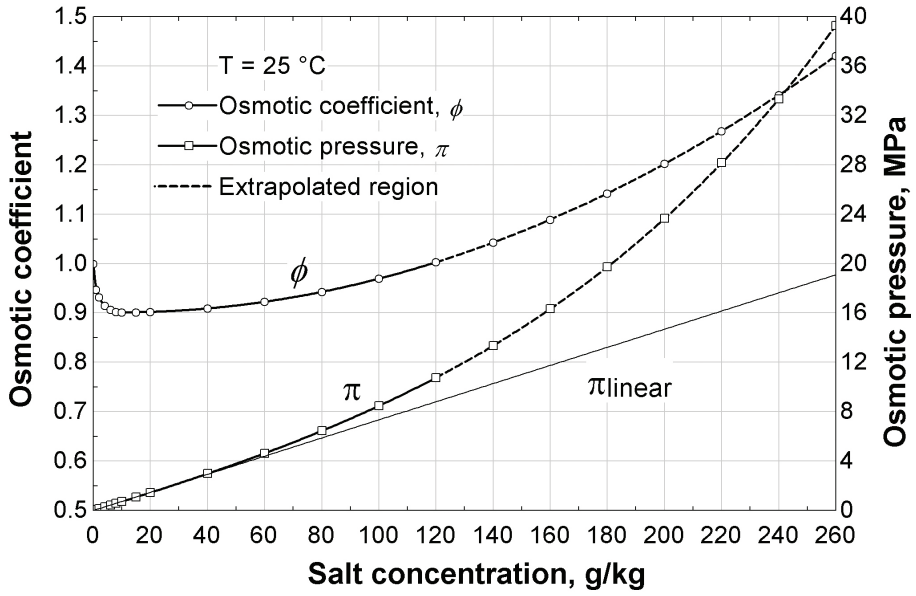

Figure 4.4: Seawater molal osmotic coefficient and osmotic pressures versus salinity for a fixed temperature shown on the left- and right-hand axes. The osmotic coefficient curve and nonlinear osmotic pressure curves are extrapolated for salinities greater than 120 g/kg and these sections are shown as bold dashed lines. The linear osmotic pressure curve is solid.

(w) of the system reach the values found in the surrounding environment (T_0, p_0, and w_0, respectively). Therefore, exergy consists of a thermomechanical exergy and a chemical exergy. The thermomechanical exergy is the maximum work obtained when the temperature and pressure of the system changes to the environment temperature and pressure (T_0, p_0) with no change in the concentration. In this case, we say that thermomechanical equilibrium with the environment occurs. The chemical exergy is the maximum work obtained when the concentration of each substance in the system changes to its concentration in the environment at the environment pressure and temperature (T_0, p_0). In that case, chemical equilibrium occurs.

For a control mass (closed system), the exergy, e, can be mathematically expressed as [16, 17]

$$e = (u - u^*) + p_0\ (v - v^*) - T_0\ (s - s^*) + \sum_{i=1}^{n} w_i \left(\mu_i^* - \mu_{i,0}\right) / M_i \tag{4.50}$$

where u, s, v, μ_i, w_i, and M_i are the specific internal energy, specific volume, specific entropy, chemical potential of species i, mass fraction of of species i, and molar mass of species i, respectively. Properties with superscript * in the above equation are determined at the temperature and pressure of the environment (T_0, p_0) but at the same composition or concentration of the initial state. This is referred to as the restricted dead state, in which only the temperature and pressure are changed to the environmental values. However, the properties with subscript $_0$ in the above equation (*i.e.*, $\mu_{i,0}$) are determined at the temperature, pressure and concentration of the environment (T_0, P_0, w_0), which is called the global dead state.

For a control volume (open system), the flow exergy, e_f, can be calculated by adding the flow work to the exergy in Eq. (4.50) which mathematically can be expressed as [16, 17],

$$e_f = e + v\,(p - p_0) \tag{4.51}$$

Knowing that $h = u + pv$, and eliminating e in Eq. (4.51) using Eq. (4.50), the flow exergy can be rewritten as

$$e_f = (h - h^*) - T_0\ (s - s^*) + \sum_{i=1}^{n} w_i \left(\mu_i^* - \mu_{i,0}\right) / M_i \tag{4.52}$$

If the system and the environment are both the same pure substance (*e.g.*, pure water), the chemical exergy, which is the last term in Eqs. (4.50) and (4.52), will vanish. However, for a multi-component system (*e.g.*, seawater, exhaust gases) the chemical exergy must be considered. Ignoring it may lead to unrealistic and illogical results for the exergy variation with the concentration.

The following section discusses the variation of exergy and flow exergy with temperature, pressure, and composition. In particular, we show that the [control mass] exergy is never negative, whereas the [control volume] flow exergy can be negative if the system pressure is less than the dead state pressure. Changes in temperature or composition relative to the dead state values create the potential to do work by transferring heat or mass between the system and the environment, leading to positive exergy values in all cases.

4.3.1 Exergy Variation

The exergy of a control mass system, given by Eq. (4.50), and the exergy of a control volume system, which is the flow exergy given by Eq. (4.52), are intensive thermodynamic properties which represent the maximum obtainable work per unit mass of the system. They are functions of the initial state as well as the environment state. However, if the environmental state is specified (T_0, p_0, w_0), the exergy is a function only of the system initial state (T, p, w).

In this section we examine how the exergy (for a control mass system) and the flow exergy (for a control volume system) change with the temperature, pressure, and mass concentration of the initial state with respect to the environmental dead state, assuming the environmental dead state is at $T = T_0$, $p = p_0$ and $w = w_0$, and assuming an ideal gas mixture that satisfies the ideal gas relation ($pv = RT$) and which has equivalent mixture properties R, c_p, and c_v (ideal gas constant $R = \bar{R}/M$, where M is the mixture average molar mass; specific heat at constant pressure; and specific heat at constant volume, respectively).

Case 1: $p = p_0$, $w = w_0$ **but** $T \neq T_0$. In this case, the chemical exergy, which is the last term in Eq. (4.50), vanishes and the exergy can be written for an ideal gas mixture as:

$$e = c_v\,(T - T_0) + p_0\left(\frac{RT}{p} - \frac{RT_0}{p_0}\right) - T_0\left[c_p \ln\left(\frac{T}{T_0}\right) - R\ln\left(\frac{p}{p_0}\right)\right] \tag{4.53}$$

For $p = p_0$

$$e = c_v\,(T - T_0) + R\,(T - T_0) - T_0 c_p \ln\left(\frac{T}{T_0}\right) \tag{4.54}$$

Using $c_p = c_v + R$, the exergy will be

$$e = c_p T_0\left[\frac{T}{T_0} - \ln\left(\frac{T}{T_0}\right) - 1\right] \tag{4.55}$$

Equation (4.55), considered for the case when the pressure and concentration are equal to the dead state, shows that the exergy is always positive at any temperature other than the dead state temperature (see Fig. 4.5). If the system has a temperature equal to the dead state ($T/T_0 = 1$), the exergy is zero. The positive exergy is due to the heat that can be transferred between the system temperature and the dead state temperature, in one direction or the other as appropriate, to operate a heat engine cycle that can produce work. The same result, Eq. (4.55), can be obtained for a control volume system using the flow exergy equation, Eq. (4.52). Therefore, as long as $p = p_0$, $w = w_0$, any temperature difference between the system state and the dead state will result in positive exergy and positive flow exergy.

Case 2: $T = T_0$, $w = w_0$ **but** $p \neq p_0$. In this case, the chemical exergy again vanishes, and the exergy of a control mass is again given by Eq. (4.53). For $T = T_0$, the exergy will be

$$e = RT_0\left[\frac{p_0}{p} + \ln\left(\frac{p}{p_0}\right) - 1\right] \tag{4.56}$$

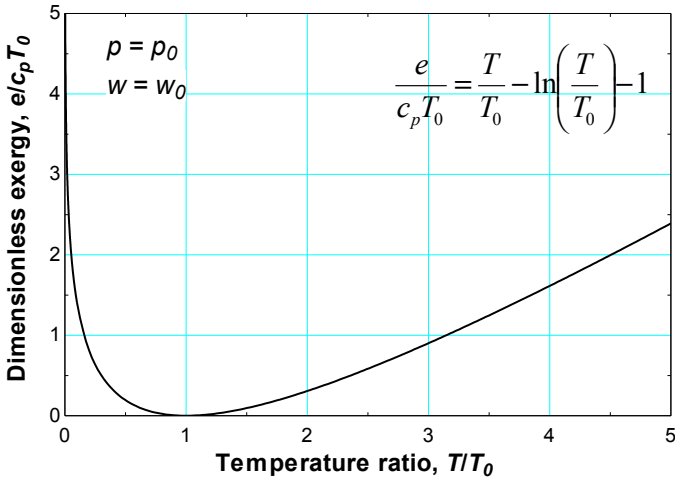

Figure 4.5: Dimensionless exergy as a function of temperature ratio

Equation (4.56) for the case when the temperature and concentration are equal to the dead state, shows that the exergy of the control mass systemâ is always positive at any pressure other than the dead state pressure (see Fig. 4.6). If the system has a pressure equal to the dead state pressure ($p/p_0 = 1$), the exergy is zero. The positive exergy is due to the mechanical work that can be obtained by expansion (if $p > p_0$) or compression (if $p < p_0$) of the system to reach the environment pressure.

For temperatures different from the dead state ($T \neq T_0$), one may show that the minimum of Eq. (4.53) with respect to pressure occurs for $p/p_0 = T/T_0$ and that the value at the minimum is positive. Thus, the control mass system has positive or zero exergy for any temperature and pressure when $w = w_0$.

For a control volume (open system), however, the signs on exergy can behave differently. The flow exergy, given by Eq. (4.52), can be written for an ideal gas mixture (with $w = w_0$) as

$$e_f = c_p\,(T - T_0) - T_0\left[c_p \ln\left(\frac{T}{T_0}\right) - R\ln\left(\frac{p}{p_0}\right)\right] \tag{4.57}$$

For $T = T_0$ the flow exergy will be

$$e_f = RT_0 \ln\left(\frac{p}{p_0}\right) \tag{4.58}$$

It is clear from Eq. (4.58) that the flow exergy of a control volume system may be positive or negative depending on the pressure of the system. If the pressure of the control volume system is higher than the dead state pressure (*i.e.*, $p > p_0$), a flow stream can be expanded reversibly (*e.g.*, using a turbine) to the environment pressure and produce work resulting in a positive flow exergy. However, if the pressure is lower than the dead state pressure (*i.e.*, $p < p_0$), an external work should be applied

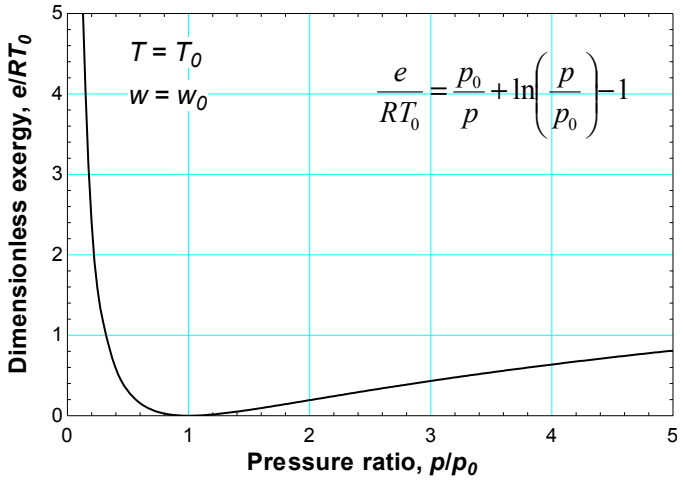

Figure 4.6: Dimensionless exergy of a control mass system as a function of pressure ratio

to compress the flow stream (*e.g.*, using a compressor) to the environment pressure resulting in a negative flow exergy (see Fig. 4.7). Therefore, the exergy of the control mass is positive at any pressure other than the dead state pressure; however the exergy of the control volume (flow exergy) can be negative at pressures lower than the dead state pressure.

Case 3: $T = T_0, p = p_0$ **but** $w \neq w_0$. In this case, when $T = T_0$ and $p = p_0$, the first two terms in the exergy equation, Eq. (4.50), and flow exergy equation, Eq. (4.52), vanish. The only remaining term is the last term which is the chemical exergy. The exergy or flow exergy in this case can be written as follows

$$e = e_f = \sum_{i=1}^{n} w_i \left(\mu_i^* - \mu_{i,0}\right) / M_i \tag{4.59}$$

For an ideal mixture model, the chemical potential differences are given, using Eqs. (4.12) and (4.13) with $\gamma_{x,i} = 1$, as

$$\mu_i - \mu_i^\circ = \bar{R}T \ln\left(x_i\right) \tag{4.60}$$

where x_i is the mole fraction, μ_i° is evaluated at a hypothetical standard state for the component i, and it is not equal to $\mu_{i,0}$. Therefore, the chemical potential differences in Eq. (4.59) can be written as

$$\mu_i^* - \mu_{i,0} = \left(\mu_i^* - \mu_i^\circ\right) - \left(\mu_{i,0} - \mu_i^\circ\right) = \bar{R}T \ln\left(\frac{x_i}{x_{i,0}}\right) \tag{4.61}$$

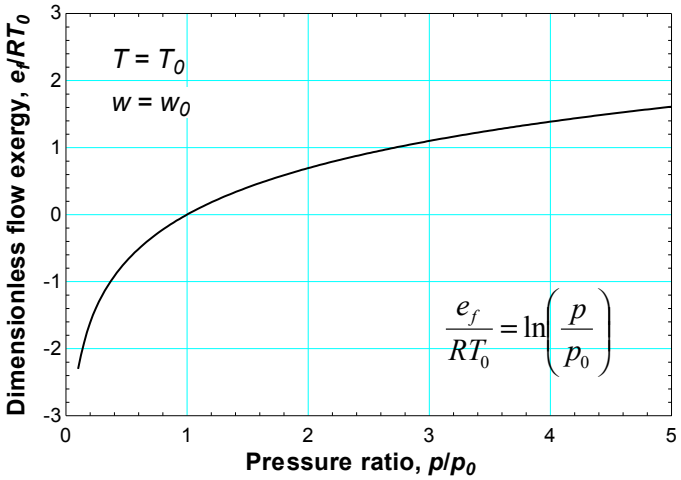

Figure 4.7: Dimensionless flow exergy as a function of pressure ratio

Substituting equation (4.61) into Eq. (4.59) yields, with $R_i = \bar{R}/M_i$,

$$e = e_f = \sum_{i=1}^{n} w_i R_i T \ln\left(\frac{x_i}{x_{i,0}}\right) \tag{4.62}$$

Assuming for simplicity that the mixture consists of two substances (1 and 2) and using $T = T_0$ yields,

$$e = e_f = w_1 R_1 T_0 \ln\left(\frac{x_1}{x_{1,0}}\right) + w_2 R_2 T_0 \ln\left(\frac{x_2}{x_{2,0}}\right) \tag{4.63}$$

We may eliminate w_i in favor of x_i using the following two relationships

$$w_1 R_1 = x_1 R \tag{4.64a}$$

$$w_2 R_2 = x_2 R \tag{4.64b}$$

where R is the gas constant for the mixture. We also know that

$$x_1 = 1 - x_2 \tag{4.65a}$$

$$x_{1,0} = 1 - x_{2,0} \tag{4.65b}$$

Substituting equations (4.64a)–(4.65b) into Eq. (4.63) and dropping the subscript 2 yields

$$e = e_f = RT_0 \left[(1-x)\ln\left(\frac{1-x}{1-x_0}\right) + x\ln\left(\frac{x}{x_0}\right)\right] \tag{4.66}$$

Now, we can prove mathematically that Eq. (4.66) is always positive at any mole fraction other than x_0 by taking the first derivative with respect to x:

$$\frac{\partial e}{\partial x} = RT_0 \left[\ln\left(\frac{x}{x_0}\right) - \ln\left(\frac{1-x}{1-x_0}\right)\right] \tag{4.67}$$

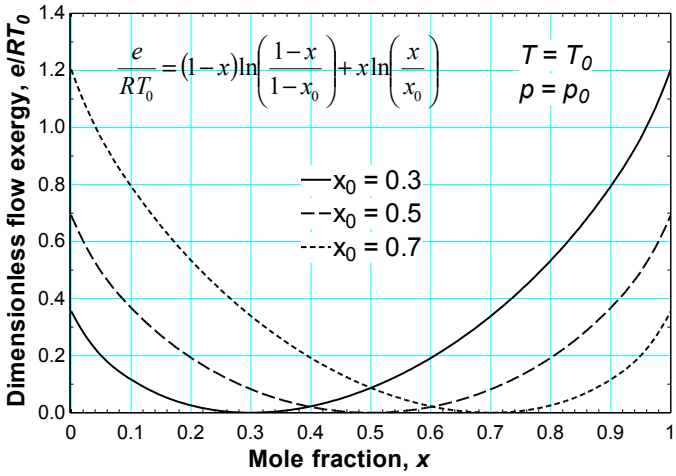

Figure 4.8: Dimensionless flow exergy as a function of concentration

From Eq. (4.66), at $x = x_0$ the exergy (and flow exergy) is zero. From Eq. (4.67) at $x < x_0$ the first derivative (slope) is negative, meaning that the exergy is decreasing. And at $x > x_0$ the first derivative (slope) is positive, meaning that the exergy is increasing. Thus, the point $x = x_0$ is a minimum.

The variation of exergy (or flow exergy) with mole fraction is shown in Fig. 4.8, in which exergy is always positive, except for a value of zero at the dead state concentration. The positive value of exergy arises from the potential for a mass transfer process, which can be used to produce work by transferring a solute between the high or low concentration of the system and the concentration of the environmental dead state. Because the chemical exergy is additive in both Eqs. (4.50) and (4.52), the same behavior will clearly occur for any selected dead state.

We have shown mathematically that, for an ideal mixture gas, the exergy of the control mass system is always positive at any temperature, pressure, and mass concentration other than the dead state, while the exergy of a control volume system (the flow exergy) may have negative values if the pressure of the system is lower than the dead state pressure. The same conclusion can be obtained for real systems using actual thermodynamic data. In the following section, the exergy and flow exergy of seawater are calculated to demonstrate the various trends.

4.3.2 Seawater Exergy

The correlations given in the Appendix for the thermodynamic properties of seawater are used to calculate the flow exergy of seawater. In this regard, the (environment) dead state should be specified[6]. In seawater desalination systems, the intake seawater condition of the desalination plant is usually taken as the environment dead state

[6]However, it is important to mention that the choice of the dead state does not affect the exergy difference between any two states.

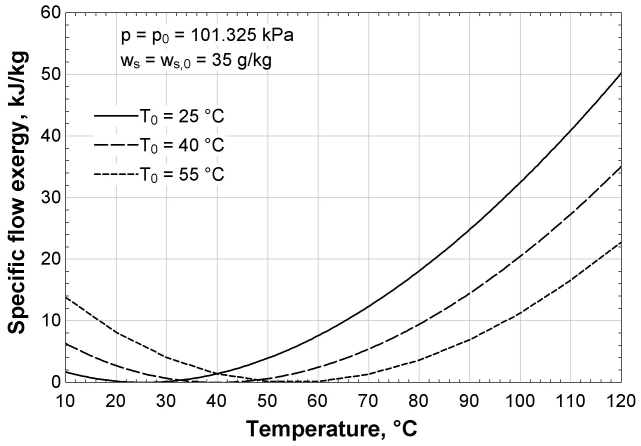

Figure 4.9: Specific flow exergy of seawater as a function of temperature

condition. This condition varies from place to place depending on the geographical location of the desalination plant (ambient temperature, altitude, salinity of the seawater source). In addition, the pressure of the intake seawater depends on the depth of the intake system which varies from 5–50 m. Therefore, the dead state pressure may change from 1 to 5 atmospheres.

The effect of changing the environmental dead state as well as the initial state on seawater flow exergy is shown in Figs. 4.9–4.11. Figure 4.9 shows the specific flow exergy of seawater as it changes with the initial state temperature when the pressure and salt concentration are equal to the dead state values. As shown in this figure, the flow exergy is zero at the dead state temperature. It is always positive at any temperature other than the dead state temperature. This is true for any selected dead state temperature, therefore whenever there is a difference in temperature between the system and environment, there will be a thermal potential difference that makes the flow exergy positive.

Figure 4.10 shows the specific flow exergy of seawater as it changes with the salt concentration of the initial state temperature when the pressure and temperature are equal to the dead state values. As shown in this figure, the flow exergy is always positive at any concentration other than the dead state concentration. This fact is true for any selected dead state salt concentration: whenever a concentration difference exists between the system and environment, the flow exergy is positive. For instance, if the salt concentration of the flow stream is higher than the salt concentration at the dead state, pure water can flow from the environment to the flow stream through a semi-permeable membrane. This will increase the static head of the flow stream and can produce work (exergy) though a hydropower turbine [18]. The same thing will happen if the salt concentration of the flow stream is lower than that of the environmental dead state, but the flow of water in this case will be from the flow stream to the environment. This is clearly illustrated in Fig. 4.10, which is applicable

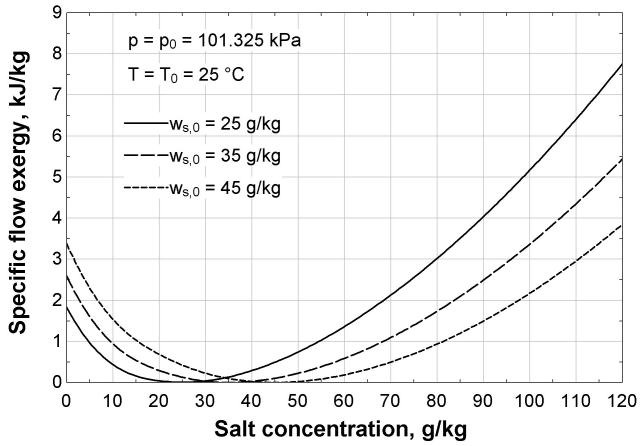

Figure 4.10: Specific flow exergy of seawater as a function of salt concentration

for any selected dead state.

The effect of changing the dead state pressure is shown in Fig. 4.11. As shown in this figure, the flow exergy is zero at the dead state pressure. Flow exergy is positive at pressures higher than the dead state pressure and negative at pressures lower than the dead state pressure. In contrast, the exergy of a control mass system (closed system) is always positive, irrespective of whether the pressure is higher or lower than the dead state pressure, as shown in Fig. 4.12.

4.4 Thermodynamic Analysis of Desalination Processes

In this section, a consistent definition of Second Law efficiency for desalination systems based on the least work of separation is presented [19]. Additionally, the required work of separation is decomposed into the least work of separation plus the contribution from all significant sources of irreversibility within the system, and methods of evaluating the entropy generation due to specific physical processes are derived. In Section 4.5, these methods are applied to four common desalination systems.

4.4.1 Derivation of Performance Parameters for Desalination

Work and Heat of Separation

Consider a simple black-box separator model for a desalination system, with a separate control volume surrounding it at some distance, as shown in Fig. 4.13. The work of separation entering the system is denoted by $\dot{W}_{\text{sep}}$ and the heat transfer into the system is $\dot{Q}$. Stream sw is the incoming seawater, stream p is pure water (product), and stream

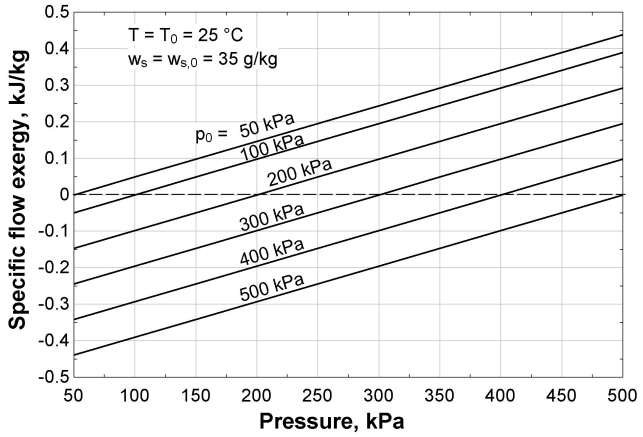

Figure 4.11: Specific flow exergy of seawater as a function of pressure

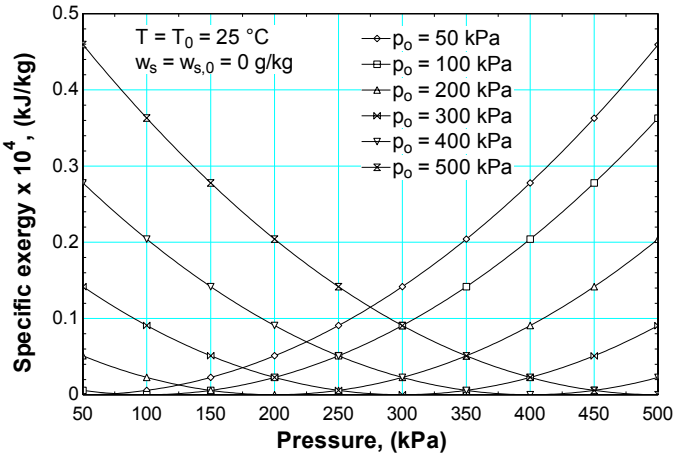

Figure 4.12: Specific exergy of water as a function of pressure (closed system)

b is the concentrated brine. By selecting the control volume sufficiently far from the physical plant, all the inlet and outlet streams enter and leave the control volume at ambient temperature, T_0, and pressure, p_0. Additionally, the heat transfer, $\dot{Q}$, occurs at ambient temperature.

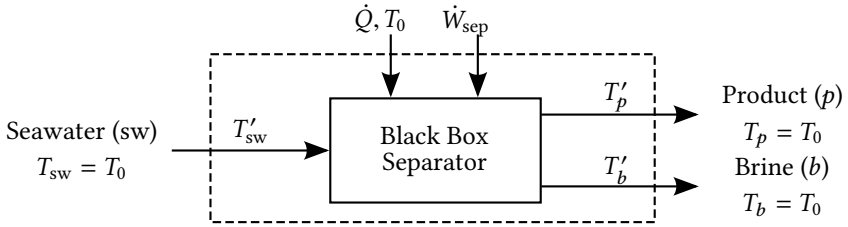

Figure 4.13: When the control volume is selected suitably far away from the physical system, all inlet and outlet streams are at ambient temperature and pressure. The temperature of the streams inside the control volume, denoted by T'_i, might not be at T_0.

The logic underlying this latter formulation is that the exergy of the outlet streams attributable to thermal disequilibrium with the environment is not deemed useful. In other words, the purpose of a desalination plant is to produce pure water, not pure *hot* water. Consider separately the thermal conditions at the desalination system boundary (solid box) and the distant control volume boundary (dashed box). Product and reject streams may exit the desalination system at temperatures T'_p and T'_b, different than ambient temperature, T_0. The exergy associated with these streams could be used to produce work that would offset the required work of separation. However, if the exergy associated with thermal disequilibrium is not harnessed in this way, but simply discarded, entropy is generated as the streams are brought to thermal equilibrium with the environment. This entropy generation is analyzed in Section 4.4.2. Similarly, pressure disequilibrium would result in additional entropy generation [18]. In general, differences in concentration between the various streams represent a chemical disequilibrium which could also be used to produce additional work; however, since the purpose of the desalination plant is to split a single stream into two streams of different concentrations, the outlet streams are not brought to chemical equilibrium with the environment.

The least work and least heat of separation are calculated by evaluating the First and Second Laws of Thermodynamics for the distant control volume. The convention that work and heat input to the system are positive is used.

$$\dot{W}_{\text{sep}} + \dot{Q} + (\dot{m}h)_{\text{sw}} = (\dot{m}h)_p + (\dot{m}h)_b \tag{4.68a}$$

$$\frac{\dot{Q}}{T_0} + (\dot{m}s)_{\text{sw}} + \dot{S}_{\text{gen}} = (\dot{m}s)_p + (\dot{m}s)_b \tag{4.68b}$$

In Eqs. (4.68a) and (4.68b), $\dot{m}_i$, h_i, and s_i are the mass flow rate, specific enthalpy and specific entropies of the seawater (sw), product (p), and brine (b) streams. The First and Second Laws are combined by multiplying Eq. (4.68b) by ambient temperature, T_0,

and subtracting from Eq. (4.68a) while noting that the specific Gibbs free energy is, $g = h - Ts$ (all evaluated at $T = T_0$):

$$\dot{W}_{\text{sep}} = \dot{m}_p g_p + \dot{m}_b g_b - \dot{m}_{\text{sw}} g_{\text{sw}} + T_0 \dot{S}_{\text{gen}} \tag{4.69}$$

Least Work and Heat of Separation

In the limit of reversible operation, entropy generation is zero and the work of separation becomes the reversible work of separation, which is also known as the least work of separation:

$$\dot{W}_{\text{least}} \equiv \dot{W}_{\text{sep}}^{\text{rev}} = \dot{m}_p g_p + \dot{m}_b g_b - \dot{m}_{\text{sw}} g_{\text{sw}} \tag{4.70}$$

Equations (4.69) and (4.70) should be evaluated using seawater properties [20].[7]

In order to gain better physical insight into the separation process, it is instructive to consider how the least work varies with recovery ratio. The recovery ratio is defined as the ratio of the mass flow rate of product water to the mass flow rate of feed seawater:

$$r \equiv \frac{\text{Product Water}}{\text{Inlet Seawater}} = \frac{\dot{m}_p}{\dot{m}_{\text{sw}}} \tag{4.71}$$

Using a simple mass balance ($\dot{m}_{\text{sw}} = \dot{m}_p + \dot{m}_b$) and normalizing Eq. (4.70) by the amount of water produced gives:

$$\frac{\dot{W}_{\text{least}}}{\dot{m}_p} = g_p + \frac{\dot{m}_{\text{sw}} - \dot{m}_p}{\dot{m}_p} g_b - \frac{\dot{m}_{\text{sw}}}{\dot{m}_p} g_{\text{sw}} = g_p + \left(\frac{1}{r} - 1\right) g_b - \frac{1}{r} g_{\text{sw}} \tag{4.72}$$

The Gibbs free energy of each of the streams in Eq. (4.72) is evaluated using seawater properties [20], as a function of temperature and salinity. Provided the inlet salinity and the product salinity is known, then the brine salinity is found using a mass balance:

$$w_{\text{s,b}} = \frac{\dot{m}_{\text{sw}} w_{\text{s,sw}} - \dot{m}_p w_{\text{s,p}}}{\dot{m}_b} = \frac{w_{\text{s,sw}}}{1 - r} - \frac{r w_{\text{s,p}}}{1 - r} \tag{4.73}$$

Since the least work is evaluated assuming all streams leave the control volume at ambient temperature, Eq. (4.72) is a function of temperature, inlet salinity, product salinity, and recovery ratio.

Holding temperature constant at 25 °C, the least work of separation is plotted as a function of these variables in Fig. 4.14.[8] It is seen that regardless of inlet salinity and product salinity, the least work is minimized as the recovery ratio approaches

[7] The least work should not depend on the thermodynamic frame of reference chosen for analysis. Indeed, using the Gibbs-Duhem relationship, we can show that the result we derive using a control volume (CV) analysis, Eq. (4.70), is identical to the result obtained from a control mass (CM) approach. As $\dot{m}g = \dot{G}$, expanding Eq. (4.70) in terms of salt (s) and water (w) using Eq. (4.11) yields: $\dot{W}_{\text{least}} = \dot{G}_p + \dot{G}_b - \dot{G}_{\text{sw}} = \dot{N}_{w,p}\mu_{w,p} + \dot{N}_{s,p}\mu_{s,p} + \dot{N}_{w,b}\mu_{w,b} + \dot{N}_{s,b}\mu_{s,b} - \dot{N}_{w,\text{sw}}\mu_{w,\text{sw}} - \dot{N}_{s,\text{sw}}\mu_{s,\text{sw}}$. Rewriting the differences as integrals, $\Delta\dot{N}\mu = \int d(\dot{N}\mu)$, and considering a pure product ($d\dot{N}_s = 0$ and $\mu_{w,p} = \mu_w^\circ$), all remaining terms like $\dot{N}d\mu$ sum to zero by Gibbs-Duhem, Eq. (4.15). The result, $W_{\text{least}} = \int_{\text{sw}}^{b} RT \ln a_w \, dN_w$, is identical to Eq. (12) in [21], which is obtained using a CM approach.

[8] These curves have been updated relative to those in [19], using the newer Gibbs energy correlation in [20] rather than the older one from [22]. This has changed the values of least work at the lowest salinities.

zero. This is true in general because, in the limit of zero recovery, the only stream that experiences an energy change is the product stream. At finite recovery, work must also be provided to supply the chemical potential energy change of the brine stream due to a change in salinity. Since the least work is defined per unit mass of product, the least work represents the amount of energy necessary to create 1 kg of pure water plus the amount of energy necessary to change the chemical potential of the brine stream.

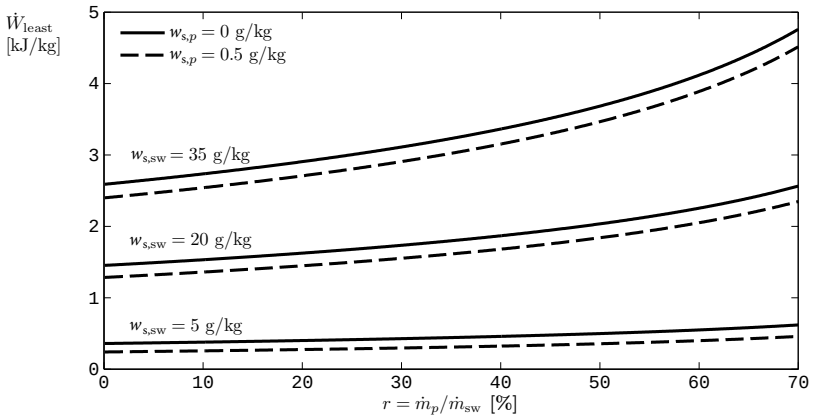

Figure 4.14: The least work of separation is minimized when the recovery ratio approaches zero.

From Fig. 4.14, it can be seen that the least work of separation is minimized as the recovery ratio approaches zero (*i.e.*, infinitesimal extraction).

$$\dot{W}_{\text{least}}^{\text{min}} \equiv \lim_{r \to 0} \dot{W}_{\text{least}} \tag{4.74}$$

Using seawater properties [20] and assuming an inlet salinity of 35 g/kg, zero salinity water product, and $T = 25\,^{\circ}\text{C}$, the least work of separation at infinitesimal recovery is 2.59 kJ/kg.

Equation (4.69) represents the amount of work required to produce a kilogram of pure water. If heat is used to power a desalination system instead of work, the heat of separation is a more relevant parameter. Recalling that heat engines produce work and reject heat, the calculation of the heat of separation is straightforward. Figure 4.15 shows the control volume from Fig. 4.13 but with a reversible heat engine providing work of separation.

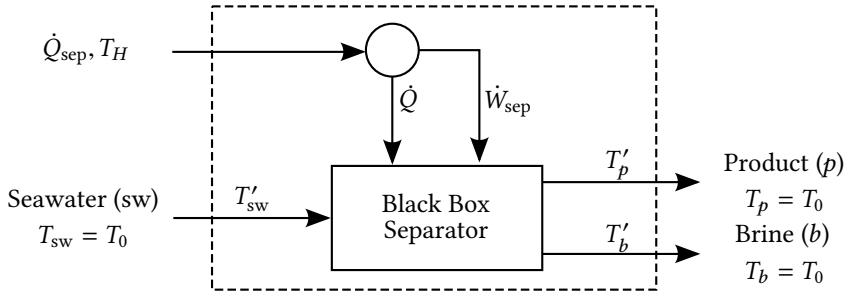

Figure 4.15: Addition of a high temperature reservoir and a Carnot engine to the control volume model shown in Fig. 4.13.

If the heat is provided from a high temperature reservoir, then the First Law for the heat engine is

$$\dot{Q}_{sep} = \dot{W}_{sep} + \dot{Q} \tag{4.75}$$

Assuming a reversible heat engine operating between the high temperature reservoir at T_H and ambient temperature T_0 and considering work per unit mass produced,

$$\frac{\dot{W}_{sep}}{\dot{m}_p} = \frac{\dot{Q}_{sep}}{\dot{m}_p} - \frac{\dot{Q}}{\dot{m}_p} = \frac{\dot{Q}_{sep}}{\dot{m}_p}\left(1 - \frac{T_0}{T_H}\right) \tag{4.76}$$

where the second equality holds as a result of the entropy transfer that occurs in a reversible heat engine operating between two heat reservoirs. Therefore, the heat of separation is:

$$\frac{\dot{Q}_{sep}}{\dot{m}_p} = \frac{\dot{W}_{sep}}{\left(1 - \frac{T_0}{T_H}\right)\dot{m}_p} = \frac{\dot{W}^{rev}_{sep} + T_0\dot{S}_{gen}}{\left(1 - \frac{T_0}{T_H}\right)\dot{m}_p} \tag{4.77}$$

where the second equality holds by combining Eqs. (4.69) and (4.70). Note that Eq. (4.77) can also be derived from Eqs. (4.68a) and (4.68b) if $\dot{W}_{sep}$ is set to zero and the temperature in the Second Law is set to T_H [23]. Equations for the least heat of separation, $\dot{Q}_{least}$ and the minimum least heat of separation, $\dot{Q}^{min}_{least}$ can be obtained from Eq. (4.77) in the same manner as the corresponding work equations.

In practice, the entropy generation term in Eqs. (4.69) and (4.77) often dominates over the least work or least heat. Therefore, the parameter, $\dot{S}_{gen}/\dot{m}_p$ is of critical importance to the performance of desalination systems [23]. This term is referred to as the specific entropy generation, $\mathcal{S}_{gen}$, and is a measure of entropy generated per unit of water produced:

$$\mathcal{S}_{gen} = \frac{\dot{S}_{gen}}{\dot{m}_p} \tag{4.78}$$

In the formulation described above, all streams enter and exit the system at ambient temperature. Therefore, the specific exergy destroyed, e_d, in the system is equal to the product of $\mathcal{S}_{gen}$ and the ambient temperature. This term is physically reflective of the same phenomenon that produces Eq. (4.78):

$$e_d = \frac{T_0\dot{S}_{gen}}{\dot{m}_p} \tag{4.79}$$

Least Work of Separation for Salt Removal

Thus far, we have considered the removal of water from a saline feed. But suppose we wished instead to remove salt from the feed, resulting in pure salt and pure water. The results are given for an NaCl solution, but the methodology can be applied to other mixtures.

Employing the same control volume formulation we've used up to this point [See Sec. 4.2.1, Eq. (4.7) and Sec. 4.4.1, Eq. (4.70)], the inlet stream is the feed F, and the outlet streams are the salt (product) p and the pure water stream d. When all three streams are at the same temperature and pressure, Eq. (4.7) applies and:

$$\dot{W}_{\text{rev}} = \dot{G}_F - \dot{G}_d - \dot{G}_p \tag{4.80}$$

Each $\dot{G}$ can be expanded in terms of water and salt, $\dot{G} = (\dot{N}\mu)_w + (\dot{N}\mu)_s$, but because the d and p streams are pure, $\dot{N}_{w,d} = \dot{N}_{w,F}$ and $\dot{N}_{s,p} = \dot{N}_{s,F}$, so:

$$\dot{W}_{\text{rev}} = \dot{N}_{w,F}(\mu_{w,F} - \mu_{w,d}) + \dot{N}_{s,F}(\mu_{s,F} - \mu_{s,p}) \tag{4.81}$$

When solid and aqueous salt are in equilibrium, *i.e.*, at the solubility equilibrium, the chemical potential of salt in the solid and aqueous phases are equal. Thus $\mu_{s,p} = \mu_s^\circ + RT \ln a_{s,p}$, where $a_{s,p}$ is the activity of the salt in a saturated solution. The d stream is pure, so $a_{w,d} = 1$, and $\mu_{w,d} = \mu_{w,d}^\circ$. Dividing the LHS side of Eq. (4.81) by $RT\,\dot{N}_{s,p}$ and the RHS by the numerically equal term $RT\,\dot{N}_{s,F}$, Eq. (4.81) reduces to

$$\frac{\dot{W}_{\text{rev}}}{RT\dot{N}_{s,p}} = \frac{1}{b_{s,F}M_w} \ln\left(a_{w,F}\right) + \ln\left(\frac{a_{s,F}}{a_{s,p}}\right) \tag{4.82}$$

At 25°C and atmospheric pressure, the solubility of NaCl is 6.147 mol/kg, $\gamma_{b,\pm} = 1.006$, and so $a_{s,p} = (\gamma_{b,\pm} b)^2 = 38.24$ (See Fig. 4.2 and [2]). For a 0.62 mol/kg NaCl solution, a rough approximation of seawater, $a_{w,F} = 0.9796$ and $a_{s,F} = 0.1734$. The least work for salt removal is thus 307 kJ/kg-salt produced, or equivalently 11.1 kJ/kg-water removed – over four times the least work required to separate saltwater into brine and water! This figure is also a good approximation to the minimum energy required for zero-liquid-discharge (ZLD) seawater desalination. (In ZLD, all of the water in the seawater is converted to fresh water, so the recovery ratio is the mass fraction of water in the seawater, or about 96.5%.)

Second Law Efficiency

The Second Law (or exergetic) efficiency is employed as a measure of the thermodynamic reversibility of a desalination system. Unlike First Law efficiency, which measures the amount of an energy source that is put to use, Second Law efficiency, η_{II}, measures the extent of irreversible losses within a system. A completely reversible system will have a Second Law efficiency of 1 even though the First Law efficiency is likely to be lower. Bejan *et al.* [24] define the exergetic efficiency as the ratio of the exergy of the process products to the process fuel. In other words, the

exergetic efficiency is the ratio of the useful exergy of the outputs of the process ($\dot{\Xi}_{\text{out,useful}}$) to the exergy of the process inputs ($\dot{\Xi}_{\text{in}}$):

$$\eta_{II} \equiv \frac{\dot{\Xi}_{\text{out,useful}}}{\dot{\Xi}_{\text{in}}} = 1 - \frac{\dot{\Xi}_{\text{destroyed}} + \dot{\Xi}_{\text{lost}}}{\dot{\Xi}_{\text{in}}} \tag{4.83}$$

The second equality in Eq. (4.83) is valid since the useful exergy out is equal to the exergy minus the sum of the exergy destroyed ($\dot{\Xi}_{\text{destroyed}}$) and the exergy lost ($\dot{\Xi}_{\text{lost}}$). Exergy destroyed represents lost available work due to irreversibilities within the system. Exergy lost represents lost available work due to discarding streams to the environment that carry exergy. Note that when the material inputs to the system are taken to be at equilibrium with the environment, Ξ_{in} equals Ξ_{fuel}, $\Xi_{\dot{W}_{\text{sep}}}$, or $\Xi_{\dot{Q}_{\text{sep}}}$, depending on the energy input. Additionally, Eq. (4.83) is equivalent to the definition used by Kahraman and Cengel [25].

Prior to applying Eq. (4.83) to desalination systems, it is important to understand the differences between the three definitions of work that are presented. The work of separation, $\dot{W}_{\text{sep}}$, is the actual amount of work necessary to produce a given amount of water from a fixed feed stream using a real separation process. The least work of separation, $\dot{W}_{\text{least}}$, represents the amount of work necessary to produce the same amount of product water from the feed stream while operating under reversible conditions. Finally, the minimum least work, $\dot{W}^{\text{min}}_{\text{least}}$, is the minimum required work of separation in the limit of reversible operation and infinitesimal extraction. As a result, the following relation will always hold:

$$\dot{W}_{\text{sep}} > \dot{W}_{\text{least}}(r > 0) > \dot{W}^{\text{min}}_{\text{least}}(r = 0) \tag{4.84}$$

In a desalination process, purified water is considered to be the useful product. The useful exergy associated with pure water is the minimum least work (or heat) of separation that is required to obtain purified water from feed water of a given salinity (*i.e.*, infinitesimal extraction of pure water with inlet and outlet streams at ambient temperature). The minimum least work (at zero recovery), rather than the least work (at finite recovery), is used since it represents the actual exergetic value of pure water. To further illustrate, when analyzing a unit of pure water, it is impossible to know the process that was used to produce it. Therefore, the minimum energy required to produce it must be the exergetic value and $\dot{\Xi}_{\text{out,useful}} = \dot{W}^{\text{min}}_{\text{least}}(r = 0)$.

Since the control volume is defined so that the inlet stream is at the dead state, the only exergy input to the system comes in the form of either a work ($\dot{W}_{\text{sep}}$) or heat ($\dot{Q}_{\text{sep}}$) input (exergy of the feed stream is zero). The work of separation is equivalent to the useful work done within the system plus the exergy destroyed within that system.

In order to calculate the work of separation, two equivalent processes may be considered. The first involves a separation process where the products are brought to thermal and mechanical equilibrium with the environment, whereas the brine is also brought into chemical equilibrium (total dead state, TDS). The reversible work required to achieve this process corresponds to the least work at zero recovery. The total work of separation is given by the sum of the reversible work required plus the exergy destruction associated with entropy generated in the separation and run-down

to equilibrium processes:

$$\dot{W}_{sep} = \dot{W}^{min}_{least}(r = 0) + T_0 \dot{S}^{TDS}_{gen} \tag{4.85}$$

The second process involves a separation process where the products are only brought to thermal and mechanical equilibrium with the environment (restricted dead state, RDS). The reversible work required to achieve this process corresponds to the least work at finite recovery. The total work of separation again is given by the sum of the reversible work required plus the exergy destruction associated with entropy generated in this process:

$$\dot{W}_{sep} = \dot{W}_{least}(r > 0) + T_0 \dot{S}^{RDS}_{gen} \tag{4.86}$$

It can be shown that Eqs. (4.85) and (4.86) are equivalent.[9] Note that the work of separation for a system can also be directly evaluated using a First Law analysis.

As result, when Eq. (4.83) is applied to a desalination system that receives both work and heat input, it should be written as:

$$\eta_{II} = \frac{\text{least exergy of separation}}{\text{exergy input}} = \frac{\dot{W}^{min}_{least}}{\dot{W}_{sep} + \dot{Q}_{sep}\left(1 - \frac{T_0}{T_H}\right)} \tag{4.87}$$

For the case of a purely work driven system, such as reverse osmosis desalination, this becomes:

$$\eta_{II} = \frac{\dot{W}^{min}_{least}}{\dot{W}_{sep}} = \frac{\dot{W}^{min}_{least}}{\dot{W}^{min}_{least} + T_0 \dot{S}^{TDS}_{gen}} = \frac{\dot{W}^{min}_{least}}{\dot{W}_{least} + T_0 \dot{S}^{RDS}_{gen}} \tag{4.88}$$

For a heat driven system, Equation (4.83) can be written in terms of the least heat of separation:

$$\eta_{II} = \frac{\dot{Q}^{min}_{least}}{\dot{Q}_{sep}} = \frac{\dot{Q}^{min}_{least}}{\dot{Q}^{min}_{least} + \left(1 - \frac{T_0}{T_H}\right)^{-1} T_0 \dot{S}^{TDS}_{gen}} = \frac{\dot{Q}^{min}_{least}}{\dot{Q}_{least} + \left(1 - \frac{T_0}{T_H}\right)^{-1} T_0 \dot{S}^{RDS}_{gen}} \tag{4.89}$$

Clearly, the two definitions of Second Law efficiency presented in Eqs. (4.88) and (4.89) are bounded by 0 and 1 because $\dot{W}_{sep} > \dot{W}_{least}$ and $\dot{Q}_{sep} > \dot{Q}_{least}$. Observe that $\dot{W}_{least}$ and $\dot{Q}_{least}$ are functions of feed salinity, product salinity, recovery ratio, and T_0. Additionally, η_{II} will only equal 1 in the limit of completely reversible operation, as expected. Note that the selection of the control volume suitably far away such that all streams are at thermal and mechanical equilibrium allows for this bounding.

Three relevant Second Law based performance parameters for desalination systems have been discussed thus far: specific entropy generation, Eq. (4.78); specific exergy destruction, Eq. (4.79); and Second Law efficiency, Eqs. (4.88) and (4.89). This section will focus on specific entropy generation and Second Law efficiency.

[9] Substitution of $\dot{W}^{min}_{least}$ from Eq. (4.124) into Eq. (4.86) while noting that $\dot{S}^{TDS}_{gen} = \dot{S}^{RDS}_{gen} + \dot{S}^{brine\,RDS\to TDS}_{gen}$ exactly gives Eq. (4.85).

Energetic Performance Parameters

Three often-used parameters are key to describing the energetic performance of desalination systems. The first, called gained output ratio (GOR), is the ratio of the enthalpy required to evaporate the distillate (or equivalently, the energy release in condensation) and the heat input to the system, or

$$\text{GOR} \equiv \frac{\dot{m}_p h_{fg}(T_0)}{\dot{Q}_{\text{sep}}} \tag{4.90}$$

In essence, GOR is a measure of how many times the latent heat of vaporization is captured in the condensation of pure water vapor and reused in a subsequent evaporation process to create additional pure water vapor from a saline source. By the First Law of Thermodynamics, a thermal desalination system that has no such heat recovery requires at least the latent heat of vaporization multiplied by the mass of pure water produced as its energy input: its GOR is approximately one (or less when feed heating and heat losses are taken into account). It is important to note that Eq. (4.90) is valid as written only for a desalination system driven by heat; that is, a thermal desalination system. A work-driven desalination system, in contrast, uses electricity or shaft work to drive the separation process. Normally, this work is produced by a thermal process, such as a heat engine. Thus, to evaluate the heat input required for a work-driven desalination system, a First Law efficiency of the process that produces the work of separation must be known.

The second parameter, known as the performance ratio (PR), is defined as the ratio of the mass flow rate of product water to that of the heating steam:

$$\text{PR} \equiv \frac{\dot{m}_p}{\dot{m}_s} \tag{4.91}$$

For a thermal desalination system in which the heat input is provided by condensing steam, as is typical of large-scale thermal processes such as MED and MSF, the values of PR and GOR are quite similar. In that case, the two parameters differ only by the ratio of the latent heat of vaporization at the distillate and heating steam temperatures. That is, $\text{GOR} = \text{PR} \times \frac{h_{fg}(T_0)}{h_{fg}(T_{\text{steam}})}$. (Some authors interchange these definitions of GOR and PR.)

The third parameter, specific electricity consumption (SEC) is best suited to work-driven desalination systems. It is defined as the ratio of the work of separation (or work input) to the mass flow rate of product water, or

$$\text{SEC} \equiv \frac{\dot{W}_{\text{sep}}}{\dot{m}_p} \tag{4.92}$$

As was the case with GOR, because thermal and electrical energy are not directly comparable, numerical values of SEC cannot be compared between thermal- and work-driven systems. SEC as defined by Eq. (4.92) should only be used for desalination systems driven by work.

4.4.2 Analysis of Entropy Generation Mechanisms in Desalination

Several common processes in desalination systems result in entropy generation, including heat transfer, pressure differentials, and non-equilibrium conditions. By utilizing the ideal gas and incompressible fluid models, simple expressions are derived to show the important factors in entropy generation for various physical processes. Physical properties, evaluated at a representative reference state of 50 °C, are provided in Table 4.3 for pure water [26] and seawater [22]. Proper selection of the reference state is discussed below. In all equations in this section, states 1 and 2 are the inlet and outlet states, respectively, for each process.

Table 4.3: Representative values of reference state constants for Eqs. (4.94a), (4.94b), (4.96a), and (4.96b).

Pure water and vapor constants, $T_{sat} = 50\,^{\circ}\text{C}$, $p_{sat} = 12.3$ kPa			
c	4.18 kJ/kg-K	h°_{IG}	2590 kJ/kg
c_p	1.95 kJ/kg-K	h°_{IF}	209 kJ/kg
R	0.462 kJ/kg-K	s°_{IG}	8.07 kJ/kg-K
v	1.01×10^{-3} m^3/kg	s°_{IF}	0.704 kJ/kg-K
Seawater constants, 50 °C, 35,000 mg/kg			
c	4.01 kJ/kg-K	h°_{IF}	200 kJ/kg
v	0.986×10^{-3} m^3/kg	s°_{IF}	0.672 kJ/kg-K

Before analyzing the entropy generation mechanisms, the ideal gas and incompressible fluid models are discussed. By definition, the density of an incompressible fluid does not vary, and the specific heat capacities at constant pressure and constant volume are the same ($c_p = c_v = c$). As a result, an incompressible fluid is one which satisfies the following equations:

$$\mathrm{d}h_{IF} = c\,\mathrm{d}T + v\,\mathrm{d}p \tag{4.93a}$$

$$\mathrm{d}s_{IF} = c\frac{\mathrm{d}T}{T} \tag{4.93b}$$

Integrating Eqs. (4.93a) and (4.93b) from an arbitrary reference state to the state of interest while assuming constant specific heat (c) yields the following expressions:

$$h_{IF} = c(T - T^{\circ}) + v(p - p^{\circ}) + h^{\circ}_{IF} \tag{4.94a}$$

$$s_{IF} = c\ln\frac{T}{T^{\circ}} + s^{\circ}_{IF} \tag{4.94b}$$

Similarly, an ideal gas follows the equation of state, $pv = RT$, and is governed by the following equations:

$$\mathrm{d}h_{IG} = c_p\mathrm{d}T \tag{4.95a}$$

$$\mathrm{d}s_{IG} = c_p\frac{\mathrm{d}T}{T} - R\frac{\mathrm{d}p}{p} \tag{4.95b}$$

Integrating Eqs. (4.95a) and (4.95b) from an arbitrary reference state to the state of interest while assuming constant specific heat at constant pressure, c_p, yields the following expressions:

$$h_{\text{IG}} = c_p(T - T^\circ) + h^\circ_{\text{IG}} \tag{4.96a}$$

$$s_{\text{IG}} = c_p \ln \frac{T}{T^\circ} - R \ln \frac{p}{p^\circ} + s^\circ_{\text{IG}} \tag{4.96b}$$

For increased accuracy, the generalized compressibility model, $pv = ZRT$ can be used instead if R is replaced with ZR in Eqs. (4.95a), (4.95b), (4.96a), and (4.96b) and all future equations.

When evaluating Eqs. (4.94a), (4.94b), (4.96a), and (4.96b), the physical properties (specific heat, volume, compressibility factor, *etc.*) and reference values of enthalpy and entropy should be evaluated at a suitable reference state. The reference state should be selected as the saturated state corresponding to the average temperature between the inlet and outlet streams. Representative values of these constants, evaluated for pure water [26] at 50 °C, are provided in Table 4.3. For seawater, the average salinity should be used. Representative values of these constants, evaluated for seawater [22] at 50 °C and 35 g/kg, are also provided in Table 4.3. It should be noted that the specific heat of seawater is significantly lowered with increasing salinity. Therefore, these approximations should not be used for processes in which composition substantially changes. Instead, Gibbs free energy should be used (see Section 4.4.2).

Flashing

When liquid water near saturation conditions passes through a throttle, a portion will vaporize as a result of the pressure drop through the device. The exiting fluid is thus a mixture of liquid and low pressure vapor and can be modeled as an incompressible fluid and ideal gas, respectively. Application of the First and Second Laws to the flash box (throttle) control volume reduces to:

$$h_{1,\text{IF}} = h_2 = (1 - x)h_{2,\text{IF}} + xh_{2,\text{IG}} \tag{4.97a}$$

$$s^{\text{flashing}}_{\text{gen}} = s_2 - s_1 = \left[(1 - x)s_{2,\text{IF}} + xs_{2,\text{IG}}\right] - s_{1,\text{IF}} \tag{4.97b}$$

Substitution of Eqs. (4.94a), (4.94b), (4.96a), and (4.96b) into Eqs. (4.97a) and (4.97b) with simplification gives the quality and entropy generation due to flashing.

The entropy generated in this process is

$$\begin{aligned} s^{\text{flashing}}_{\text{gen}} = c \ln \frac{T_2}{T_1} + x \Big\{ &(c_p - c) \ln T_2 - R \ln p_2 \\ &+ \left[s^\circ_{\text{IG}} - s^\circ_{\text{IF}} - (c_p - c) \ln T^\circ + R \ln p^\circ\right] \Big\} \end{aligned} \tag{4.98}$$

where the quality, x, is given by:

$$x = \frac{c(T_1 - T_2) + v(p_1 - p_2)}{(c_p - c)T_2 - vp_2 + [h^\circ_{\text{IG}} - h^\circ_{\text{IF}} - (c_p - c)T^\circ + vp^\circ]} \tag{4.99}$$

and c_p is the specific heat at constant pressure, c is the specific heat of an incompressible fluid, R is the ideal gas constant for steam, v is the specific volume of the liquid, h°_{IG} and s°_{IG} are the enthalpy and entropy for steam at the reference state, and h°_{IF} and s°_{IF} are the enthalpy and entropy for liquid water at the reference state.

Flow through an expansion device without phase change

Although the physical causes for pressure drops differ when considering flow through expanders, pipes, throttles, membranes, and other flow constrictions, the control volume equations that govern the entropy generated remains constant. As with the analysis of the flashing case, the First and Second Laws for an isenthalpic process simplify to:

$$w = \frac{\dot{W}}{\dot{m}} = h_2 - h_1 \tag{4.100a}$$

$$s_{\text{gen}} = s_2 - s_1 \tag{4.100b}$$

For an expansion device, the isentropic efficiency, η_e, is defined as:

$$\eta_e \equiv \frac{w}{w^s} = \frac{h_2 - h_1}{h_2^s - h_1} \tag{4.101}$$

where w is the work produced per unit mass through the device and w^s is the work produced assuming isentropic expansion.

For entropy generation in the expansion of an incompressible fluid, Eq. (4.94b) shows that for an isentropic expansion from p_1 to p_2, $T_2^s = T_1$. Combining this result with Eqs. (4.94a), (4.100a), and (4.101) and solving for T_2 gives

$$T_2 = T_1 + \frac{v}{c}(p_1 - p_2)\,(1 - \eta_e) \tag{4.102}$$

Substitution of Eqs. (4.94b) and (4.102) into Eq. (4.100b) yields the entropy generated due to irreversible expansion of an incompressible fluid:

$$s_{\text{gen}}^{\text{expansion,IF}} = c \ln\left[1 + \frac{v}{cT_1}(p_1 - p_2)\,(1 - \eta_e)\right] \approx \frac{v}{T_1}(p_1 - p_2)\,(1 - \eta_e) \tag{4.103}$$

In the limit of a completely irreversible pressure drop (such as through a throttle) in which no work is generated, $\eta_e = 0$ and (4.103) reduces to:

$$s_{\text{gen}}^{\Delta p,\text{IF}} = c \ln\left[1 + \frac{v}{cT_1}(p_1 - p_2)\right] \approx \frac{v}{T_1}(p_1 - p_2) \tag{4.104}$$

For entropy generation in the expansion of an ideal gas, Eq. (4.96b) shows that for an isentropic expansion from p_1 to p_2,

$$T_2^s = T_1 \left(\frac{p_2}{p_1}\right)^{R/c_p}$$

Combining this result with Eqs. (4.96a), (4.100a), and (4.101) and solving for T_2 gives

$$T_2 = T_1 \left\{ 1 + \eta_e \left[\left(\frac{p_2}{p_1} \right)^{R/c_p} - 1 \right] \right\} \tag{4.105}$$

Substitution of Eqs. (4.96b) and (4.105) into Eq. (4.100b) yields the entropy generated due to irreversible expansion of an ideal gas:

$$s_{\text{gen}}^{\text{expansion,IG}} = c_p \ln \left\{ 1 + \eta_e \left[\left(\frac{p_2}{p_1} \right)^{R/c_p} - 1 \right] \right\} - R \ln \frac{p_2}{p_1} \tag{4.106}$$

In the limit of a completely irreversible pressure drop (such as through a throttle) in which no work is generated, $\eta_e = 0$ and Eq. (4.106) reduces to:

$$s_{\text{gen}}^{\Delta p,\text{IG}} = -R \ln \frac{p_2}{p_1} \tag{4.107}$$

Based on Eqs. (4.104) and (4.107), for an incompressible fluid, entropy generation is determined by the pressure difference, whereas for an ideal gas, it is determined by the pressure ratio.

Pumping and compressing

Application of the First and Second Laws to a pump (or compressor) control volume yields Eqs. (4.100a) and (4.100b). For pumping and compressing, the isentropic efficiency, η_p, is defined as:

$$\eta_p \equiv \frac{w^s}{w} = \frac{h_2^s - h_1}{h_2 - h_1} \tag{4.108}$$

For entropy generation in pumping, assume that the liquid can be modeled as an incompressible fluid. Equation (4.94b) shows that for an isentropic expansion from p_1 to p_2, $T_2^s = T_1$. Combining this result with Eqs. (4.94a), (4.100a), and (4.108) and solving for T_2 gives

$$T_2 = T_1 + \frac{v}{c}(p_2 - p_1)\left(\frac{1}{\eta_p} - 1 \right) \tag{4.109}$$

Substitution of Eqs. (4.94b) and (4.109) into Eq. (4.100b) yields the entropy generated due to irreversible pumping:

$$s_{\text{gen}}^{\text{pumping}} = c \ln \left[1 + \frac{v}{cT_1}(p_2 - p_1)\left(\frac{1}{\eta_p} - 1 \right) \right] \approx \frac{v}{T_1}(p_2 - p_1)\left(\frac{1}{\eta_p} - 1 \right) \tag{4.110}$$

The entropy generated due to irreversible pumping can also be derived by noticing that the difference between the actual work and the reversible work is simply the exergy destruction. Since irreversibilities during the compression process of an incompressible fluid will result in only minor changes in temperature (*i.e.*, $T_2 \approx T_1$),

the entropy generation can be determined by dividing the exergy destruction by the inlet temperature in accordance with Gouy-Stodola theorem [16]:

$$s_{\text{gen}}^{\text{pumping}} = \frac{\Xi_d}{T_1} = \frac{w - w^s}{T_1} = \frac{h_2 - h_2^s}{T_1} = \frac{h(T_2, p_2) - h(T_1, p_2)}{T_1}$$
$$= \frac{v}{T_1}(p_2 - p_1)\left(\frac{1}{\eta_p} - 1\right) \tag{4.111}$$

Note that Eq. (4.111) is simply the Taylor series expansion of the second term of Eq. (4.110). This alternate derivation is only appropriate because the pumping process is nearly isothermal.

For entropy generation in vapor compression, assume that both the inlet and outlet vapor can be modeled as an ideal gas that follows the generalized compressibility form. Equation (4.96b) shows that for an isentropic expansion from p_1 to p_2,

$$T_2^s = T_1\left(\frac{p_2}{p_1}\right)^{R/c_p}$$

Combining this result with Eqs. (4.96a), (4.100a), and (4.108) and solving for T_2 gives

$$T_2 = T_1\left\{1 - \frac{1}{\eta_p}\left[1 - \left(\frac{p_2}{p_1}\right)^{R/c_p}\right]\right\} \tag{4.112}$$

Substitution of Eqs. (4.96b) and (4.112) into Eq. (4.100b) yields the entropy generated due to irreversible compression:

$$s_{\text{gen}}^{\text{compression}} = c_p \ln\left\{1 - \frac{1}{\eta_p}\left[1 - \left(\frac{p_2}{p_1}\right)^{R/c_p}\right]\right\} - R\ln\frac{p_2}{p_1} \tag{4.113}$$

Note that unlike in the incompressible fluid case, Eq. (4.113) cannot be derived through the use of the Gouy-Stodola theorem since the compression of a gas is not an isothermal process.

Approximately isobaric heat transfer process

Actual heat exchangers always have a pressure drop associated with viscous forces. However, without knowledge of specific flow geometry or the local temperature and pressure fields, it is impossible to partition entropy generation according to particular transport phenomena. For example, Bejan [27] has shown that for a simple, single-fluid heat exchanger, comparing the trade off between entropy generation due to heat transfer across a finite temperature difference and pressure drop across a finite flow volume yields a thermodynamically optimal heat exchanger geometry.

In heat exchangers within typical desalination processes, however, the effect of pressure drop on physical properties is insignificant. Thus, entropy generation may be calculated as a function of terminal temperatures alone. For the range of temperatures and flow configurations encountered in the present analysis, this approximation holds for fluids that may be modeled as both ideal gases and incompressible fluids.

The entropy generation equation for a heat exchanger is

$$\dot{S}_{\text{gen}}^{\text{HX}} = [\dot{m}(s_2 - s_1)]_{\text{stream 1}} + [\dot{m}(s_2 - s_1)]_{\text{stream 2}} \tag{4.114}$$

In the case of a device that transfers heat at a relatively constant pressure, an approximate expression may be developed for entropy generation as a function of inlet and outlet temperatures alone. Entropy may be written as:

$$\mathrm{d}s = \frac{1}{T}\mathrm{d}h - \frac{v}{T}\mathrm{d}p \tag{4.115}$$

Integrating Eq. (4.115) at constant pressure gives:

$$s_2 - s_1 = \int_1^2 \frac{1}{T}\mathrm{d}h \tag{4.116}$$

For an ideal gas, Eq. (4.115) is written as Eq. (4.95b) which can be integrated at constant pressure to give:

$$s_2 - s_1 = c_p \ln \frac{T_2}{T_1} \tag{4.117}$$

For an incompressible fluid, entropy is not a function of pressure as seen in Eq. (4.93b). Therefore, the entropy difference is given by:

$$s_2 - s_1 = c \ln \frac{T_2}{T_1} \tag{4.118}$$

If it is now assumed that the heat exchanger is adiabatic with respect to the environment and that there is no work, then the above equations can be substituted into Eq. (4.114).

For an isobaric phase change from a saturation state (either liquid or vapor), the entropy change is

$$s_2 - s_1 = x s_{fg} = x(s_{\text{IG}} - s_{\text{IF}}) \qquad \text{for evaporation} \tag{4.119a}$$

$$= (x - 1)s_{fg} = (x - 1)(s_{\text{IG}} - s_{\text{IF}}) \qquad \text{for condensation} \tag{4.119b}$$

where x is the quality at the exit of the process.

Thermal disequilibrium of discharge streams

Referring again to Fig. 4.13, the entropy generated in bringing outlet streams from the system control volume to the ambient temperature reached at the exit of the distant control volume may be calculated. Consider a stream that is in mechanical, but not thermal equilibrium with the environment (Fig. 4.16). The environment acts as a heat reservoir, and through an irreversible heat transfer process, the stream is brought to thermal equilibrium.

The First and Second Laws for this control volume give:

$$\dot{Q} = \dot{m}_i(h_i - h_i') \tag{4.120a}$$

$$\dot{S}_{\text{gen}} = \dot{m}_i \left[(s_i - s_i') - \frac{\dot{Q}}{T_0}\right] = \dot{m}_i \left[(s_i - s_i') - \frac{h_i - h_i'}{T_0}\right] \tag{4.120b}$$

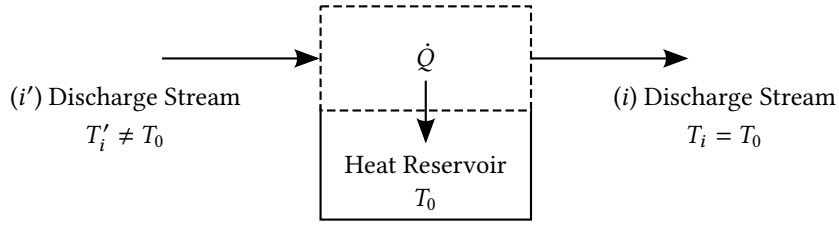

Figure 4.16: Entropy is generated in the process of a stream reaching thermal equilibrium with the environment.

For incompressible fluids at mechanical equilibrium with the environment, $s_i - s_i' = c_i \ln \frac{T_0}{T_i}$ and $h_i - h_i' = c_i(T_0 - T_i)$. Substituting into Eq. (4.120b) gives the entropy generated in bringing a stream of incompressible fluid to thermal equilibrium with the environment:

$$\dot{S}_{\text{gen}}^{T\text{ disequilibrium}} = \dot{m}_i c_i \left[\ln\left(\frac{T_0}{T_i}\right) + \frac{T_i}{T_0} - 1 \right] \tag{4.121}$$

Chemical disequilibrium of concentrate stream

When considering a desalination system, the concentrate is typically considered to be waste and is discharged back to the ocean. Since the concentrate is at higher salinity than the ocean, entropy is generated in the process of restoring the concentrate to chemical equilibrium (also called distributive equilibrium) with the seawater. This entropy generation can be calculated in one of two ways.

First, consider the addition of the concentrate stream at the restricted dead state to a large reservoir of seawater at the total dead state. An exergy balance governing the mixing of the concentrate stream with the seawater reservoir is written as follows:

$$\dot{\Xi}_{\text{destroyed}}^{\text{mixing}} = -[(\dot{m}_c + \dot{m}_{\text{sw}}^{\text{reservoir}})g_{\text{out}} - \dot{m}_c g_c - \dot{m}_{\text{sw}}^{\text{reservoir}} g_{\text{sw}}] \tag{4.122}$$

where $\dot{\Xi}_{\text{destroyed}}^{\text{mixing}}$ is the exergy destroyed as a result of irreversible mixing. In the limit that $\dot{m}_c / \dot{m}_{\text{sw}}^{\text{reservoir}} \to 0$, the mixed state g_{out} approaches g_{sw} and the concentrate stream is brought to chemical equilibrium with the environment. Using the Gouy-Stodola theorem [16], the exergy destroyed due to irreversible mixing can be used to evaluate the entropy generated as the concentrate stream runs down to chemical equilibrium:

$$\dot{S}_{\text{gen}}^{\text{concentrate RDS}\to\text{TDS}} = \frac{\dot{\Xi}_{\text{destroyed}}^{\text{mixing}}}{T_0} \tag{4.123}$$

The mixing process described by Eq. (4.122) is analogous to the separation process shown in Fig. 4.13 performed in reverse.

A second method to evaluate the entropy generation due to chemical disequilibrium of the concentrate stream is based on the least work of separation. When considering the control volume given by Fig. 4.13 and the minimum least work of separation, there is an infinitesimally small product stream of pure water along with a stream

of concentrate of salinity that is infinitesimally above that of seawater. Therefore, the concentrate stream is in thermal, mechanical, and nearly chemical equilibrium with the environment. If, however, there is a finite recovery ratio, the concentrate stream salinity is greater than that of seawater. Additionally, as the recovery ratio increases, the flow rate of the concentrate stream decreases and flow rate of the product water increases (assuming fixed input feed rate). Since the concentrate stream is not at equilibrium with the environment, there is a chemical potential difference that can be used to produce additional work. This additional work is exactly equal to the difference between the least work of separation, Eq. (4.70), and the minimum least work of separation, Eq. (4.74). When the concentrated concentrate is discarded to the ocean, this work potential is lost. Therefore, entropy generation due to chemical disequilibrium of the concentrate stream can also be evaluated through the use of the Gouy-Stodola theorem as follows:

$$T_0 \dot{S}_{\text{gen}}^{\text{concentrate RDS}\to\text{TDS}} = \dot{W}_{\text{least}}(r > 0) - \dot{W}_{\text{least}}^{\text{min}}(r = 0) \tag{4.124}$$

Evaluation of entropy generation using Eqs. (4.123) and (4.124) gives equivalent results.

4.5 Entropy Generation Mechanisms in Seawater Desalination Technologies

Using the methods developed in preceding section, the component and system level entropy production and Second Law efficiency of several common seawater desalination technologies are now evaluated. Four simple examples of common systems are considered: forward feed, multiple effect distillation (MED); direct contact membrane distillation (DCMD); single effect mechanical vapor compression (MVC); and single-stage reverse osmosis (RO). These examples serve to illustrate the application of the models and methods to both thermally driven and work driven desalination processes. These analyses may alternatively be done using the flow exergy function described in Sec. 4.3.

4.5.1 Multiple Effect Distillation

A very simple model based on approximations from Mistry *et al.* [28], El-Sayed and Silver [29], Darwish *et al.* [30], and El-Dessouky and Ettouney [31] is used to generate all the temperature profiles and mass flow rates within a forward feed (FF) multiple effect distillation (MED) cycle (Fig. 4.17).

Several common approximations are made: The temperature drop between effects is assumed to be constant, $\Delta T = (T_{\text{steam}} - T_{\text{last effect}})/n$. Additionally, the driving temperature difference between condensing vapor and evaporating brine and the temperature rise across feed heaters are both taken to be ΔT. The temperature rise in the condenser is set to 10 °C. The distillate is approximated as pure water, and it is assumed that distillate is produced in each effect (D_i) at a rate of 99% of that produced in the previous effect (*i.e.*, $D_{i+1} = 0.99 D_i$) to approximate the effect of increasing latent heat with decreasing effect temperature. Distillate produced from flashing in each

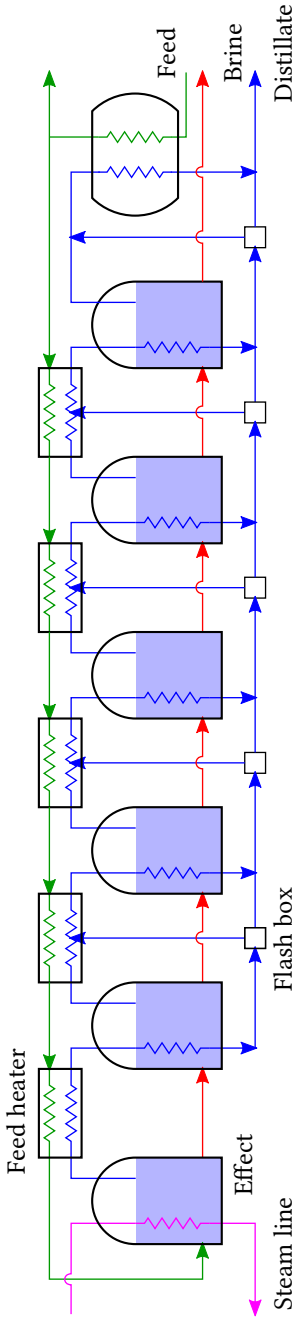

Figure 4.17: A typical flow path for a forward feed multiple effect distillation system.

effect is given by $D_{f,i} = \dot{m}_{b,i-1} c_{p,i} \Delta T / h_{fg,i}$ where $m_{b,i-1}$ is the brine from the previous effect which becomes the feed to the current effect. The remainder of the distillate is produced from boiling in the effect. There is no flashing in the first effect. Distillate produced from flashing in the flash boxes is given by $D_{fb,i} = \sum_{j=1}^{i-1} D_j c_{p,i} \Delta T / h_{fg,i}$, for $i \geq 2$. The quality of the distillate leaving the feed heater is calculated using an energy balance on the heater, $\dot{m}_F c_{p,i} \Delta T = (D_i + D_{fb,i})(1 - x_i) h_{fg}$, where $\dot{m}_F$ is the mass flow rate of the feed seawater.

Water and salinity mass balances for the effects are:

$$\dot{m}_{b,i-1} = D_i + \dot{m}_{b,i} \tag{4.125}$$

$$\dot{m}_{b,i-1} w_{s,b,i-1} = \dot{m}_{b,i} w_{s,b,i} \tag{4.126}$$

where $w_{s,b,i}$ is the salinity of the i^{th} brine stream.

An energy balance on the first effect gives the required amount of heating steam: $\dot{m}_s h_{fg,s} = D_1 h_{D,1} + \dot{m}_{b,1} h_{b,1} - \dot{m}_F h_F$. Accurate properties for seawater [22] and steam [26], including enthalpies, entropies, specific heats, *etc.*, are used and evaluated at each state.

The inputs to the simplified MED FF model with 6 effects include: 1 kg/s of distillate, seawater salinity of 42 g/kg, maximum salinity of 70 g/kg, steam temperature of 70 °C, last effect temperature of 40 °C, and seawater (and environment) temperature of 25 °C.

Using the above approximations and inputs, all thermodynamic states for the MED FF system are found. Entropy generation in each component is computed by using a control volume for each component. Pumping work and entropy generated due to flashing in effects are evaluated using Eqs. (4.98) and (4.110), respectively.

Figure 4.18 shows the entropy generated in each component, whereas Fig. 4.19 shows the percentage of entropy generated in each type of component. Entropy generated during pumping is not included in the figure since it is much less than 1% of the overall amount. Looking at Fig. 4.19, it is clear that heat transfer is the dominant source of entropy generation in MED systems since most of the generation occurs in the heat exchange devices (effects, feed heaters, and condenser). It was found that entropy generated due to flashing in the effects was very small.

Although the effects result in the greatest portion of the entropy generated, it is important to note that the condenser is the single greatest source of irreversibility, as seen in Fig. 4.18. The condenser is such a large source of entropy generation as a result of the large temperature difference between the condensed vapor and the cooling water or feed stream.

Many modern MED plants operate using a thermal vapor compressor (TVC). The TVC is used to entrain the vapor from the final effect and re-inject it into the first effect. MED-TVC plants have much higher performance ratios than non-TVC plants and they reduce the size of the final condenser, thus reducing this large source of irreversibilities. It is important to note, however, that the TVC is also a highly irreversible device so that total entropy production may not be as much reduced.

Finally, it is seen that for this MED plant, entropy generated as a result of the non-equilibrium discharge of the brine and distillate corresponds to approximately 8.7% of the plant's overall losses. The Second Law efficiency, accounting for disequilibrium of the discharge, is $\eta_{II} = 5.9\%$. Additionally, PR = 5.2 and GOR = 5.4.

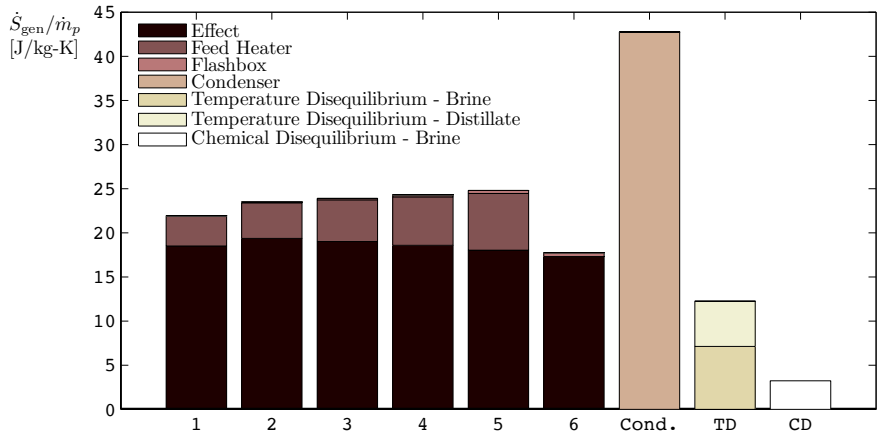

Figure 4.18: Entropy production in the various components of a six effect forward feed multiple effect distillation system.

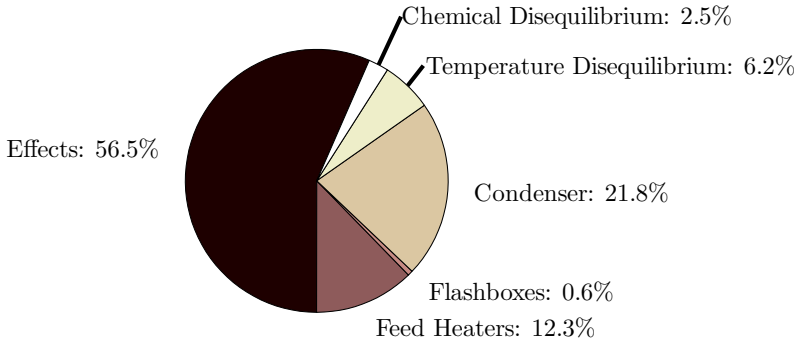

Figure 4.19: Relative contribution of sources of entropy generation in a forward feed multiple effect distillation system. Irreversibilities in the effects dominate. Total specific entropy generation is 196 J/kg-K.

4.5.2 Direct Contact Membrane Distillation

Direct contact membrane distillation (DCMD) is a membrane-based thermal distillation process in which heated feed passes over a hydrophobic microporous membrane [32]. The membrane holds back a meniscus of water near the pores. On the opposing side, cooled fresh water passes over the membrane. The temperature difference between the water streams induces a vapor pressure difference that drives evaporation through the pores. This can be described in terms of a vapor pressure difference multiplied by a membrane distillation coefficient B, which represents the diffusion resistance through the pores. It is based on material properties and pore geometry, and depends weakly on temperature and is assumed to be constant for this calculation. On the feed side, boundary layers in concentration, temperature, and momentum are present, with corresponding diffusional transport of heat and mass. On the cooler fresh water side, there is condensation of vapor and warming of the fresh water, with boundary layer processes similar to those on the feed side. Direct contact membrane distillation has been successfully used to produce fresh water at small scale (0.1 m^3/day) [33–36].

A transport process model for DCMD based on validated models by Bui *et al.* [37] and Lee *et al.* [36] was implemented to obtain the permeate flux, and outlet temperatures of a DCMD module. The calculation of system performance used heat transfer coefficients calculated from correlations based on module geometry [38]. While the Bui *et al.* [37] model used a hollow-fiber membrane configuration, the present calculations are done for a flat-sheet configuration. Membrane geometry and operating conditions are taken from some pilot-sized plants the literature [39, 40]. Seawater enters the system at 27 °C and 35,000 mg/kg total dissolved solids at a mass flow rate of 1 kg/s, The inlet feed is preheated to a constant temperature of 85 °C, and the required heat is provided by a 90 °C source. The permeate side contains fresh water with an inlet flow rate of 1 kg/s. The resulting recovery ratio for this system is 4.4%. The regenerator is a liquid-liquid heat exchanger with a terminal temperature difference of 3 K. The pressure drop through the thin channel in the membrane module was found to be the dominant pressure drop in the system and was the basis for calculating the entropy generation due to pumping power. Properties for seawater [22] were used in the calculation. A schematic diagram of the system is shown in Fig. 4.20, with module geometry and constants shown.

Entropy generation was calculated for each component in the system by using a control volume analysis. Figure 4.21 shows the breakdown of entropy generation in each component.

The greatest source of entropy generation is the module. This is owed mostly to diffusion through the pores and to a lesser extent heat conduction losses, as only a thin membrane separates the cold and hot streams in the module. The small pore size contributes substantially to the diffusion resistance; the pore diameter is usually on the order of 1000 times less than the membrane thickness. Recent work [41] has also shown that equating the inlet flowrate of one stream with the outlet flow rate of the other stream instead of equating the module streams' inlet flow rates, as done here, achieves better thermal balancing in DCMD. Such thermal balancing reduces the entropy generation [42] in the module and can result in a 10–20% improvement in efficiency [41]. The heater contributes substantially due to

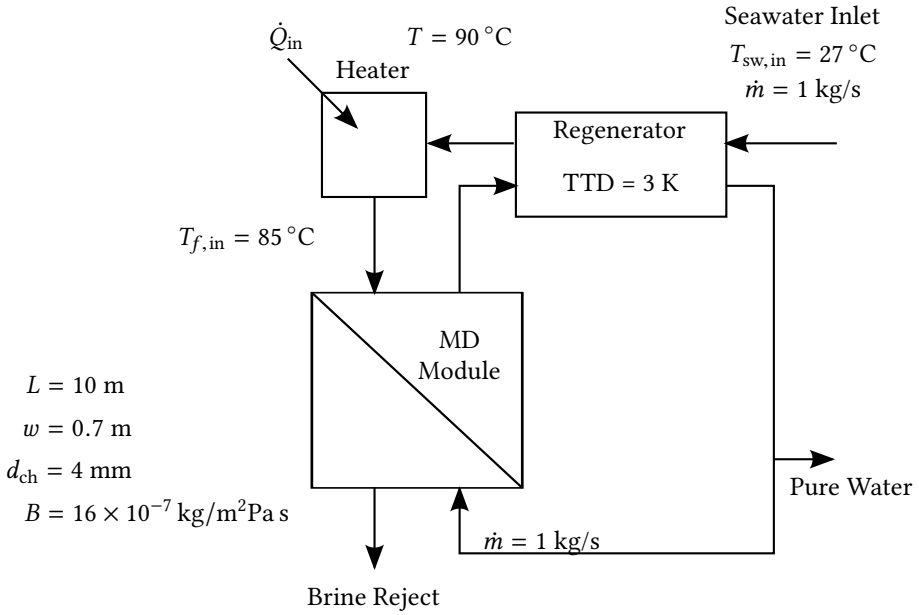

Figure 4.20: Flow path for a basic direct contact membrane distillation system.

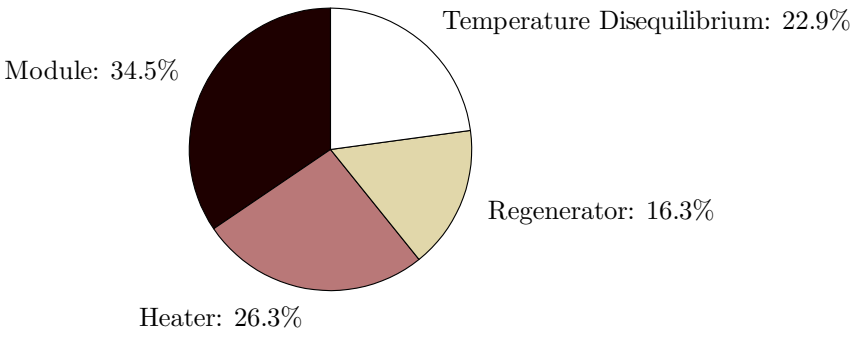

Figure 4.21: Relative contribution of sources of entropy generation in a direct contact membrane distillation system. Total specific entropy generation is 925.4 J/kg-K.

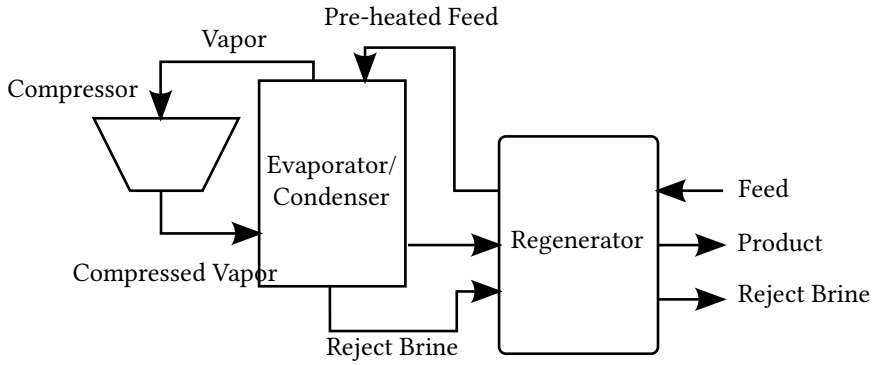

Figure 4.22: Single effect mechanical vapor compression process.

the large amount of heat transferred, and the large temperature difference between the source temperature (usually a steam saturation temperature) and the heater inlet. The regenerator has lower entropy generation as it transfers energy through a lower temperature difference, which remains constant throughout its length. The discharge temperature disequilibrium entropy generation is low compared to other thermal systems, as the brine reject temperature is lower. Additionally, since the recovery ratio is low, the chemical disequilibrium of the brine is also negligible (entropy generation due to brine disequilibrium is approximately three orders of magnitude smaller than from other sources). Like most other systems discussed here, the entropy generation contributed by low pressure-rise circulation pumping is negligible.

Reducing the top temperature, $T_{f,\text{in}}$, results in a net increase in specific entropy generation. This is primarily due to the heater, as a lower top temperature gives rise to a higher temperature difference in the heater. Specific entropy generation in the module goes down slightly, as evaporation happens at a lower temperature; however, this is negated by an increase in specific entropy generation in the regenerator, as water production decreases faster than the temperature gradient in the regenerator. Entropy generation to temperature disequilibrium goes up primarily owing to the lower recovery ratio and additional brine reject.

Given the MD's low recovery ratio and high discharge temperature, entropy generation is high when compared to other desalination systems, and as a result $\eta_{II} = 1.0\%$, as calculated with Eq. (4.88) and taking account all sources of entropy generation. Other configurations of MD, such as conductive-gap MD (CGMD), can cut overall energy consumption in half relative to DCMD [43].

4.5.3 Mechanical Vapor Compression

A simple single effect mechanical vapor compression (MVC) model is considered. A schematic diagram of the process is shown in Fig. 4.22. The design values chosen for the process are guided by those reported for single stage MVC plants analyzed by Veza [44] and Aly [45] and are listed in Table 4.4.

The inlet pressure to the compressor is taken to be the average of the saturation

Table 4.4: MVC design inputs.

Input	Value
Seawater inlet temperature	25 °C
Seawater inlet salinity	35 g/kg
Product water salinity	0 g/kg
Discharged brine salinity	58.33 g/kg
Top brine temperature	60 °C
Pinch: evaporator-condenser	2.5 K
Recovery ratio	40%
Isentropic compressor efficiency	70%
Compressor inlet pressure	19.4 kPa

Table 4.5: MVC model outputs.

Output	Value
Specific electricity consumption	8.84 kWh/m^3
Discharged brine temperature	27.2 °C
Product water temperature	29.7 °C
Compression ratio	1.15
Second Law efficiency, η_{II}	8.5%

pressure of seawater at a salinity corresponding to the average of the feed and reject salinity. The regenerating heat exchanger is thermally balanced and thus the temperature difference is taken to be constant between the rejected brine and the feed stream and also between the product water and the feed stream. By employing energy conservation equations for each component, the unknown thermodynamic states may be computed (an explicit model for energy consumption is given in [46]). Knowing the thermodynamic states at each point, the entropy generated within each component may be calculated along with the entropy generated when the discharged brine is returned to a body of water with the same composition and temperature as the feed. The key outputs from the model are reported in Table 4.5. The breakdown of entropy generation among components is indicated within Fig. 4.23.

The majority of entropy generation may be attributed to heat transfer across a finite temperature difference from the condensation process to the evaporation process. Entropy generation within the regenerator is less significant, primarily because the sensible heat transferred in the regenerator is substantially smaller than the large amount of latent heat recovered in the evaporator-condenser. Entropy generation due to irreversibility within the compressor is important and depends upon the compression ratio and its isentropic efficiency. Entropy generated in returning concentrated brine to a body of seawater is considerable as the recovery ratio is high (40%). Entropy generated in returning product streams to the temperature of inlet seawater is small as the regenerator is effective in bringing these streams to a temperature close to that

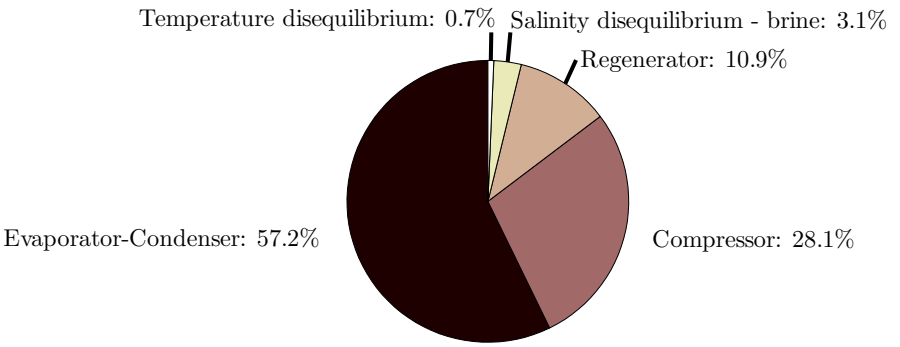

Figure 4.23: Relative contribution of sources of entropy generation in a mechanical vapor compression system. Total specific entropy generation is 98.0 J/kg-K. Contributions of the temperature disequilibrium of the distillate and brine streams are 0.5% and 0.2%, respectively.

of the inlet seawater.

The MVC system modeled above is a simple single effect system, satisfactory for demonstrating the distribution of entropy generation throughout MVC plants. Detailed thermoeconomic models with multiple effects have been analyzed in literature [47]. Research has also been undertaken on improving the heat transfer coefficients within the evaporation and condensation processes of phase change. Lara *et al.* [48] investigated high temperature and pressure MVC, where dropwise condensation can allow greatly enhanced heat transfer coefficients. Lukic *et al.* [49] also investigated the impact of dropwise condensation upon the cost of water produced. Such improvements in heat transfer coefficients reduce the driving temperature difference in the evaporator-condenser leading to a lower compression ratio and thus reduced compressor work requirements per unit of water produced. As the present analysis shows, reduction of entropy generation within the evaporator-condenser and the compressor are crucial if exergetic efficiency is to be improved.

4.5.4 Reverse Osmosis

A typical flow path for a single stage reverse osmosis (RO) plant with energy recovery is shown in Fig. 4.24 [50]. Since RO is a mechanically driven system and thermal effects are of second order to pressure effects, reasonably accurate calculations can be performed while only considering pressure work. The following approximations are made:

Feed seawater is assumed to enter at ambient temperature and pressure (25 °C, 1 bar) and at standard seawater salinity (35 g/kg). Pure water (0 g/kg salinity) is assumed to be produced at a recovery ratio of 40%. Further, it is assumed that 40% of the feed is pumped to 69 bar using a high pressure pump while the remaining 60% is pumped to the same pressure using a combination of a pressure exchanger driven by the rejected brine as well as a booster pump. The high pressure, booster,

and feed pump efficiencies are assumed to be 85%. The concentrated brine loses 2 bar of pressure through the RO module while the product leaves the module at 1 bar. Energy Recovery Inc. [50] makes a direct contact pressure exchanger that features a single rotating part. The pressure exchanger pressurizes part of the feed using work produced through the depressurization of the brine in the rotor. Equations (4.94a), (4.101), and (4.108) are used to match the work produced in expansion to the work required for compression. Assuming the expansion and compression processes are 98% efficient [50], the recovered pressure is calculated as follows:

$$p_{\text{recovered}} = p_{\text{feed}} - \eta_{\text{expansion}}\eta_{\text{compression}}\left(\frac{\rho_{\text{feed}}}{\rho_{\text{brine}}}\right)(p_{\text{brine}} - p_{\text{atm}}) \tag{4.127}$$

and the pressure exchanger efficiency is evaluated using ERI's definition [50]:

$$\eta_{\text{PX}} = \frac{\sum_{\text{out}} \text{Pressure} \times \text{Flow}}{\sum_{\text{in}} \text{Pressure} \times \text{Flow}} \tag{4.128}$$

Density of seawater is evaluated using seawater properties [22].

Using the above assumptions, approximations, and inputs, the entropy generated in the various components can be directly calculated using equations derived in Section 4.4.2. The entropy generated in the high pressure pump, booster pump, and the feed in the pressure exchanger is evaluated using Eq. (4.110). The entropy generated through the expansion of the pressurized brine in the pressure exchanger is evaluated using Eq. (4.103).

Additional consideration is necessary for the entropy generation in the RO module because both the mechanical and chemical state of the seawater is changing. The pure product stream's pressure is 68 bar less than the feed, and the brine is 2 bar less with an outlet salinity of 58.3 g/kg. To capture these effects, the Second Law of Thermodynamics may be applied to a control volume surrounding the module, accounting for entropy flow in and out, entropy generation, and heat transfer, $\dot{Q}_{\text{mod}}$, into the control volume boundary. Heat transfer is necessary if we evaluate the outlet streams at the inlet temperature, and to find the heat transfer we must also use the First Law on the same volume:

$$(\dot{m}h)_{\text{p}} + (\dot{m}h)_{\text{b}} - (\dot{m}h)_{\text{sw}} = \dot{Q}_{\text{mod}} \tag{4.129a}$$

$$(\dot{m}s)_{\text{p}} + (\dot{m}s)_{\text{b}} - (\dot{m}s)_{\text{sw}} = \dot{S}_{\text{gen,mod}} + \frac{\dot{Q}_{\text{mod}}}{T_0} \tag{4.129b}$$

To evaluate the enthalpy and entropy changes, the physical properties of seawater are needed as function of temperature, pressure, and salinity. Since seawater is nearly incompressible, its entropy is essentially independent of p and could be evaluated without accounting for pressure change (e.g., using the package of Sharqawy et al. [22]). The effect of pressure on enthalpy cannot be ignored, although it can also be approximated using an incompressible substance model. Instead, the pressure dependent property package of Nayar et al. [20] can be used. The property changes

$$\Delta\dot{H} = \dot{m}_{\text{p}}\, h(T_0, p_{\text{atm}}, w_{\text{s,p}}) + \dot{m}_{\text{b}}\, h(T_0, p_{\text{brine}}, w_{\text{s,b}}) - \dot{m}_{\text{f}}\, h(T_0, p_{\text{HP}}, w_{\text{s,f}})$$
$$\Delta\dot{S} = \dot{m}_{\text{p}}\, s(T_0, p_{\text{atm}}, w_{\text{s,p}}) + \dot{m}_{\text{b}}\, s(T_0, p_{\text{brine}}, w_{\text{s,b}}) - \dot{m}_{\text{f}}\, s(T_0, p_{\text{HP}}, w_{\text{s,f}})$$

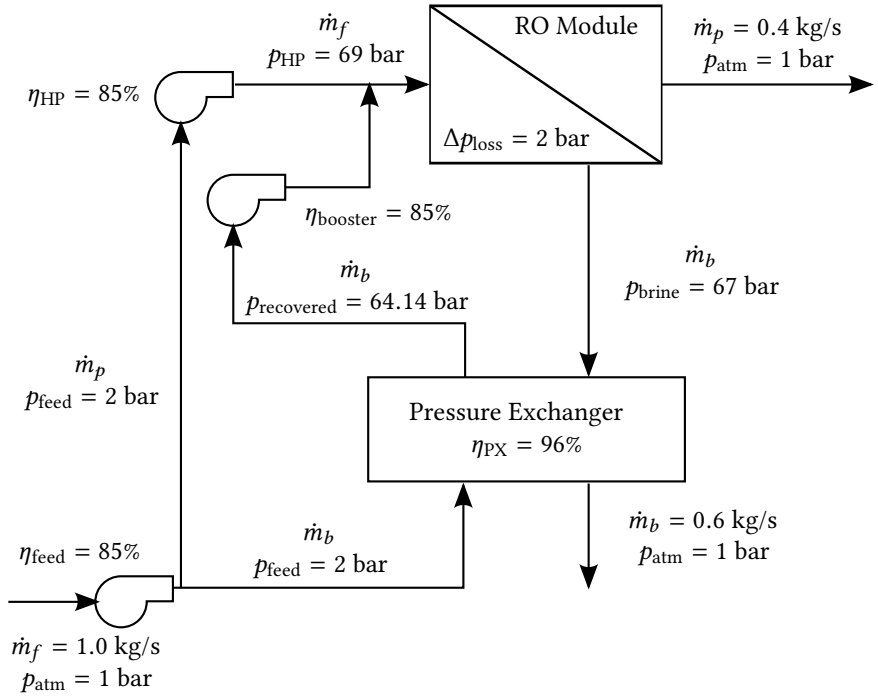

Figure 4.24: A typical flow path for a single stage reverse osmosis system.

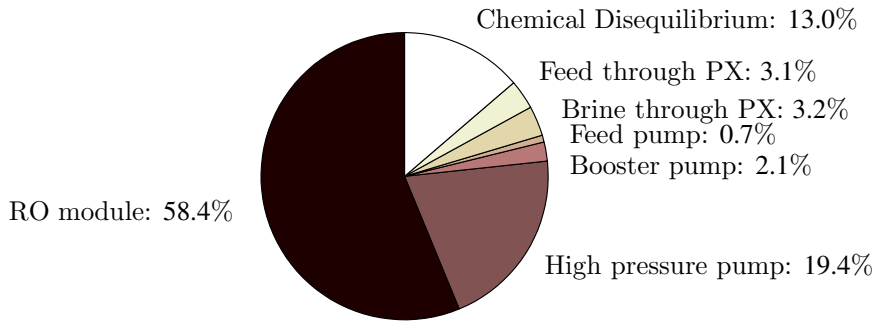

Figure 4.25: Relative contribution of sources to entropy generation in the reverse osmosis system. Irreversibilities associated with product flow through the membrane dominates. Total specific entropy generation, omitting the chemical disequilibrium, is $S_{\text{gen}}^{\text{TDS}} = 19.9$ J/kg-K.

are found to have the values $\Delta\dot{H} = -2.70$ kW and $\Delta\dot{S} = -4.42$ W/K. From these, the First and Second Laws give $\dot{Q}_{\text{mod}} = -2.70$ kW (out of the control volume) and $\dot{S}_{\text{gen,mod}} = 4.65$ W/K.

Regarding the heat transfer, if the system were adiabatic, the outlet streams would be warmer (by roughly 0.7 K if they had the same temperature) but the value of $\dot{S}_{\text{gen,mod}}$ would be essentially the same. The energy dissipated by pump inefficiency results in small increases in the high pressure feed temperature (around 0.4 K), which is also assumed to be removed by heat transfer to the environment. Only negligible entropy generation results from these heat transfers out of the system because the temperature differences above T_0 are so small [see Eq. (4.121)].

Mistry et al. [19] used the incompressible fluid model to find the module entropy generation as the sum of the entropy change of composition (at fixed T and p), the entropy generation from depressurizing the product ($\Delta p = 68$ bar), and the entropy generation from depressurizing the brine ($\Delta p = 2$ bar). Algebra shows that that approach is also consistent with the First and Second Laws.

Figure 4.25 is a pie chart showing the relative amounts of entropy generation within the single-stage RO system. The greatest irreversibility occurs within the RO module, and the diffusion of water through the very high pressure drop of the RO membrane is the principal source of this irreversibility. Note that the high pressure pump moves this same mass of water through the same pressure difference, but does so at 85% efficiency and therefore generates substantially less entropy than the zero efficiency flow through the membrane.

For these conditions, the minimum least work is found to be $\dot{W}_{\text{least}}^{\min}(r = 0) = 2.59$ kJ/kg, and the total entropy generation is $S_{\text{gen}}^{\text{TDS}} = 19.9$ J/kg-K. Therefore, from Eq. (4.85) the required work of separation is 8.53 kJ/kg (2.37 kWh/m^3) and the Second Law efficiency, per Eq. (4.88), is 30.4%.

Since RO systems tend to operate at higher Second Law efficiency than thermal plants, the irreversibility due to discharge disequilibrium of the brine stream has a

larger contribution to the total entropy generation. As seen in Fig. 4.25, the high salinity of the brine accounts for 13% of the plant's total irreversibility. The only way to reduce this effect is to lower the recovery ratio or to implement an osmotic power recovery device (such as a pressure-retarded osmosis system) on the reject brine stream.

Based on these conditions, the minimum least work is found to be $\dot{W}^{\min}_{\text{least}}(r = 0) = 2.59$ kJ/kg and the total entropy generation is $S^{\text{TDS}}_{\text{gen}} = 18.9$ J/kg-K. Therefore, from Eq. (4.85) the required work of separation is 8.23 kJ/kg (2.28 kWh/m^3) and the Second Law efficiency, per Eq. (4.88), is 31.4%.

Since RO systems tend to operate at higher Second Law efficiency than thermal plants, the irreversibility due to discharge disequilibrium of the brine stream has a larger contribution to the total entropy generation. As seen in Fig. 4.25, the high salinity of the brine accounts for 13% of the plant's total irreversibility. The only way to reduce this effect is to lower the recovery ratio or to implement an osmotic power recovery device on the reject brine stream.

When trying to improve RO systems, designers target the irreversibilities in the module. The simplest way to improve the performance of the system is to use a two (or more) stage RO system (*e.g.*, as described in [51]). In a two stage system, water is extracted at a lower recovery ratio from the first stage, resulting in a lower brine concentration. Since the required pressure of the feed is dependent on the osmotic pressure, which itself is a function of the feed concentration, a lower recovery ratio means that lower pressures are needed in the first stage. Next, the brine from the first stage is then further pressurized to the top pressure and additional water is extracted in a second stage. Even though the same top pressure is reached, since the first stage operates with a lower pressure across the membranes, less total entropy is generated in the two stage system.

Batch processing of seawater, in which a charge of seawater is slowly pressurized as permeate is removed through membranes, can maintain a relatively smaller difference between hydraulic and osmotic pressure throughout the process [42]. This reduces the entropy generation and lowers the energy consumption per unit permeate. Semi-batch processes have been commercialized, *e.g.*, by Desalitech Ltd. [52], and report significant reductions in energy. True batch processes, such as those recently invented at MIT, could cut the energy requirements even further [53].

4.6 Second Law Efficiency for a Desalination System Operating as Part of a Cogeneration Plant

Many large-scale desalination processes use a cogeneration scheme, in which low temperature steam and electricity from a power plant are used to drive a desalination plant. Additional primary energy (fuel), beyond that needed for electricity production, must be provided to drive the desalination plant. Thus, it is useful to consider the amount of additional heat energy that must be provided to the power plant in order to generate the heat and work needed to power the desalination plant. In order to do so, consider a cogeneration system in which a power plant is connected to a desalination

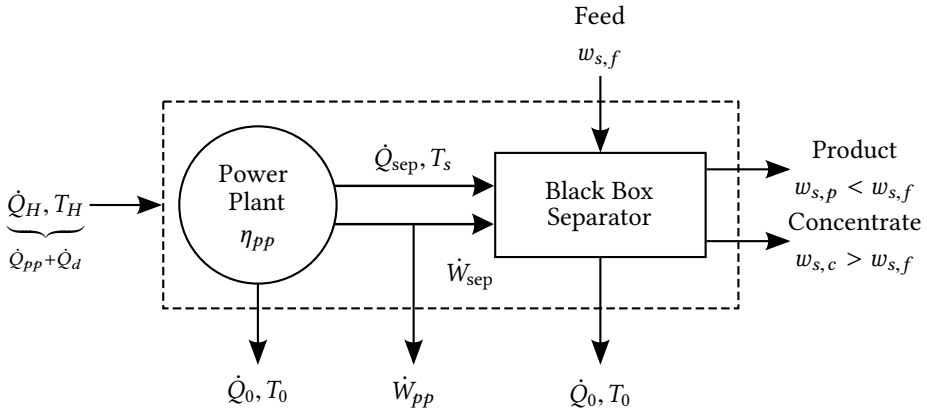

Figure 4.26: The power plant converts heat input into work output, work for the desalination plant (represented as an unspecified black box separator), and heat for the desalination plant. It is assumed that the power plant operates at a Second Law efficiency of η_{pp}.

plant as shown in Fig. 4.26. In this system, a heat input ($\dot{Q}_H$) is provided to a power plant. This heat input is equal to the amount of heat necessary to drive the power plant ($\dot{Q}_{pp}$) plus the additional amount necessary to generate steam and electricity for the desalination plant ($\dot{Q}_d$ to produce $\dot{Q}_{\text{sep}}$ and $\dot{W}_{\text{sep}}$). The power plant produces a net amount of work equal to the desired plant work production ($\dot{W}_{pp}$) plus the amount of work necessary to drive the desalination plant ($\dot{W}_{\text{sep}}$). Note that typically, fuel, rather than heat, is the primary energy input to cogeneration systems and therefore, the analysis should be done in terms of the amount of fuel required to drive the power plant plus the additional amount of fuel required to produce the heat and work necessary to drive the desalination plant ($\dot{m}_{\text{fuel}} = \dot{m}_{pp} + \dot{m}_d$). However, for simplicity and with the goal of highlighting the difference between work and heat driven systems, the control volume for this analysis is drawn under the assumption that heat, and not fuel, is transferred into the system. The effect of including the combustor in the analysis is now discussed briefly.

The following derivation is based on the work of Mistry and Lienhard [54] and El-Sayed and Silver [29]. The First and Second Laws of Thermodynamics are written about the power plant control volume:

$$\dot{Q}_{pp} + \dot{Q}_d = \dot{Q}_{\text{sep}} + \dot{Q}_0 + \dot{W}_{pp} + \dot{W}_{\text{sep}} \tag{4.130a}$$

$$\dot{S}_{\text{gen}} + \frac{\dot{Q}_{pp}}{T_H} + \frac{\dot{Q}_d}{T_H} = \frac{\dot{Q}_{\text{sep}}}{T_s} + \frac{\dot{Q}_0}{T_0} \tag{4.130b}$$

Multiplying the Second Law by T_0 and substituting into the First Law to eliminate heat transfer to the ambient environment ($\dot{Q}_0$) gives:

$$\dot{W}_{pp} + \dot{W}_{\text{sep}} = \left(\dot{Q}_{pp} + \dot{Q}_d\right)\left(1 - \frac{T_0}{T_H}\right) - \dot{Q}_{\text{sep}}\left(1 - \frac{T_0}{T_s}\right) - T_0\dot{S}_{\text{gen}} \tag{4.131}$$

In order to deal with the irreversibilities within the system, the rate of entropy generation is assumed to be proportional to the amount of work produced by a reversible power plant operating within the same heat transfer loads. That is

$$T_0\dot{S}_{\text{gen}} \propto \left(\dot{W}_{pp,\text{rev}} + \dot{W}_{\text{sep,rev}}\right) = \left(\dot{Q}_{pp} + \dot{Q}_d\right)\left(1 - \frac{T_0}{T_H}\right) - \dot{Q}_{\text{sep}}\left(1 - \frac{T_0}{T_s}\right) \tag{4.132}$$

Letting the constant of proportionality be $(1-\eta_{pp})$, where $\eta_{pp} = \eta/\eta_{\text{Carnot}}$ is the Second Law efficiency of the power plant, η is the First Law (energy) efficiency of the plant, and η_{Carnot} is the Carnot efficiency of a power plant operated between T_H and T_0,

$$T_0\dot{S}_{\text{gen}} = \left[\left(\dot{Q}_{pp} + \dot{Q}_d\right)\left(1 - \frac{T_0}{T_H}\right) - \dot{Q}_{\text{sep}}\left(1 - \frac{T_0}{T_s}\right)\right]\left(1 - \eta_{pp}\right) \tag{4.133}$$

Substituting $T_0\dot{S}_{\text{gen}}$ into Eq. (4.131) gives:

$$\dot{W}_{pp} + \dot{W}_{\text{sep}} = \left(\dot{Q}_{pp} + \dot{Q}_d\right)\left(1 - \frac{T_0}{T_H}\right)\eta_{pp} - \dot{Q}_{\text{sep}}\left(1 - \frac{T_0}{T_s}\right)\eta_{pp} \tag{4.134}$$

Since the goal is to determine how much additional heat is necessary to drive the desalination system, $\dot{Q}_d$ must be independent of the amount of work produced by the power plant. Consider the same power plant in which the desalination system is not operating and the power plant is producing a net output of $\dot{W}_{pp}$. Then, setting $\dot{Q}_d$, $\dot{Q}_{\text{sep}}$, and $\dot{W}_{\text{sep}}$ to zero, $\dot{Q}_{pp}$ is found to be:

$$\dot{Q}_{pp} = \frac{\dot{W}_{pp}}{\left(1 - \frac{T_0}{T_H}\right)\eta_{pp}} \tag{4.135}$$

which is consistent with the definition of the First Law efficiency, η. Substituting this back into the above equation results in $\dot{Q}_{pp}$ and $\dot{W}_{pp}$ canceling out. Solving for $\dot{Q}_d$,

$$\dot{Q}_d = \frac{\dot{W}_{\text{sep}}}{\left(1 - \frac{T_0}{T_H}\right)\eta_{pp}} + \dot{Q}_{\text{sep}}\frac{\left(1 - \frac{T_0}{T_s}\right)}{\left(1 - \frac{T_0}{T_H}\right)} \tag{4.136}$$

In order to evaluate the Second Law efficiency of the desalination plant, one might think to use the exergetic value of the work and heat inputs to the plant,

$$\dot{\Xi}_{\text{sep}} = \dot{W}_{\text{sep}} + \left(1 - \frac{T_0}{T_s}\right)\dot{Q}_{\text{sep}}, \tag{4.137}$$

for the denominator in Eq. (4.83) since it represents the total exergy input to the desalination system. While this would be correct for a stand-alone system, $\dot{W}_{\text{sep}}$ and $\dot{Q}_{\text{sep}}$ do not represent the true exergy inputs for entire separation system which is contained within the dashed border in Fig. 4.26. Instead, the exergy input to drive the desalination system is that due to the extra heat transfer provided to the power plant,

$\dot{Q}_d$. Therefore, the Second Law efficiency should be evaluated based on this quantity. Substituting Eq. (4.136) into Eq. (4.83) gives:

$$\eta_{II} = \frac{\dot{\Xi}^{\min}_{\text{least}}}{\dot{\Xi}_{\text{sep}}} = \frac{\dot{W}^{\min}_{\text{least}}}{\dot{Q}_d \left(1 - \frac{T_0}{T_H}\right)} = \frac{\dot{W}^{\min}_{\text{least}}}{\frac{\dot{W}_{\text{sep}}}{\eta_{pp}} + \dot{Q}_{\text{sep}} \left(1 - \frac{T_0}{T_s}\right)} \tag{4.138}$$

The important difference between using Eq. (4.137) and Eq. (4.136) is the fact that the work input ($\dot{W}_{\text{sep}}$) is divided by the Second Law efficiency of the power plant. This effectively accounts for the fact that the work is not produced reversibly from the heat source, and therefore cannot be directly compared with the thermal exergy input. If there is no work input, then $\dot{W}_{\text{sep}} = 0$ and Eq. (4.138) correctly reduces to the ratio of the least heat of separation (based on T_s) to the actual heat input to the desalination system itself. Similarly, if there is no heat input, then $\dot{Q}_{\text{sep}} = 0$ and Eq. (4.138) reduces to:

$$\eta_{II} = \eta_{pp} \frac{\dot{W}^{\min}_{\text{least}}}{\dot{W}_{\text{sep}}} \tag{4.139}$$

In the limit of reversible operation for the power plant (*i.e.*, $\eta_{pp} = 1$), Eq. (4.139) reduces to Eq. (4.88). The Second Law efficiency of the power plant is present in Eq. (4.139) since the work used to power the desalination plant is produced irreversibly. Had the losses in the combustor been included in this analysis, both $\dot{W}_{\text{sep}}$ and $\dot{Q}_{\text{sep}}$ in Eq. (4.138) would be divided by the Second Law efficiency of the combustor, $\eta_{II,\text{combustor}}$. This would have the effect of reducing the Second Law efficiency of the desalination process in proportion to the Second Law efficiency of the combustor. Both the heat and work terms would be affected equally since the losses occur prior to the power generation process.

In order to better understand the energetic behavior of both membrane and thermal systems, a parametric study of Eq. (4.138) is conducted in the following two sections for systems using standard seawater as the feed source (35 g/kg, 25 °C). Under these conditions, the minimum least work of separation of seawater per kilogram of product is 2.71 kJ/kg [19].[10] The Second Law efficiency is evaluated under two different conditions: (1) work is the only input to the desalination system; and (2) heat at 100 °C is the primary input and the amount of pumping work is varied.

Desalination Powered by Work

For desalination systems that are powered entirely using work, $\dot{Q}_{\text{sep}} = 0$ and Eq. (4.138) reduces to Eq. (4.139). As a result, it is clear that unless the power plant operates reversibly, a work powered desalination system can never achieve 100% Second Law efficiency, even if the desalination process is conducted reversibly. This result is unavoidable because the primary energy source in the cogeneration scheme is heat to the power plant, not electricity to the desalination plant. For the following study, the power plant is assumed to be a representative combined cycle plant operating between

[10] More recent values of seawater thermodynamic properties reduce this value by 4.4%, to 2.59 kJ/kg. For consistency with [19] we retain the older value for the calculations that follow.

1400 and 298.15 K with a First Law efficiency of $\eta = 52.8\%$ and a Second Law efficiency of $\eta_{pp} = 67.2\%$ [55]. The Second Law efficiency of a work-driven desalination plant is shown in Fig. 4.27 as a function of $\dot{W}_{\text{sep}}$ starting at a minimum value of $\dot{W}_{\text{sep}} = \dot{W}_{\text{least}}$.

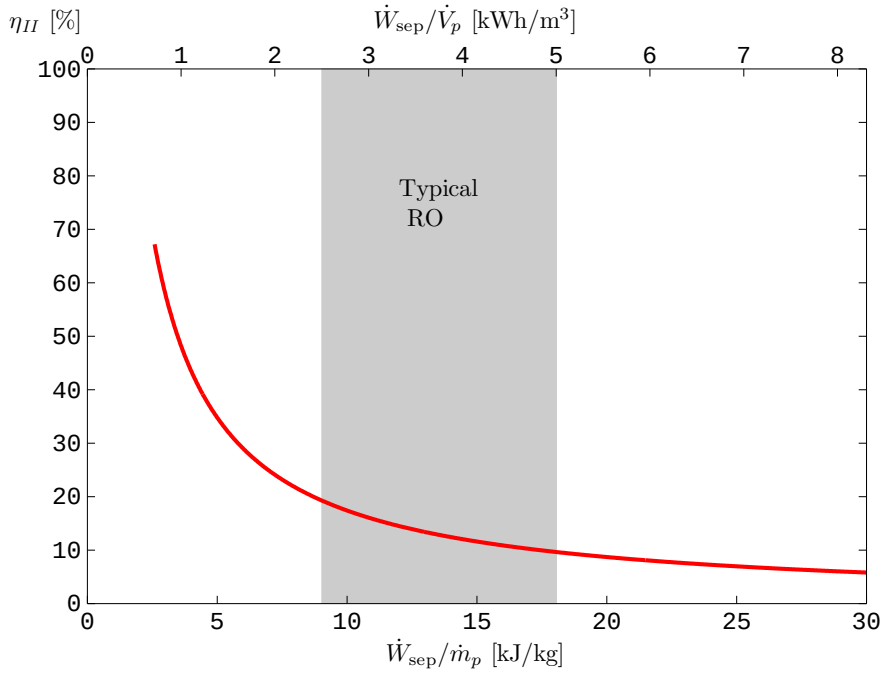

Figure 4.27: The Second Law efficiency of a work-driven desalination system operating in a cogeneration scheme can never reach 100% unless the power plant operates reversibly. Typical values for current reverse osmosis systems are highlighted. Feed water is at $T_0 = 25\,^{\circ}\text{C}$ and $w_{s,f} = 35$ g/kg.

All work-driven systems in this cogeneration scheme pay an energetic penalty on efficiency since the initial energy source (heat) must go through a conversion process (power plant) that operates irreversibly, and therefore, the limiting Second Law efficiency as $\dot{W}_{\text{sep}} \to \dot{W}_{\text{least}}$ is η_{pp}, not 1. If the primary source of energy was considered to be mass of fuel, then the limiting Second Law efficiency would be equal to the product of the Second Law efficiencies of the combustor and the power plant. That is, $\eta_{II,\text{combustor}}\eta_{pp}$. The typical range of operation for current RO technologies is in 2.5–5 kWh/m^3 and is highlighted in Fig. 4.27. RO systems with energy recovery tend to be on the lower end of this range while systems without energy recovery tend to be on the higher end of this range. Exact values are a function of system design and feed water characteristics [56–61]. This corresponds to Second Law efficiency values ranging from approximately 10% to 20%.

Desalination Powered by Co-Generated Heat and Work

Nearly all large-scale thermal desalination systems are connected to a power plant since large quantities of steam are required to provide heating to the feed. The Second Law efficiency of a thermal desalination plant operating using steam at 100 °C with pump work requirements ranging from 0 to 4 kWh/m^3 is shown in Fig. 4.28. In the case of zero pump work, 100% Second Law efficiency is theoretically possible. However, once pump work is required, the possible Second Law efficiency drops substantially (*e.g.*, approximately 50% for 0.5 kWh/m^3 of electrical work to drive pumps). Clearly, regardless of what the required heat of separation is, the additional requirement of pump work results in a decrease in the Second Law efficiency.

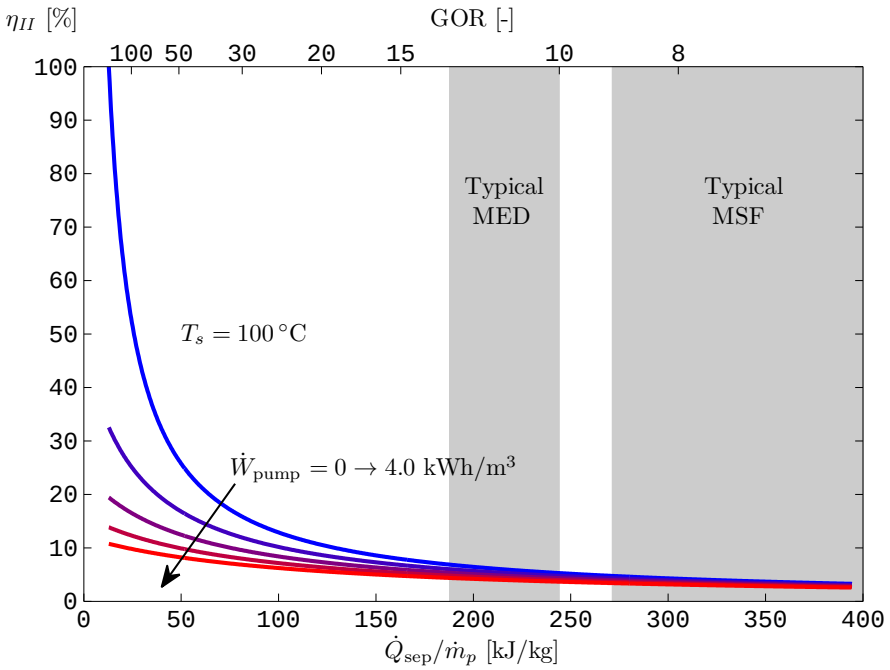

Figure 4.28: Second Law efficiency for a thermal desalination plant requiring work for pumping. Lines for pump work are in increments of 0.5 kWh/m^3. As the pump work increases, the Second Law efficiency decreases. Feed water is at $T_0 = 25\,^\circ$C and $w_{s,f} = 35$ g/kg.

The results shown in Fig. 4.28 are generated based on the assumption that all energy provided to the desalination system originally comes from a common energy source, $\dot{Q}_d$. This value of heat input is then substituted into Eqs. (4.83) and (4.137) to get Eq. (4.138). Should a desalination plant have energy inputs from multiple primary energy sources, then the analysis to derive the correct form of η_{II} will change slightly. All energy inputs should be traced to their primary sources (as was done for $\dot{W}_{\text{sep}}$ and $\dot{Q}_{\text{sep}}$ from $\dot{Q}_d$) and then each primary input should be combined based on the exergetic

value as done in Eq. (4.137).

Based on Figs. 4.27 and 4.28, when a desalination plant operates as part of a cogeneration scheme, the work-driven systems (based on currently available technology) always behave in an exergetically more favorably manner than the thermal driven systems (*i.e.*, higher η_{II}). This is true even when accounting for the energy penalty that comes from converting the source heat to work, and it is even further exemplified when considering that thermal systems typically require large amounts of electrical work for pumping (these are sometimes as high as the work requirements for an RO system by itself).

The present results are based on a Second Law efficiency of $\eta_{pp} = 67\%$, representative of a combined cycle plant. If a less efficient Rankine cycle plant were considered, having a First Law efficiency of 30–35%, a representative η_{pp} might be 45–55%, depending on the top steam temperature. The difference between the work-driven and heat systems would decrease somewhat, but work driven (membrane) systems would remain much more efficient than thermal systems.

Although current membrane systems are more efficient from a Second Law viewpoint, it should not be concluded that there is no role for thermal systems. Ultimately, several factors are considered when selecting a desalination technology including capital and operating costs, quality of feed water, and existing expertise and infrastructure. Although the work systems are favored energetically, these other factors can lead to thermal systems being more desirable for a given location or application.

4.7 Summary

Reducing energy consumption is a key tool for minimizing the environmental footprint and increasing the sustainability of desalination. Using thermodynamic analysis, we have shown how to benchmark systems and process designs against physical limits, how to model the thermodynamic properties of saline waters, and how feed water properties and environmental conditions can affect actual and minimum energy consumption. Entropy generation has been shown to characterize the energetic deficit relative to reversible systems, and equations were developed to quantify the degree of irreversibility, or inefficiency, in individual processes and desalination system components. Identifying components with relatively large entropy production focuses efficiency-driven (re-)design onto those components that will have the greatest impact on overall system performance.

In Section 4.5, we applied these tools to analyze a suite of desalination systems, including both established and emerging technologies. The results of this analysis are shown in Fig. 4.29, where we see that work-driven technologies operate closest to the reversible limit, and that one or two components in each technology stand out as the largest sources of irreversibility in each system. Tow *et al.* [62], reported the Second Law efficiency of a range of real systems operating at various salinities, as shown in Fig. 4.30. The highest efficiencies are found for seawater reverse osmosis plants.[11]

[11] These results are based on the exergy entering the desalination system itself, in contrast to the results of Section 4.6 which refer exergy inputs to the power plant of a coproduction system.

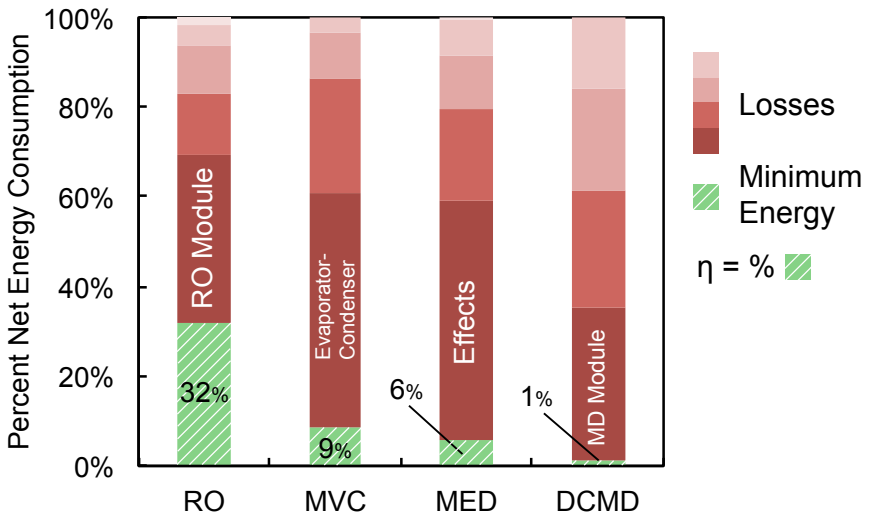

Figure 4.29: The net energy consumption for each technology assessed in Sec. 4.5 is divided into minimum energy (or efficiency) and losses on a percentage basis. Only the primary loss mechanism is labeled. The two work-driven technologies, MVC and RO, have the highest exergetic efficiency. In each system, the core component doing the separation is the greatest source of inefficiency, but auxiliary components also contribute significantly to overall irreversibility.

Other studies that capitalize on thermodynamic methods of this chapter have considered: high salinity brine desalination [46]; balancing of forward osmosis (FO) mass exchangers [62]; energy efficiency of FO relative to RO for seawater desalination [63]; performance optimization of humidification-dehumidification desalination [23, 64–67]; efficiency of desalination driven by waste heat [68]; energy requirements of a variety of hybrid desalination systems, *e.g.*, [69, 70]; and even Second Law efficiencies that incorporate the costs of electricity and heat [71].

Population growth is increasingly straining our limited supply of renewable fresh water, and associated fossil energy emissions threaten our atmosphere. Projections of rising climate variability necessitate greater resilience in our water systems. For all these reasons, the need for more efficient and sustainable desalination is urgent. The concepts and methods developed here provide a framework for assessing and improving the efficiency of both established and emerging desalination technologies.

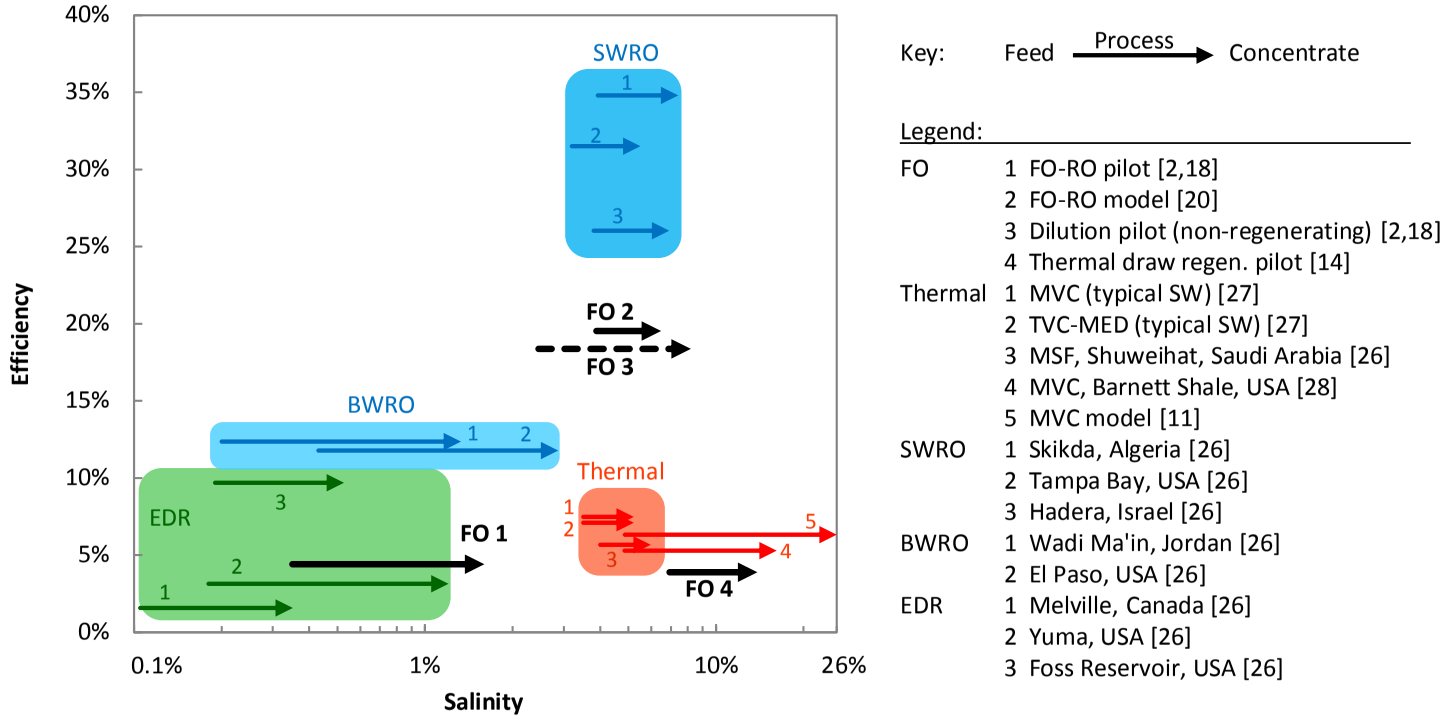

Figure 4.30: Efficiency-salinity map of desalination processes, with salinity in percent by weight. Processes are represented with arrows that begin and end at the feed and concentrate salinities, respectively. Citation numbers in chart refer to those in [62].

APPENDICES

4.A Seawater Properties Correlations

Seawater is a complex electrolyte solution of water and salts. The salt concentration, w_s, is the mass fraction of all dissolved solids present in a unit mass of seawater. It is usually expressed by the salinity (on reference-composition salinity scale) as defined by Millero *et al.* [72] which is currently the best estimate for the absolute salinity of seawater. In this appendix, correlations of seawater thermodynamic properties namely specific volume, specific enthalpy, specific entropy, specific heat, chemical potential, and osmotic coefficient to be used in thermodynamic analysis calculations of this chapter are given. In this regard, the thermodynamic properties of seawater are calculated using the correlations provided by Sharqawy *et al.* [22]. These correlations fit the data extracted from the seawater Gibbs energy function of IAPWS 2008 [73]. They are polynomial equations given as functions of temperature and salinity at atmospheric pressure (or saturation pressure for temperatures over normal boiling temperature). In these correlations, the reference state for the enthalpy and entropy values is taken to be the triple point of pure water (0.01 °C) and at zero absolute salinity.

For other correlations of seawater thermophysical properties, including pressure dependence, the equations provided by Nayar *et al.* [20] are recommended. A full set of codes for calculating seawater thermophysical properties are available without charge at: http://web.mit.edu/seawater.

4.A.1 Specific Volume

The specific volume is the inverse of the density as given by Eq. (4.A.1). Both are intensive properties however in thermodynamics literature it is preferred to use the specific volume instead of the density because it is directly related to the flow work. The density of seawater is higher than that of pure water due to the salts; consequently the specific volume is lower. The seawater density can be calculated by using Eq. (4.A.2) given by Sharqawy *et al.* [22] which fits the data of Isdale and Morris [74] and that of Millero and Poisson [75] for a temperature range of 0–180 °C and salt concentration of 0–0.16 kg/kg and has an accuracy of ±0.1%. The pure water density is given by Eq. (4.A.3) which fits the data extracted from the IAPWS [76] with an accuracy of ±0.01%.

$$v_{sw} = 1/\rho_{sw} \tag{4.A.1}$$

$$\rho_{sw} = \rho_w + w_s \left(a_1 + a_2\, T + a_3\, T^2 + a_4\, T^3 + a_5 w_s\, T^2\right) \tag{4.A.2}$$

$$\begin{aligned}\rho_w = {} & 9.999 \times 10^2 + 2.034 \times 10^{-2} T - 6.162 \times 10^{-3} T^2 \\ & + 2.261 \times 10^{-5} T^3 - 4.657 \times 10^{-8} T^4\end{aligned} \tag{4.A.3}$$

where v_{sw} is the specific volume of seawater in m^3/kg, ρ_{sw} and ρ_w are the density of seawater and pure water respectively in kg/m^3, T is the temperature in °C, w_s is the

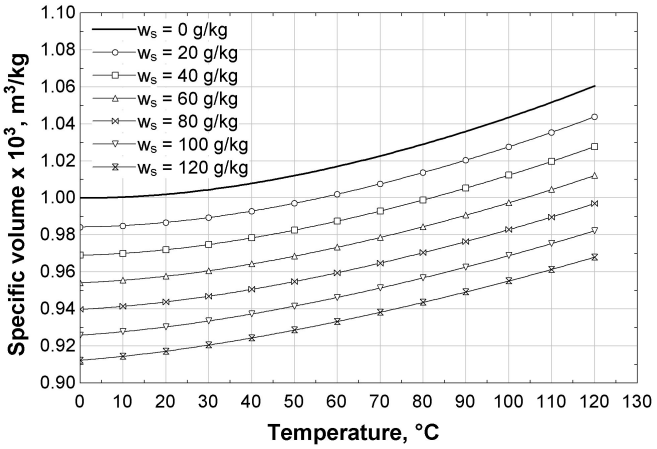

Figure 4.A.1: Seawater specific volume variations with temperature and salt concentration

salt concentration in kg_s/kg_{sw} and

$$a_1 = 8.020 \times 10^2,\ a_2 = -2.001,\ a_3 = 1.677 \times 10^{-2}$$
$$a_4 = -3.060 \times 10^{-5},\ a_5 = -1.613 \times 10^{-5} \tag{4.A.4}$$

Figure 4.A.1 shows the specific volume of seawater calculated from Eq. (4.A.1) as it changes with temperature and salt concentration. It is shown that the specific volume of seawater is less than that of pure water by about 8.6% at 0.12 kg/kg salt concentration and 120 °C. It is important to mention that for incompressible fluids (e.g., seawater) the variation of the specific volume with pressure is very small and can be neglected in most desalination practical problems. The error in calculating the specific volume is less than 1% when the pressure is varying from the saturation pressure to the critical pressure in the compressed liquid region. Therefore, Eq. (4.A.1) can be used at pressures higher than the atmospheric pressure (up to the critical pressure) and at pressure lower than the atmospheric pressure (up to the saturation pressure) with a negligible error (less than 1%).

4.A.2 Specific Enthalpy

The specific enthalpy of seawater is lower than that of pure water since the heat capacity of seawater is less than that of pure water. It can be calculated using Eq. (4.A.5) given by Sharqawy *et al.* [22] which fits the data extracted from the seawater Gibbs energy function of IAPWS [73] for a temperature range of 10–120 °C and salt concentration range of 0–0.12 kg/kg and has an accuracy of ±0.5%. The pure water specific enthalpy is given by Eq. (4.A.6) which fits the data extracted from the IAPWS [76] with an

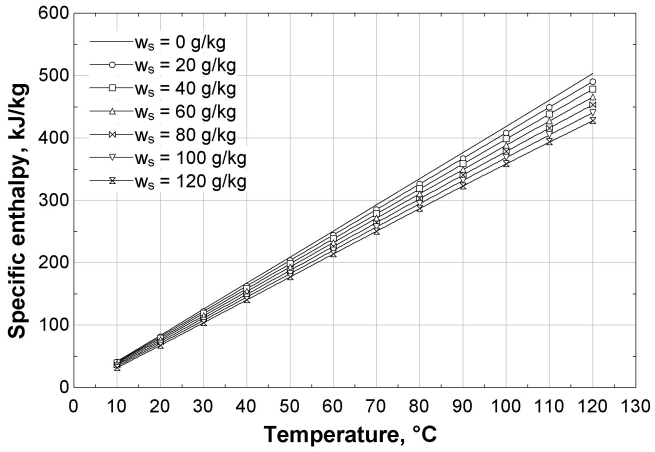

Figure 4.A.2: Seawater specific enthalpy variations with temperature and salt concentration

accuracy of ±0.02%. It is valid for temperature range of 5–200 °C.

$$h_{sw} = h_w - w_s \left(b_1 + b_2 w_s + b_3 w_s^2 + b_4 w_s^3 + b_5 T + b_6 T^2 + b_7 T^3 + b_8 w_s T + b_9 w_s^2 T + b_{10} w_s T^2\right) \quad (4.A.5)$$

$$h_w = 141.355 + 4202.070 \times T - 0.535 \times T^2 + 0.004 \times T^3 \quad (4.A.6)$$

where h_{sw} and h_w are the specific enthalpy of seawater and pure water respectively in (J/kg), $10 \leq T \leq 120$ °C, $0 \leq w_s \leq 0.12$ kg/kg and

$$\begin{aligned} &b_1 = -2.348 \times 10^4, b_2 = 3.152 \times 10^5, b_3 = 2.803 \times 10^6, b_4 = -1.446 \times 10^7 \\ &b_5 = 7.826 \times 10^3, b_6 = -4.417 \times 10^1, b_7 = 2.139 \times 10^{-1}, b_8 = -1.991 \times 10^4 \\ &b_9 = 2.778 \times 10^4, b_{10} = 9.728 \times 10^1 \end{aligned} \quad (4.A.7)$$

Figure 4.A.2 shows the specific enthalpy of seawater calculated from Eq. (4.A.5) as it changes with temperature and salt concentration. The specific enthalpy of seawater is less than that of pure water by about 14% at 0.12 kg/kg salt concentration and 120 °C.

The influence of pressure on the specific enthalpy has been analyzed and correlated by Nayar *et al.* [20].

4.A.3 Specific Entropy

The specific entropy of seawater is lower than that of pure water. It can be calculated using Eq. (4.A.8) given by Sharqawy *et al.* [22] which fits the data extracted from the seawater Gibbs energy function of IAPWS [73] for a temperature range of 10–120 °C and salt concentration range of 0–0.12 kg/kg and has an accuracy of ±0.5%. The pure water specific entropy is given by Eq. (4.A.9) which fits the data extracted from the

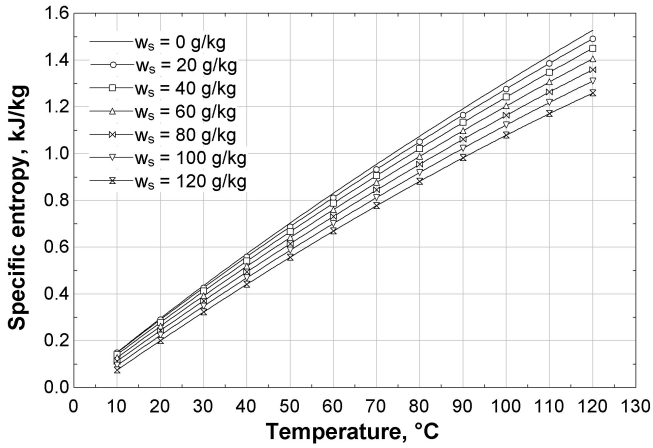

Figure 4.A.3: Seawater specific entropy variations with temperature and salt concentration

IAPWS [76] with an accuracy of ±0.1%. It is valid for $T = 5$–$200\,^{\circ}\text{C}$.

$$\begin{aligned} s_{sw} &= s_w - w_s \left(c_1 + c_2 w_s + c_3 w_s^2 + c_4 w_s^3 + c_5 T + c_6 T^2 + c_7 T^3 \right. \\ &\quad \left. + c_8 w_s T + c_9 w_s^2 T + c_{10} w_s T^2\right) \qquad (4.A.8) \\ s_w &= 0.1543 + 15.383 \times T - 2.996 \times 10^{-2} \times T^2 \\ &\quad + 8.193 \times 10^{-5} \times T^3 - 1.370 \times 10^{-7} \times T^4 \qquad (4.A.9) \end{aligned}$$

where s_{sw} and s_w are the specific entropy of seawater and pure water respectively in (J/kg K), $10 \le T \le 120\,^{\circ}\text{C}$, $0 \le w_s \le 0.12$ kg/kg and

$$\begin{aligned} &c_1 = -4.231 \times 10^2, c_2 = 1.463 \times 10^4, c_3 = -9.880 \times 10^4, c_4 = 3.095 \times 10^5 \\ &c_5 = 2.562 \times 10^1, c_6 = -1.443 \times 10^{-1}, c_7 = 5.879 \times 10^{-4}, c_8 = -6.111 \times 10^1 \\ &c_9 = 8.041 \times 10^1, c_{10} = 3.035 \times 10^{-1} \end{aligned} \qquad (4.A.10)$$

Figure 4.A.3 shows the specific entropy of seawater calculated from Eq. (4.A.8) as it changes with temperature and salt concentration. It is shown that the specific entropy of seawater is less than that of fresh water by about 18% at 0.12 kg/kg salt concentration and 120 °C. It is important to mention that for incompressible fluids (e.g., seawater) the variation of specific entropy with pressure is very small and can be neglected in most practical cases [17]. Therefore, Eq. (4.A.8) can be used at pressures different than the atmospheric pressure.

4.A.4 Chemical Potential

The chemical potentials of water in seawater and salts in seawater may be calculated using the equations given by Nayar *et al.* [20]. Figure 4.A.4 shows the chemical potential

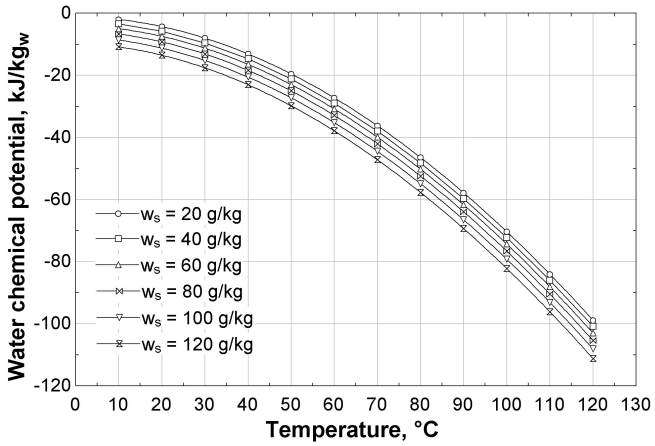

Figure 4.A.4: Chemical potential of water in seawater

of water in seawater calculated as it changes with temperature and salt concentration. Figure 4.A.5 shows the chemical potential of salts in seawater as it changes with temperature and salt concentration. It is seen in Fig. 4.A.4 that the chemical potential of water in seawater decreases with both temperature and salt concentration, while the chemical potential of salts in seawater increases with both temperature and salt concentration as seen in Fig. 4.A.5.

4.A.5 Osmotic Coefficient

The molal osmotic coefficient of a solution, Eq. (4.14b), can be determined from vapor pressure, boiling point elevation, and freezing point measurements. Sharqawy *et al.* [22] reviewed the literature for osmotic coefficient data and provided a correlation that is based on the data of Bromley *et al.* [77] due its wide parameter range of 0–200 °C in temperature and 10–120 g/kg in salinity with a maximum deviation of ±1.4% and a correlation coefficient of 0.991. This correlation is copied here:

$$\begin{aligned}\phi_b = {} & a_1 + a_2 T + a_3 T^2 + a_4 T^4 + a_5 w_s \\ & + a_6 w_s T + a_7 w_s T^3 + a_8 {w_s}^2 + a_9 {w_s}^2 T + a_{10} {w_s}^2 T^2\end{aligned} \tag{4.A.11}$$

where

$$\begin{aligned}&a_1 = 8.9453 \times 10^{-1}, a_2 = 4.1561 \times 10^{-4}, a_3 = -4.6262 \times 10^{-6} \\ &a_4 = 2.2211 \times 10^{-11}, a_5 = -1.1445 \times 10^{2}, a_6 = -1.4783 \times 10^{0} \\ &a_7 = -1.3526 \times 10^{-5}, a_8 = 7.0132 \times 10^{6}, a_9 = 5.696 \times 10^{4} \\ &a_{10} = -2.8624 \times 10^{2}\end{aligned} \tag{4.A.12}$$

Equation (4.A.11) has a validity of $0 \leq T \leq 200$ °C and $0.010 \leq w_s \leq 0.120$ g/kg, with an accuracy of ±1.4%. However, this correlation is limited to a salinity of

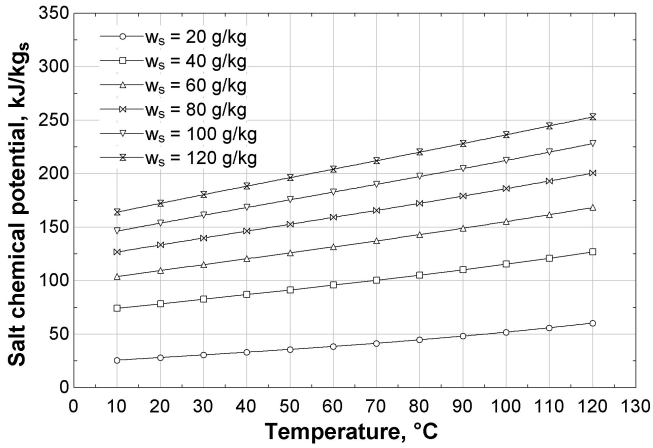

Figure 4.A.5: Chemical potential of salts in seawater

10 g/kg and cannot be extended to lower salinities (i.e. for dilute solutions). It is possible for a seawater stream to become diluted to a salinity below 10 g/kg in certain osmotically-driven processes. Literature values and correlations of the osmotic coefficient for diluted seawater with a salinity of 10 g/kg and below which adhere to this proper physical limit are difficult to find. As described by Debye-Hückel theory, the osmotic coefficient for a mixture approaches a value of 1 with decreasing salinity and does so independently of temperature. Therefore, an extension of the correlation provided by Sharqawy *et al.* [22] 2010 was developed by Sharqawy *et al.* [78] in 2013. By using the theoretical expression for the osmotic coefficient of dilute solutions given by Brønsted [79], the correct behavior as $b \to 0$ can be obtained

$$\phi_b = 1 - \kappa\sqrt{b} + \lambda b \tag{4.A.13}$$

where b is the molality of the solution given by Eq. (4.47), and κ and λ are two fitting parameter constants. To find the value of these constants, Eq. (4.A.13) and its first derivative with respect to salt concentration are set to equal the value of ϕ_b given by Eq. (4.A.11) its first derivative with respect to salt concentration at 0.010 kg/kg, forming two equations with the two constants as unknowns. At 25 °C, the two constants are found to be $\kappa = 0.3484$ and $\lambda = 0.3076$. (For the complete correlation of κ and λ as function of temperature, please see [20].) The final osmotic coefficient function is now set to be a piece-wise function with Eq. (4.A.13) forming the function for $0 \leq w_s < 0.010$ kg/kg and Eq. (4.A.11) forming the $0.010 \leq w_s \leq 0.120$ kg/kg section.

4.A.6 Specific Heat Capacity at Constant Pressure

The specific heat capacity at constant pressure for seawater is less than that of freshwater which reduces the amount of sensible heat that can be transferred at the same temperature difference. The specific heat capacity can be calculated by using

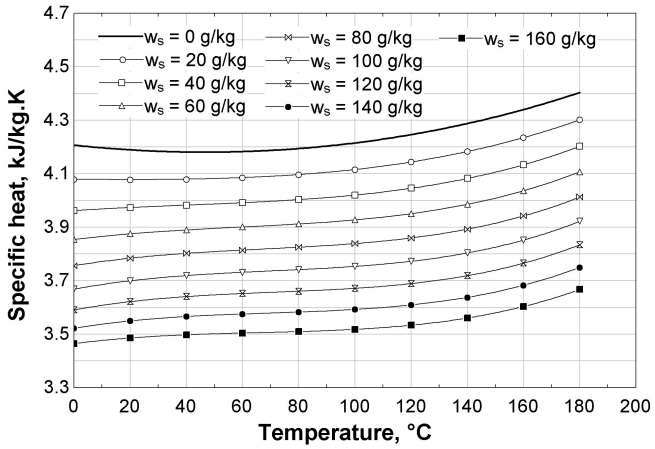

Figure 4.A.6: Specific heat of seawater

Eq. (4.A.14) given by Jamieson *et al.* [80] which fits the experimental measurements with an accuracy of ±0.3%. Equation (4.A.14) is valid for temperatures of 0–180 °C and salt concentration range of 0–0.18 kg/kg.

$$c_{p,sw} = A + B\,(T + 273.15) + C\,(T + 273.15)^2 + D\,(T + 273.15)^3 \tag{4.A.14}$$

where $c_{p,sw}$ is in kJ/kg K, T in °C, w_s in g/kg (*not* kg/kg for this particular correlation), and

$$A = 5.328 - 9.76 \times 10^{-2} w_s + 4.04 \times 10^{-4} w_s^2 \tag{4.A.15}$$

$$B = -6.913 \times 10^{-3} + 7.351 \times 10^{-4} w_s - 3.15 \times 10^{-6} w_s^2 \tag{4.A.16}$$

$$C = 9.6 \times 10^{-6} - 1.927 \times 10^{-6}\, w_s + 8.23 \times 10^{-9}\, w_s^2 \tag{4.A.17}$$

$$D = 2.5 \times 10^{-9} + 1.666 \times 10^{-9} w_s - 7.125 \times 10^{-12} w_s^2 \tag{4.A.18}$$

Figure 4.A.6 shows the specific heat of seawater calculated from Eq. (4.A.14) as a function of temperature and salt concentration. It is shown that the specific heat of seawater is less than that of fresh water by about 16% at a salt concentration of 0.16 kg/kg.

It is important to mention here that the last coefficient in Eq. (4.A.16) was printed with a positive sign in the original paper [80]. However, the correlation matches the experimental data given in the original paper only if a negative sign is used. We believe that there is a typographical error in the original paper, and we have adopted a negative sign here.

4.A.7 Tabulated Data

Tabulated data for seawater thermodynamic properties are given in Table 4.A.1 using the equations presented in this Appendix, and the equations for chemical potential

Table 4.A.1: Seawater Thermodynamic Properties: $T_0 = 25\,^{\circ}\text{C}$, $p = p_0 = 101.325$ kPa, $w_s = w_{s,0} = 0.035$ kg/kg

T °C	v m^3/kg	u kJ/kg	h kJ/kg	s kJ/kg·K	μ_w kJ/kg	μ_s kJ/kg	e_f kJ/kg
10	0.000974	40.0	40.1	0.144	−3.12	64.57	1.71
15	0.000975	59.8	59.9	0.214	−4.10	66.54	0.77
20	0.000976	79.7	79.8	0.282	−5.45	68.50	0.20
25	0.000977	99.7	99.8	0.350	−7.15	70.46	0.00
30	0.000978	119.6	119.7	0.416	−9.20	72.41	0.14
35	0.000980	139.6	139.7	0.482	−11.60	74.38	0.62
40	0.000982	159.6	159.7	0.546	−14.33	76.35	1.42
45	0.000984	179.7	179.8	0.610	−17.40	78.35	2.53
50	0.000986	199.7	199.8	0.672	−20.80	80.36	3.94
55	0.000989	219.8	219.9	0.734	−24.52	82.41	5.64
60	0.000991	239.9	240.0	0.795	−28.56	84.49	7.62
65	0.000994	260.0	260.1	0.855	−32.92	86.61	9.87
70	0.000997	280.1	280.2	0.914	−37.58	88.77	12.37
75	0.000999	300.3	300.4	0.972	−42.55	90.98	15.13
80	0.001003	320.4	320.5	1.029	−47.82	93.25	18.14
85	0.001006	340.5	340.6	1.086	−53.38	95.57	21.39
90	0.001009	360.7	360.8	1.142	−59.23	97.95	24.86

given by Nayar *et al.* [20]. The properties include specific volume, specific internal energy, specific enthalpy, specific entropy, chemical potentials, and specific flow exergy. These are given at temperature of 10–90 °C, salt concentration of 0.035 kg/kg (absolute salinity 35 g/kg) and pressure of 101.325 kPa. However, the equations presented in the appendix can be used up to temperature of 120 °C. In this case for temperatures higher than the normal boiling temperature, the pressure is the saturated pressure and the state of the seawater is the saturated liquid state. For the flow exergy values given in Table 4.A.1, the environment dead state is selected at $T_0 = 25\,^{\circ}\text{C}$, $p_0 = 101.325$ kPa and $w_{s,0} = 0.035$ kg/kg.

As previously noted, a full set of codes for calculating seawater thermophysical properties are available without charge at: `http://web.mit.edu/seawater`.

4.B Pitzer Parameters

This appendix discusses the terms in the Pitzer equations for the activity and osmotic coefficients (Eqs. (4.33)–(4.36)) in aqueous solutions. The term F is based on an extended Debye-Hückel function [6], reflecting the characteristic first-order-square-root

dependence on ionic strength caused by long-range electrostatic interactions:

$$F = -A^{\phi}\left(\frac{\sqrt{I}}{1+1.2\sqrt{I}} + \frac{2}{1.2}\ln(1+1.2\sqrt{I})\right) + \sum_{c}\sum_{a} b_c b_a B'_{ca} + \sum_{c<c'}\sum b_c b_{c'}\Phi'_{cc'} + \sum_{a<a'}\sum b_a b_{a'}\Phi'_{aa'} \tag{4.B.1}$$

The parameter A^{ϕ} is related to the Debye-Hückel limiting law, and is given by

$$A^{\phi} = \frac{1}{3}\left[\frac{e^3\,(2N_0\rho_w)^{1/2}}{8\pi\,(\epsilon_r\epsilon_0 k_b T)^{3/2}}\right] \tag{4.B.2}$$

where ρ_w is the density of pure water. Data for the relative permittivity of pure water as a function of temperature can be obtained from [81].

Interactions between cations and anions are represented by the functions B_{ij}, B'_{ij}, B^{ϕ}_{ij}, and C_{ij}:

$$B_{MX} = \beta^{(0)}_{MX} + \beta^{(1)}_{MX} g(\alpha_{MX}\sqrt{I}) + \beta^{(2)}_{MX} g(12\sqrt{I}) \tag{4.B.3a}$$

$$B'_{MX} = \beta^{(1)}_{MX} g'(\alpha_{MX}\sqrt{I})/I + \beta^{(2)}_{MX} g'(12\sqrt{I})/I \tag{4.B.3b}$$

$$B^{\phi}_{MX} = \beta^{(0)}_{MX} + \beta^{(1)}_{MX}\exp(-\alpha_{MX}\sqrt{I}) + \beta^{(2)}_{MX}\exp(-12\sqrt{I}) \tag{4.B.3c}$$

$$C_{MX} = \frac{C^{\phi}_{MX}}{2|z_M z_X|^{1/2}} \tag{4.B.3d}$$

where $\alpha_{MX} = 2.0$ for j-1 electrolytes and $\alpha_{MX} = 1.4$ for 2-2 and higher electrolytes. The parameters $\beta^{(i)}_{MX}$ are tabulated for a given ion pair, and $\beta^{(2)}_{MX}$ is associated with complex formation and generally only non-zero for 2-2 electrolytes. The functions $g(x)$ and $g'(x)$ are

$$g(x) = 2(1-(1+x)e^{-x})/x^2 \tag{4.B.4a}$$

$$g'(x) = -\frac{2}{x^2}\left[1-\left(1+x+\frac{x^2}{2}\right)e^{-x}\right] \tag{4.B.4b}$$

Interactions between like-charged pairs are represented by Φ_{ij} and Φ'_{ij}:

$$\Phi_{ij} = \theta_{ij} + {}^{E}\theta_{ij}(I) \tag{4.B.5a}$$

$$\Phi'_{ij} = {}^{E}\theta'_{ij}(I) \tag{4.B.5b}$$

$$\Phi^{\phi}_{ij} = \theta_{ij} + {}^{E}\theta_{ij}(I) + I^{E}\theta'_{ij}(I) \tag{4.B.5c}$$

Here, the only adjustable parameter for a given ion pair is θ_{ij}. The terms ${}^{E}\theta_{ij}(I)$ and ${}^{E}\theta'_{ij}(I)$ represent excess free energy arising from electrostatic interactions between

asymmetric electrolytes (*i.e.*, ions with charge of like sign and unlike magnitude), and are functions of ionic strength only:

$$ {}^{E}\theta_{ij} = \frac{z_i z_j}{4I}\left(J_0(x_{ij}) - \frac{1}{2}J_0(x_{ii}) - \frac{1}{2}J_0(x_{jj})\right) \tag{4.B.6a} $$

$$ {}^{E}\theta'_{ij} = \frac{z_i z_j}{8I^2}\left(J_1(x_{ij}) - \frac{1}{2}J_1(x_{ii}) - \frac{1}{2}J_1(x_{jj})\right) - \frac{{}^{E}\theta_{ij}}{I} \tag{4.B.6b} $$

where

$$ J_0(x) = \frac{1}{4}x - 1 + \frac{1}{x}\int_0^\infty \left[1 - \exp\left(-\frac{x}{y}e^{-y}\right)\right] y^2\, dy \tag{4.B.6c} $$

$$ J_1(x) = \frac{1}{4}x - \frac{1}{x}\int_0^\infty \left[1 - \left(1 + \frac{x}{y}e^{-y}\right) \times \exp\left(-\frac{x}{y}e^{-y}\right)\right] y^2\, dy \tag{4.B.6d} $$

and

$$ x_{ij} = 6 z_i z_j A^\phi \sqrt{I} \tag{4.B.6e} $$

The integrals in Eqs. (4.B.6c) and (4.B.6d) can be calculated numerically.

In summary, the adjustable parameters are as follows. There are 3 to 4 per unlike-charged pair, $\beta^{(0)}_{MX}$, $\beta^{(1)}_{MX}$, $\beta^{(2)}_{MX}$, and C^ϕ_{MX}; one per like-charged pair, θ_{ij}; and one per cation-cation-anion and anion-anion-cation triplet, Ψ_{ijk}. The values of these parameters can be found in a variety of sources, some of which contain slightly different values. Tables of values can be found in, *e.g.*, [7, 10, 12, 82–84].

In principle, each of the adjustable binary and ternary parameters ($\beta^{(i)}_{MX}$, C^ϕ_{MX}, θ_{ij}, and Ψ_{ijk}) are functions of temperature. Unfortunately, a complete set of these data as a function of temperature over the range of interest are generally unavailable in open literature (although some significant collections are available, *e.g.*, [10, 83, 84]). However, Silvester and Pitzer have noted that the temperature derivatives of these parameters are often small [85], and much of the temperature variation in activity coefficient is confined to A^ϕ (Eq. (4.B.2)) both in the parameter's explicit temperature dependence, as well as implicitly through variations in the dielectric constant [86]. In addition, solubility computations by DeLima and Pitzer [87] were not impaired by using room temperature values for the mixing parameters (θ_{ij} and Ψ_{ijk}) up to 473 K—well outside the temperature range of typical desalination systems.

4.C Nomenclature

Symbols

A^ϕ	Modified Debye-Hückel parameter [kg$^{1/2}$/mol$^{1/2}$]
a	Activity
B_{ij}, B^ϕ_{ij}	Pitzer parameter, second virial coefficient [kg/mol]
B'_{ij}	Pitzer binary interaction parameter [kg^2/mol^2]
B	Membrane distillation coefficient [kg/m^2-Pa-s]
b	Molality [mol/kg]
C	Modified van 't Hoff coefficient [kPa-kg/g]

C_{ij}, C_{ij}^{ϕ}	Pitzer parameter, unlike-charged interactions [kg^2/mol^2]
C_p	Heat capacity at constant pressure [J/K]
CV	Control volume
c	Concentration [mol/L]; specific heat capacity [J/kg-K]
c_p	Specific heat capacity at constant pressure [J/kg-K]
c_v	Specific heat capacity at constant volume [J/kg-K]
D_i	Distillate from effect i [kg/s]
$D_{f,i}$	Distillate from flashing in effect i [kg/s]
$D_{fb,i}$	Distillate from flashing in flash box i [kg/s]
d_{ch}	Flow channel depth [m]
e	Elementary charge [C]; specific exergy [J/kg]
e_d	Specific exergy destroyed [J/kg]
e_f	Specific flow exergy [J/kg]
F	Extended Debye-Hückel function, Eq. (4.B.1)
G	Gibbs free energy [J]
g	Specific Gibbs free energy [J/kg]
H	Enthalpy [J]
h	Specific enthalpy [J/kg]
h_{fg}	Latent heat of vaporization [J/kg]
h_{sf}	Latent heat of freezing [J/kg]
I	Ionic strength [mol/kg]
i	van 't Hoff factor [-]
K_b	Ebullioscopic constant [K-mol/kg]
K_f	Cryoscopic constant [K-mol/kg]
k_B	Boltzmann's constant [J/K]
L	Length [m]
M_i	Molar mass of species i [g/mol]
M	Mixture average molar mass [g/mol]
m	Mass [kg]
$\dot{m}$	Mass flow rate [kg/s]
N_A	Avogadro's number (6.022140×10^{23}) [mol^{-1}]
N_i	Amount of species i [mol]
n	Number of effects or stages [-]
p	Pressure [kPa]
$\dot{Q}$	Heat transfer rate [W]
$\dot{Q}_{\text{least}}$	Least heat of separation [W]
$\dot{Q}_{\text{least}}^{\text{min}}$	Minimum least heat of separation [W]
$\dot{Q}_{\text{sep}}$	Heat of separation [W]
R	Ideal gas constant [J/kg-K]
$\bar{R}$	Molar gas constant, 8.31446 [J/mol-K]
r	Recovery ratio [(kg/s product)/(kg/s feed)]
S	Entropy [J/K]
$\dot{S}_{\text{gen}}$	Entropy generation rate [W/K]
s	Specific entropy [J/kg-K]
s_{gen}	Specific entropy generation per unit fluid [J/kg-K]

$\mathcal{S}_{\text{gen}}$	Specific entropy generation per unit water produced [J/kg-K]
T	Temperature [K]
T_0	Ambient (dead state) temperature [K]
T_H	Temperature of hot-side reservoir [K]
U	Internal energy [J]
u	Specific internal energy [J/kg]
V	Volume [m^3]
$\overline{v}$	Molar volume [m^3 mol^{-1}]
v	Specific volume [m^3/kg]
$\dot{W}$	Work transfer rate [W]
$\dot{W}_{\text{least}}$	Least work of separation [W]
$\dot{W}^{\text{min}}_{\text{least}}$	Minimum least work of separation [W]
$\dot{W}_{\text{rev}}$	Reversible work [W]
$\dot{W}_{\text{sep}}$	Work of separation [W]
w	Specific work [J/kg]; mass fraction [kg/kg or g/kg]; width [m]
w_s	Mass fraction of salts [kg/kg or g/kg]
x	Quality [kg/kg]; mole fraction
Z	Pitzer function, $\sum_i b_i \lvert z_i \rvert$ [mol/kg]; generalized compressibility [-]
z	Charge number

Greek

α	Pitzer parameter [$kg^{1/2}/mol^{1/2}$]
β	Pitzer parameter [kg/mol]
γ_x, γ_b, γ_c	Rational, molal, and molar activity coefficient
δ_b	Boiling point elevation [K]
δ_f	Freezing point depression [K]
Δ	Change in a variable
Δp_{sat}	Vapor pressure lowering [Pa]
ε_0	Vacuum permittivity
ε_r	Relative permittivity
η	Mole ratio of salt in seawater [-], efficiency
η_e	Isentropic efficiency of expander [-]
η_p	Isentropic efficiency of pump/compressor [-]
η_{II}	Second Law/exergetic efficiency [-]
θ	Pitzer parameter [kg/mol]
κ	Constant in Eq. (4.A.13)
λ	Constant in Eq. (4.A.13)
λ_{ij}	Pitzer parameter, uncharged interactions [kg/mol]
μ	Chemical potential [J/mol]
ν	Stoichiometric coefficient
$\dot{\Xi}_{\text{destroyed}}$	Exergy destruction rate [W]
$\dot{\Xi}$	Exergy flow rate [W]
π	Osmotic pressure [Pa]
ρ	Density [kg/m^3]
Φ_{ij}, Φ^{ϕ}_{ij}	Pitzer parameter, like-charged interactions [kg/mol]

Φ'_{ij}	Pitzer parameter, like-charged interactions [kg^2/mol^2]
ϕ	Osmotic coefficient
Ψ_{ijk}	Pitzer parameter, ternary interactions [kg^2/mol^2]

Subscripts

0	Environment, or global dead state
a, X	Anion
atm	Atmospheric
b	Brine, molal basis
c, M	Cation
d	Desalination, diluent
f	Flashing
F	Feed
i	ith species, inlet state
n, N	Neutral species
o	Outlet state
p	Product
pp	Power plant
s	Steam; salt
sat	Saturated state
sw	Seawater
w	Water

Superscripts

id	Ideal solution
ex	Excess property
s	Isentropic
$'$	Stream before exiting CV
$^\circ$	Standard (reference) state
*	Restricted dead state

Acronyms

BH	Brine heater
CAOW	Closed air open water
CD	Chemical disequilibrium
ERI	Energy Recovery Inc.
FF	Forward feed
GOR	Gained output ratio
HP	High pressure
HX	Heat exchanger
IF	Incompressible fluid
IG	Ideal gas
MED	Multiple effect distillation
MVC	Mechanical vapor compression
OT	Once through
PR	Performance ratio

PX	Pressure exchanger
RDS	Restricted dead state
RO	Reverse osmosis
TD	Temperature disequilibrium
TDS	Total dead state
WH	Water heated

References

[1] S. Glasstone, *Thermodynamics for Chemists*. D. Van Nostrand Company, Inc., 1947. 8, 18, 19

[2] K. S. Pitzer, J. C. Peiper, and R. H. Busey, "Thermodynamic properties of aqueous sodium chloride solutions," *Journal of Physical and Chemical Reference Data*, vol. 13, no. 1, pp. 1–102, 1984. 8, 16, 34

[3] R. A. Robinson and R. H. Stokes, *Electrolyte Solutions*. Dover, 2nd revised ed., 2002. 8, 13, 18

[4] P. Atkins and J. de Paula, *Atkins' Physical Chemistry*. W. H. Freeman and Company, 8th ed., 2006. 9

[5] W. Hamer and Y. Wu, "Osmotic coefficients and mean activity coefficients of uni-univalent electrolytes in water at 25 °C," *Journal of Physical and Chemical Reference Data*, vol. 1, no. 4, pp. 1047–1099, 1972. 12

[6] P. Debye and E. Hückel, "Zur theorie der elektrolyte," *Physikalische Zeitschrift*, vol. 24, pp. 185–206, May 1923. 13, 73

[7] J. F. Zemaitis, D. M. Clark, M. Rafal, and N. C. Scrivner, *Handbook of Aqueous Electrolyte Thermodynamics*. Wiley-AIChE, 1986. 13, 75

[8] C. W. Davies, "The Extent of Dissociation of Salts in Water. Part VIII. An Equation for the Mean Ionic Activity Coefficient of an Electrolyte in Water, and a Revision of the Dissociation Constants of Some Sulphates.," *Journal of the Chemical Society*, pp. 2093–2098, 1938. 13

[9] K. S. Pitzer and J. J. Kim, "Thermodynamics of Electrolytes. IV. Activity and Osmotic Coefficients for Mixed Electrolytes," *Journal of the American Chemical Society*, vol. 96, pp. 5701–5707, September 1974. 13

[10] K. S. Pitzer, "A thermodynamic model for aqueous solutions of liquid-like density," *Reviews in Mineralogy and Geochemistry*, vol. 17, pp. 97–142, 1987. 13, 14, 75

[11] C. E. Harvie and J. H. Weare, "The prediction of mineral solubilities in natural waters: the Na-K-Mg-Ca-Cl-SO_4-H_2O system from zero to high concentration at 25 °C," *Geochimica et Cosmochimica Acta*, vol. 44, pp. 981–997, 1980. 14

[12] C. E. Harvie, N. Møller, and J. H. Weare, "The prediction of mineral solubilities in natural waters: The Na-K-Mg-Ca-H-Cl-SO_4-OH-HCO_3-CO_3-CO_2-H_2O system to high ionic strengths at 25 °C," *Geochimica et Cosmochimica Acta*, vol. 48, pp. 723–751, 1984. 13, 75

[13] K. S. Pitzer, "Thermodynamics of Electrolytes. I. Theoretical Basis and General Equations," *Journal of Physical Chemistry*, vol. 77, no. 2, pp. 268–277, 1973. 13

[14] K. H. Mistry, H. A. Hunter, and J. H. Lienhard V, "Effect of composition and nonideal solution behavior on desalination calculations for mixed electrolyte solutions with comparison to seawater," *Desalination*, vol. 318, pp. 34–47, 2013. 13

[15] A. Saul and W. Wagner, "International equations for the saturation properties of ordinary water substance," *Journal of Physical and Chemical Reference Data*, vol. 16, pp. 893–901, 1987. 16

[16] A. Bejan, *Advanced Engineering Thermodynamics*. Hoboken, New Jersey: John Wiley & Sons, Inc., 3rd ed., 2006. 21, 42, 44

[17] M. J. Moran, *Availability Analysis: A guide to efficient energy use*. New York, NY: ASME Press, corrected ed., 1989. 21, 69

[18] M. H. Sharqawy, J. H. Lienhard V, and S. M. Zubair, "On exergy calculations of seawater with applications in desalination systems," *International Journal of Thermal Sciences*, vol. 50, no. 2, pp. 187–196, 2011. 27, 30

[19] K. H. Mistry, R. K. McGovern, G. P. Thiel, E. K. Summers, S. M. Zubair, and J. H. Lienhard V, "Entropy generation analysis of desalination technologies," *Entropy*, vol. 13, no. 10, pp. 1829–1864, 2011. 28, 31, 56, 60

[20] K. G. Nayar, M. H. Sharqawy, L. D. Banchik, and J. H. Lienhard V, "Thermophysical properties of seawater: A review and new correlations that include pressure dependence," *Desalination*, vol. 387, pp. 1–24, July 2016. http://web.mit.edu/seawater/. 31, 32, 54, 66, 68, 69, 71, 73

[21] R. W. Stoughton and M. H. Lietzke, "Calculation of some thermodynamic properties of sea salt solutions at elevated temperature from data on NaCl solutions," *Journal of Chemical and Engineering Data*, vol. 10, pp. 254–260, July 1965. 31

[22] M. H. Sharqawy, J. H. Lienhard V, and S. M. Zubair, "Thermophysical properties of seawater: A review of existing correlations and data," *Desalination and Water Treatment*, vol. 16, pp. 354–380, April 2010. http://web.mit.edu/seawater. 31, 38, 39, 47, 49, 54, 66, 67, 68, 70, 71

[23] K. H. Mistry, J. H. Lienhard V, and S. M. Zubair, "Effect of entropy generation on the performance of humidification-dehumidification desalination cycles," *International Journal of Thermal Sciences*, vol. 49, no. 9, pp. 1837–1847, 2010. 33, 64

[24] A. Bejan, G. Tsatsaronis, and M. Moran, *Themal Design & Optimization*. New York: John Wiley & Sons, Inc., 1996. 34

[25] N. Kahraman and Y. A. Çengel, "Exergy analysis of a MSF distillation plant," *Energy Conversion and Management*, vol. 46, no. 15-16, pp. 2625–2636, 2005. 35

[26] W. Wagner and A. Pruss, "The IAPWS formulation 1995 for the thermodynamic properties of ordinary water substance for general and scientific use," *Journal of Physical and Chemical Reference Data*, vol. 31, no. 2, pp. 387–535, 2002. 38, 39, 47

[27] A. Bejan, "General criterion for rating heat-exchanger performance," *International Journal of Heat and Mass Transfer*, vol. 21, no. 5, pp. 655–658, 1978. 42

[28] K. H. Mistry, M. A. Antar, and J. H. Lienhard V, "An improved model for multiple effect distillation," *Desalination and Water Treatment*, vol. 51, no. 4-6, pp. 807–821, 2013. 45

[29] Y. M. El-Sayed and R. S. Silver, *Principles of Desalination*, vol. A, ch. 2: Fundamentals of Distillation, pp. 55–109. New York, NY: Academic Press, 2nd ed., 1980. 1980. 45, 58

[30] M. Darwish, F. Al-Juwayhel, and H. K. Abdulraheim, "Multi-effect boiling systems from an energy viewpoint," *Desalination*, vol. 194, no. 1-3, pp. 22–39, 2006. 45

[31] H. T. El-Dessouky and H. M. Ettouney, *Fundamentals of Salt Water Desalination*. Amsterdamn, The Netherlands: Elsevier, 2002. 45

[32] K. W. Lawson and D. R. Lloyd, "Membrane distillation," *Journal of Membrane Science*, vol. 124, no. 1, pp. 1–25, 1997. 49

[33] J. Rodriguez-Maroto and L. Martinez, "Bulk and measured temperatures in direct contact membrane distillation," *Journal of Membrane Science*, vol. 250, no. 1-2, pp. 141–149, 2005. 49

[34] L. Martinez-Diez and F. Florido-Diaz, "Desalination of brines by membrane distillation," *Desalination*, vol. 137, no. 1-3, pp. 267–273, 2001.

[35] L. Song, B. Li, K. K. Sirkar, and J. L. Gilron, "Direct contact membrane distillation-based desalination: Novel membranes, devices, larger-scale studies, and a model," *Industrial & Engineering Chemistry Research*, vol. 46, no. 8, pp. 2307–2323, 2007.

[36] H. Lee, F. He, L. Song, J. Gilron, and K. K. Sirkar, "Desalination with a cascade of cross-flow hollow fiber membrane distillation devices integrated with a heat exchanger," *AIChE Journal*, vol. 57, no. 7, pp. 1780–1795, 2011. 49

[37] V. Bui, L. Vu, and M. Nguyen, "Modelling the simultaneous heat and mass transfer of direct contact membrane distillation in hollow fibre modules," *Journal of Membrane Science*, vol. 353, no. 1-2, pp. 85–93, 2010. 49

[38] J. H. Lienhard IV and J. H. Lienhard V, *A Heat Transfer Textbook*. Mineola, NY: Dover Publications, 4th ed., 2011. http://ahtt.mit.edu. 49

[39] H. E. Fath, S. M. Elsherbiny, A. A. Hassan, M. Rommel, M. Wieghaus, J. Koschikowski, and M. Vatansever, "PV and thermally driven small-scale, stand-alone solar desalination systems with very low maintenance needs," *Desalination*, vol. 225, no. 1-3, pp. 58–69, 2008. 49

[40] F. Banat, N. Jwaied, M. Rommel, J. Koschikowski, and M. Wieghaus, "Desalination by a "compact SMADES" autonomous solar-powered membrane distillation unit," *Desalination*, vol. 217, no. 1-3, pp. 29–37, 2007. 49

[41] J. Swaminathan, H. W. Chung, D. M. Warsinger, and J. H. Lienhard V, "Simple method for balancing direct contact membrane distillation," *Desalination*, vol. 383, pp. 53–59, 2016. 49

[42] G. P. Thiel, R. K. McGovern, S. M. Zubair, and J. H. Lienhard V, "Thermodynamic equipartition for increased second law efficiency," *Applied Energy*, vol. 118, pp. 292–299, 2014. 49, 57

[43] J. Swaminathan, H. W. Chung, D. M. Warsinger, F. A. Al-Marzooqi, H. A. Arafat, and J. H. Lienhard V, "Energy efficiency of permeate gap and novel conductive gap membrane distillation," *Journal of Membrane Science*, vol. 502, pp. 171–178, 2016. 51

[44] J. M. Veza, "Mechanical vapour compression desalination plants — a case study," *Desalination*, vol. 101, no. 1, pp. 1–10, 1995. 51

[45] S. E. Aly, "Gas turbine total energy vapour compression desalination system," *Energy Conversion and Management*, vol. 40, no. 7, pp. 729–741, 1999. 51

[46] G. P. Thiel, E. W. Tow, L. D. Banchik, H. Chung, and J. H. Lienhard V, "Energy consumption in desalinating produced water from shale oil and gas extraction," *Desalination*, vol. 366, pp. 94–112, 2015. 52, 64

[47] A. Nafey, H. Fath, and A. Mabrouk, "Thermoeconomic design of a multi-effect evaporation mechanical vapor compression (MEE-MVC) desalination process," *Desalination*, vol. 230, no. 1-3, pp. 1–15, 2008. 53

[48] J. Lara, G. Noyes, and M. Holtzapple, "An investigation of high operating temperatures in mechanical vapor-compression desalination," *Desalination*, vol. 227, no. 1-3, pp. 217–232, 2008. Issue 1 First Oxford and Nottingham Water and Membranes Research Event 2-4 July 2006, Oxford, UK. 53

[49] N. Lukic, L. Diezel, A. Fröba, and A. Leipertz, "Economical aspects of the improvement of a mechanical vapour compression desalination plant by dropwise condensation," *Desalination*, vol. 264, no. 1-2, pp. 173–178, 2010. 53

[50] Energy Recovery Inc, "ERI power model." Online http://www.energyrecovery.com/resource/power-model/, 2010. San Leandro, CA. 53, 54

[51] M. Elimelech and W. A. Phillip, "The future of seawater desalination: Energy, technology, and the environment," *Science*, vol. 333, no. 6043, pp. 712–717, 2011. 57

[52] Desalitech Ltd, "Doing away with RO energy-recovery devices," *Desalination & Water Reuse*, vol. 20, no. 2, pp. 26–28, 2010. 57

[53] D. M. Warsinger, E. W. Tow, K. G. Nayar, L. A. Maswadeh, and J. H. Lienhard V, "Energy efficiency of batch and semi-batch reverse osmosis desalination," *Water Research*, 2016. under review. 57

[54] K. H. Mistry and J. H. Lienhard V, "Generalized least energy of separation for desalination and other chemical separation processes," *Entropy*, vol. 15, no. 6, pp. 2046–2080, 2013. 58

[55] M. J. Moran and H. N. Shapiro, *Fundamentals of Engineering Thermodynamics*. New Jersey: John Wiley & Sons, Inc., 6th ed., 2007. 61

[56] Global Water Intelligence, "Desaldata.com." Online http://desaldata.com, 2013. 61

[57] J. E. Miller, "Review of water resources and desalination technologies," Tech. Rep. SAND 2003-0800, Sandia National Laboratories, Livermore, CA, March 2003.

[58] G. J. Crisp, "Actual energy consumption and water cost for the swro systems at perth," in *Desalination: An Energy Solution*, no. IDA_HB2010-Crisp, (Huntington Beach, CA, USA), International Desalination Association, November 2–3, 2010.

[59] R. L. Stover, "Isobaric energy recovery technology — history and future opportunities," in *Desalination: An Energy Solution*, no. IDA_HB2010-Stover, (Huntington Beach, CA, USA), International Desalination Association, November 2–3, 2010.

[60] R. L. Stover, "Seawater reverse osmosis with isobaric energy recovery devices," *Desalination*, vol. 203, no. 1–3, pp. 168–175, 2007. EuroMed 2006: Conference on Desalination Strategies in South Mediterranean Countries.

[61] C. Fritzmann, J. Löwenberg, T. Wintgens, and T. Melin, "State-of-the-art of reverse osmosis desalination," *Desalination*, vol. 216, no. 1âĽ"3, pp. 1–76, 2007. 61

[62] E. W. Tow, R. K. McGovern, and J. H. Lienhard V, "Raising forward osmosis brine concentration efficiency through flow rate optimization," *Desalination*, vol. 366, pp. 71–79, 2015. 63, 64, 65

[63] R. K. McGovern and J. H. Lienhard V, "On the potential of forward osmosis to energetically outperform reverse osmosis desalination," *Journal of Membrane Science*, vol. 469, pp. 245–250, 2014. 64

[64] R. K. McGovern, G. P. Thiel, G. P. Narayan, S. M. Zubair, and J. H. Lienhard V, "Performance limits of single and dual stage humidification dehumidification desalination systems," *Applied Energy*, vol. 102, pp. 1081–1090, Feb 2013. 64

[65] G. P. Narayan, K. M. Chehayeb, R. K. McGovern, G. P. Thiel, S. M. Zubair, and J. H. Lienhard V, "Thermodynamic balancing of the humidification dehumidification desalination system by mass extraction and injection," *International Journal of Heat and Mass Transfer*, vol. 57, pp. 756–770, February 2013.

[66] F. Al-Sulaiman, G. P. Narayan, and J. H. Lienhard V, "Exergy analysis of a high-temperature-steam-driven, varied-pressure, humidification-dehumidification system coupled with reverse osmosis," *Applied Energy*, vol. 103, pp. 552–561, March 2013.

[67] K. M. Chehayeb, G. P. Narayan, S. M. Zubair, and J. H. Lienhard V, "Thermodynamic balancing of a fixed-size two-stage humidification dehumidification desalination system," *Desalination*, vol. 369, pp. 125–139, 2015. 64

[68] D. M. Warsinger, K. H. Mistry, K. G. Nayar, H. W. Chung, and J. H. Lienhard V, "Entropy generation of desalination powered by variable temperature waste heat," *Entropy*, vol. 17, pp. 7530–7566, October 2015. 64

[69] R. K. McGovern, S. M. Zubair, and J. H. Lienhard V, "The benefits of hybridizing electrodialysis with reverse osmosis," *Journal of Membrane Science*, vol. 469, pp. 326–335, November 2014. 64

[70] J. Swaminathan, K. G. Nayar, and J. H. Lienhard V, "Mechanical vapor compression-membrane distillation hybrids for reduced specific energy consumption," *Desalination and Water Treatment*, vol. 57, no. 55, pp. 26507–26517, 2016. 64

[71] K. H. Mistry and J. H. Lienhard V, "An economics-based second law efficiency," *Entropy*, vol. 15, pp. 2736–2765, 2013. http://www.mdpi.com/1099-4300/15/7/2736. 64

[72] F. J. Millero, R. Feistel, D. G. Wright, and T. J. McDougall, "The composition of standard seawater and the definition of the reference-composition salinity scale," *Deep Sea Research Part I: Oceanographic Research Papers*, vol. 55, pp. 50–72, 2008. 66

[73] "Release on the IAPWS formulation for the thermodynamic properties of seawater," tech. rep., International Association for the Properties of Water and Steam, 2008. 66, 67, 68

[74] J. D. Isdale and R. Morris, "Physical properties of sea water solutions: density," *Desalination*, vol. 10, pp. 329–339, 1972. 66

[75] F. J. Millero and A. Poisson, "International one-atmosphere equation of state of seawater," *Deep Sea Research Part A: Oceanographic Research Papers*, vol. 28, pp. 625–629, 1981. 66

[76] "Release on the IAPWS formulation 1995 for the thermodynamic properties of ordinary water substance for general and scientific use," tech. rep., International Association for the Properties of Water and Steam, 1996. 66, 67, 69

[77] L. A. Bromley, D. Singh, P. Ray, S. Sridhar, and S. M. Read, "Thermodynamic properties of sea salt solutions," *AIChE Journal*, vol. 20, pp. 326–335, 1974. 70

[78] M. H. Sharqawy, L. D. Banchik, and J. H. Lienhard V, "Effectiveness-mass transfer units (ε-MTU) model of an ideal pressure retarded osmosis membrane mass exchanger," *Journal of Membrane Science*, vol. 445, pp. 211–219, 2013. 71

[79] K. S. Pitzer, *Thermodynamics*. New York: McGraw-Hill, Inc., 3rd ed., 1995. 71

[80] D. T. Jamieson, J. S. Tudhope, R. Morris, and G. Cartwright, "Physical properties of sea water solutions: heat capacity," *Desalination*, vol. 7, pp. 23–30, 1969. 72

[81] M. Uematsu and E. U. Franck, "Static dielectric constant of water and steam," *Journal of Physical and Chemical Reference Data*, vol. 9, no. 4, pp. 1291–1306, 1980. 74

[82] H.-T. Kim and W. J. Frederick, "Evaluation of Pitzer Ion Interaction Parameters of Aqueous Electrolyte Solutions at 25 °C. 2. Ternary Mixing Parameters," *Journal of Chemical Engineering Data*, vol. 33, pp. 278–283, 1988. 75

[83] R. T. Pabalan and K. S. Pitzer, "Thermodynamics of concentrated electrolyte mixtures and the prediction of mineral solubilities to high temperatures for mixtures in the system Na-K-Mg-Cl-SO_4-OH-H_2O," *Geochimica et Cosmochimica Acta*, vol. 51, pp. 2429–2443, 1987. 75

[84] F. J. Millero and D. Pierrot, "A chemical equilibrium model for natural waters," *Aquatic Geochemistry*, vol. 4, pp. 153–199, 1998. 75

[85] L. F. Silvester and K. S. Pitzer, "Thermodynamics of Electrolytes X. Enthalpy and the effect of Temperature on the Activity Coefficients," *Journal of Solution Chemistry*, vol. 7, no. 5, pp. 327–337, 1978. 75

[86] L. F. Silvester and K. S. Pitzer, "Thermodynamics of Electrolytes. 8. High-Temperature Properties, Including Enthalpy and Heat Capacity, with Application to Sodium Chloride," *The Journal of Physical Chemistry*, vol. 81, no. 19, pp. 1822–1828, 1977. 75

[87] M. P. de Lima and K. S. Pitzer, "Thermodynamics of saturated electrolyte mixtures of NaCl with Na_2SO_4 and with $MgCl_2$," *Journal of Solution Chemistry*, vol. 12, no. 3, pp. 187–199, 1983. 75